UNIVERSITY OF CALIFORNIA
RIVERSIDE

A Study of Aluminum Dependent Root Growth Inhibition in *Arabidopsis thaliana*

A Dissertation submitted in partial satisfaction
of the requirements for the degree of

Doctor of Philosophy

in

Biochemistry and Molecular Biology

by

Cynthia Nezames

June 2011

Dissertation Committee:
Dr. Paul Larsen, Chairperson
Dr. Daniel Gallie
Dr. Hailing Jin

The Dissertation of Cynthia Nezames is approved:

_____

_____

_____

Committee Chairperson

University of California, Riverside

ABSTRACT OF THE DISSERTATION

A Study of Aluminum Dependent Root Growth Inhibition in *Arabidopsis thaliana*

by

Cynthia Nezames

Doctor of Philosophy, Graduate Program in Biochemistry and Molecular Biology
University of California, Riverside, June 2011
Dr. Paul Larsen, Chairperson

Aluminum (Al) toxicity is a global agricultural problem and is one of the major factors that limit crop productivity on acidic soils. Plant Al toxicity is involved in many hypothesized mechanisms since it can interact with many intracellular and extracellular structures of the root. Mechanisms of Al exclusion, which confers Al-tolerance and resistance, have been studied in depth while internalized Al-tolerance mechanisms have not been fully described due to the complexity of the predicted cellular targets of Al.

Several Al hypersensitive mutants have been identified suggesting that they represent mutations in genes that are required for Al-tolerance or resistance. One of these mutants, *als7* was identified as a mutation in *Slow Walker2*. Molecular analysis revealed that Al hypersensitivity in *als7-1* is correlated with loss of expression of a factor required for methionine recycling, which leads to reduced levels of endogenous polyamines. Further analysis shows that Al-dependent root growth inhibition is reversed by addition

of exogenous spermine. Spermine likely functions to compete with Al^{3+} for binding to extra- and intracellular anionic sites, which is shown by the severe reduction in Al accumulation in spermine-treated roots.

Several suppressor mutations were identified that masked the Al hypersensitivity of *als3-1*. One of these mutations, *alt2-1* was isolated and represents a mutation in a WD40 protein that contains a DWD motif. Loss of *alt2-1* causes the plant to fail to detect DNA damage caused by Al stress. This prevents a halt in the cell cycle for DNA repair, which in turn maintains the quiescent center and allows the plant to tolerate high levels of Al. Furthermore, *alt2-1* is hypersensitive to the interstrand and intrastrand crosslinking agents. From *in vitro* studies, Al has been shown to be a DNA crosslinker, suggesting that *alt2-1* is required to detect DNA crosslinks. These results taken together suggest that Al is acting as a DNA crosslink mimic or a weak DNA crosslinker, which has minor immediate consequence on the plant if the crosslink is not detected.

Table of Contents

List of Figures

Introduction

Plants are exposed to variety of abiotic and biotic stressors throughout their life cycle. Unlike most organisms, plants must cope with these stressors in order to survive and have developed sophisticated methods of tolerance, avoidance and resistance. One major factor in plant health is soil quality since plants are soil bound. It is key to understand how soil stresses such as salinity, heat, acidity, and availability of nutrients affect plant health since it can ultimately improve crop yield from agriculturally important plant species.

In acidic soils, aluminum (Al) is considered to be the most important growth-limiting factor for plants due to its naturally occurring abundance. Al toxicity causes reduced root growth that ultimately leads to reduced shoot growth and crop yields. Even though Al toxic soils are widespread, they represent some of the most biologically diverse regions in terms of plant life and unfortunately the mechanisms of tolerance are poorly understood. This creates an opportunity to study plants that are hypersensitive as well as tolerant to Al to understand mechanisms that allow plants to tolerate levels of Al that are otherwise highly inhibitory. The mechanisms to increase Al tolerance my then be applied to agriculturally important crop species.

CHAPTER ONE

Aluminum Occurrence

Aluminum (Al) toxicity is a global agricultural problem and is one of the major factors that limit crop productivity on acidic soils. Acidic soils comprise greater than 30% of the land in the world (von Uexhüll 1995), with varying estimates having 50-70% of the potentially arable lands in the acidic range (Hede 2001). Originally this problem was considered to be restricted to tropical agricultural regions, or areas of high rainfall with highly weathered soils, but soil acidity has now attracted global attention. Acid soils occur primarily in two belts, a northern belt with a cool, humid climate and a southern tropical belt with a warm, humid climate (Figure 1). In addition, two thirds of the acid soils are found primarily in forested areas and 17% are covered by prairie, savanna, or steppe vegetation. Only 5.6% of the world's acid soils are used for agriculture (von Uexhüll 1995), indicating that acid soils severely compromise agricultural production due to mineral deficiencies, unavailability of essential nutrients and mineral toxicities. Because acid soils are detrimental to crop production, especially several cereal species, the widespread occurrence of acid soils serves as a severe limitation on agricultural production in these areas.

Soil acidity is determined by the concentration of hydrogen ions in the soil solution. A variety of factors including biological, environmental and the characteristics of the soil affect this acidity. Decay of organic material which forms carbonic acid and other weak acids can add to the acidity of the soil solution. In addition the amount

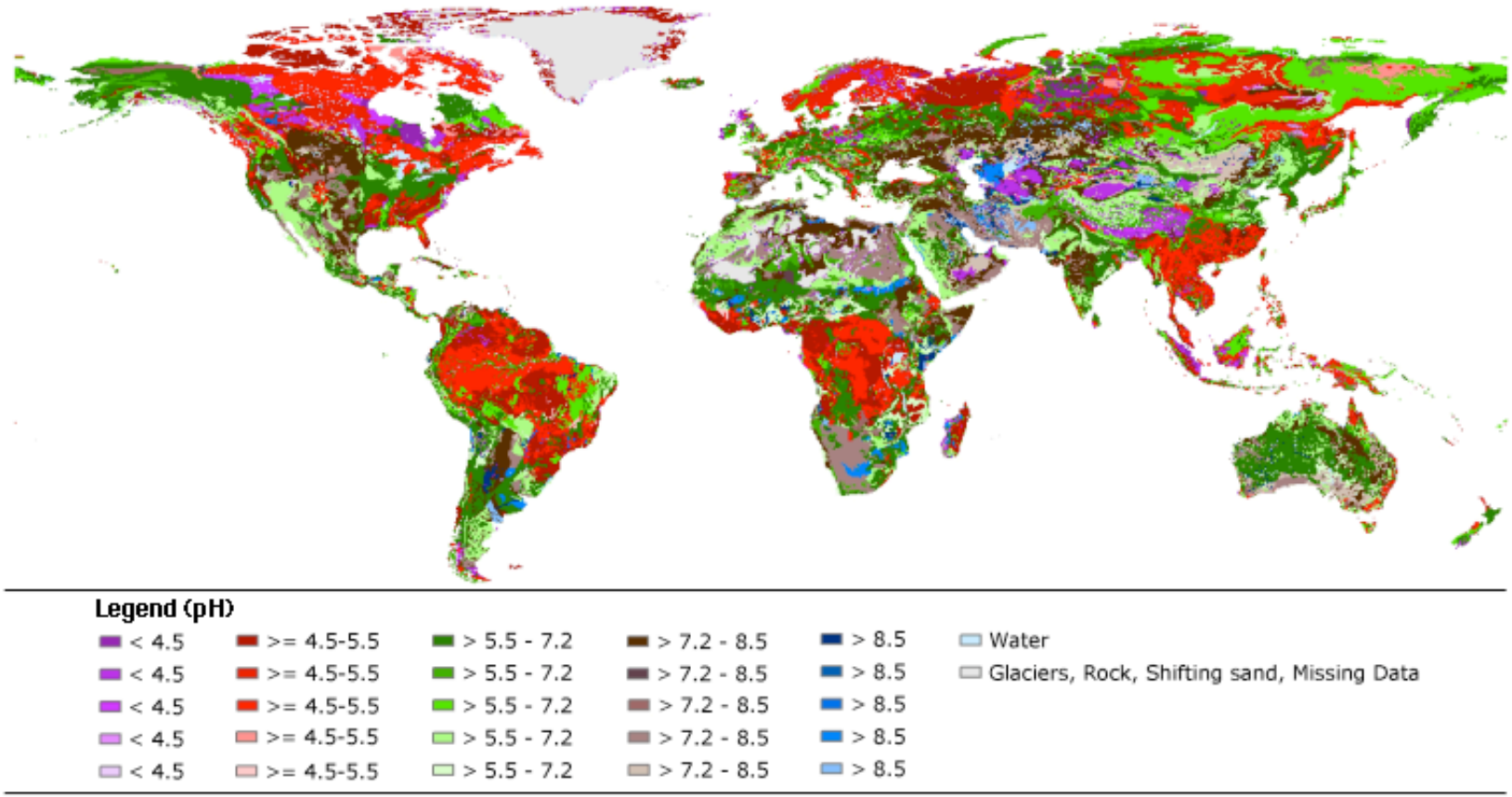

Figure 1. World acid soils. Areas that have a pH 5.5 and lower are depicted as the pink to purple areas of the map. The Americas account for the majority of the world's acid soils containing 40.9% of the world's acid soils. Asia accounts for 26.4% of the world's acid soils, but Southeast Asia and the Pacific have 63% of their regional land comprised of acid soils. For the remaining continents, Africa accounts for 16.7%, Europe 9.9% and Australia and New Zealand combined account for 6.1% of the world's acid soils (von Uexküll 1995)

of rainfall can affect the rate of soil acidification depending on the rate of flow through the soil solution. Finally, soils that develop from granite materials acidify faster than soils that have developed from calcareous materials. Also, sandy soils acidify more rapidly due to their higher leaching potential and reduced buffering capacity. The cumulative effect of these factors is practically immeasurable over the course of a few years and therefore may contribute relatively little to total soil acidity, indicating there are other factors that contribute to rapidly acidification of the soil solution (Carver 1995).

Surface soil acidity can be accelerated by certain agricultural practices such as high output farming and excessive utilization of ammonium-based fertilizers. Over cropping can also lead to the depletion of basic cations from the soil solution such as calcium, potassium, magnesium and sodium. Even harvesting methods can affect the rate of acidification of the soil solution. For example, removal of the straw alone from wheat cropping depletes basic cations to the greatest extent and actually enhances acidification by nitrification (Westerman 1987).

Poor acid fertility can result from many mineral deficiencies and mineral toxicities, with Al toxicity being the single most important factor. Al is the third most common element and the most common metal in the Earth's crust, accounting for 8% of the Earth's crust by weight. The majority of Al is contained within aluminosilicate compounds in the primary mineral, which is the parent rock, or as aluminum oxides and aluminosilicates in the secondary mineral, which are formed during weathering (McBride 1994). However, Al in these forms is not phytotoxic and only a small percentage of Al in the soil solution contributes to aluminum toxicity in plants (Mossor-Pietraszewska 2001).

Even though Al exists in many forms such as aluminum ions, aluminum oxides, aluminum sulfates, aluminum fluorides and the complex Al_{13}, only the trivalent aluminum cation and Al_{13} complex have been proven to be toxic to plants (Kochian 1995). Of these two forms of Al, the trivalent cation Al^{3+} is the most prevalent species in soils that are pH <4.7, therefore the most significant form for aluminum phototoxicity.

Al toxicity is dependent on the pH of the soil solution and also the predominate clay mineral. Al can also become dissociated from the primary and secondary minerals in acidic conditions, which can add to the soil acidity. In soils of pH <5.5, Al speciates to Al^{3+} in the soil solution to levels that rapidly inhibit root growth. As the pH decreases further, the concentration of Al in the soil solution increases. Between pH of 4.0 to 4.5 in the soil solution, a small change in the acidity can cause large changes in the solubility of Al (Tyler 1987). For example, at pH <4.2, Al^{3+} can be found at extremely high concentrations ranging from 0.1 to 1.0 mmol/L (Ulrich 1983).

Al toxicity is also influenced by organic matter content, concentration of other cations, plant species and individual genetic properties of the plants. In developed countries, soil acidity can be alleviated by the addition of lime to neutralize the acidic soil solution. This practice has limited impact on subsoil acidity due to the lime being spread on the soil surface then tilled into the soil. Free Al^{3+} in the soil solution can also complex with several organic acids such as malic, citric and oxalic acids, which results in reduced concentrations and solubility of Al^{3+} (Andersson 1988, Wong 2003). Since it is difficult to manage Al subsoil toxicity, it becomes of interest to understand how plants cope with Al toxicity.

CHAPTER TWO

Effects of Aluminum Toxicity on Plants

The toxic effects of plants grown on Al have been extensively reported for almost a century, and plant Al toxicity is speculated to be complex since it can interact with many intracellular and extracellular structures of the root. Primary negative effects on the root have been shown to be at or near the root tip (Kochian 1995). Al targets are both apoplastic and symplastic resulting in reduced cell elongation, damage to the cell wall, changes in Ca^{2+} levels within the cell, as well as a variety of other cellular alterations (Kochian 1995). Mechanisms of Al exclusion that confer Al-resistance by preventing Al uptake have been studied in depth while internalized Al-tolerance mechanisms that increase the capability to cope with internalized Al have not been fully described due to the complexity of predicted cellular targets of Al.

The primary target of Al toxicity has been shown to be at the root and more specifically at the root tip. This is not surprising since the primary contact of Al with the plant is between the soil solution and the root. The immediate effect of Al toxicity is reduced elongation of the root, which can occur as quickly as 30 minutes to two hours (Ryan 1992, Barceló 2002). Upon extended treatment with Al, the root begins to swell, concomitant with distortion of differentiated cells and root discoloration. Meristematic and root cap cells also become increasingly more vacuolated. There are also changes in root cell patterning, irregular cell division, alterations in cell shape, cell wall thickening, callose accumulation, disintegration of the cytoskeleton, formation of myelin figures,

alteration of the plasma membrane, and the production of reactive oxygen species (Illíš 2006). The rapid inhibition of root growth is likely caused by interference with cell elongation, while long-term inhibition of root growth is likely due to inhibition of cell division (Kochian 1995).

Even though it is known that the primary effect of Al toxicity occurs at the root tip, the response to Al at the tip varies. The root tip is divided into many different zones of development. At the end of the root tip is the root cap, which protects the apical meristem of the root and the meristematic zone replaces cells of the root cap. The meristematic zone is the zone of cell division, which contains the root apical meristem. Within this region there is a core of slow dividing cells called the quiescent center, which produces the rapidly dividing initial cells. The zone of elongation where the root cells elongate and then begin to differentiate follows this region. Between these two zones is the transition zone where the cells prepare to differentiate. This zone is further divided into the proximal and distal transition zones. The final zone of root development is the zone of cell differentiation, where final differentiation occurs and the root hairs develop. A recent study using fluorescent lifetime imaging (FILM) in plants quantified Al^{3+} uptake *in vivo*. This report confirmed that the primary sites for Al^{3+} entry are the meristem and distal transition zones, while Al^{3+} uptake is limited in the cortex and epidermis of the mature root zone (Babourina 2009). It was also determined that the maximum rates of Al uptake into the cytoplasm was 2–3 μmol m^{-3} min^{-1} for the meristematic root zone and 3–7 μmol m^{-3} min^{-1} for the mature zone after a 30-min exposure to 100 μm $AlCl_3$ at a pH of 4.2 (Babourina 2009).

Al localizes to both the apoplast and the symplast, but it is unclear where the primary site of Al action is. Al accumulation in the apoplast appears to be correlated with the pectin content of the cell wall (Wang 2009). Accelerator mass spectrometry in single cells of *Chara corallina* revealed that the major portion of Al uptake is apoplastic (Taylor 2000). Al accumulation in the symplasm has been much more difficult to establish and historically has been a controversial topic. Al has been observed to enter the cell walls and vacuoles of maize root tips cells after four hours of treatment, but after 24 hours of treatment, Al is found primarily in the vacuoles (Vázquez 1999). Al has also been found in the cytoplasm where it alters microtubule structure and polar transport of actin (Kollmeier 2000). Al accumulation has also been shown to occur in the endosomes, where it is speculated that endocytosis of cell wall pectins occurs and causes internalization of Al (Illéš 2006). It is also possible that aluminum uptake occurs through ion channels that transport cations of similar ionic radius to Al^{3+}, such as Fe^{3+} and Mg^{2+} (Kochian 1995).

Al causes its toxic effects at the cell walls and plasma membranes of the root, since the cell wall is the primary site of Al accumulation. Interaction with the cell wall accounts for the initial rapid phase of Al accumulation by the roots and is due to the degree of methylation of the pectin at the cell wall, which is controlled by pectin methylesterase. Intact roots of maize were found to have increased Al accumulation and Al dependent root inhibition when pectin methylesterase was enhanced (Horst 2010). Al treatment also causes reduced root cell wall flexibility and binding of Al to the pectic

matrix may prevent cell wall extension physically and/or physiologically by decreasing the effectiveness of cell wall-loosening enzymes (Wehr 2004).

Al rapidly alters the plasma membrane as well as interacts with membrane lipids and proteins, which causes changes in its structural properties such as membrane fluidity and permeability (Khan 2009). These changes, as well as an increase in cytosolic Ca^{2+} are required for the induction of callose synthesis (Kauss 1989), which is a sensitive response to Al stress in the root apex. Al also induces membrane depolarization, specifically in the distal transition zone, which may be related to the inhibition of the H^+-ATPase activity (Ahn 2001) and in turn may cause a disruption of H^+ homeostasis in the cytosol. These changes in the plasma membrane properties by Al affect its ion transport properties, such as causing a rapid decrease of K^+ efflux without changing K^+ influx (Horst 1992). Al-induced damage of membrane integrity also may be related to Al-enhanced oxidative stress through the formation of reactive oxygen species leading to lipid peroxidation (Jones 2006) and protein oxidation (Boscolo 2003). Oxidative stress genes have been shown to be induced upon Al treatment and over expression of these genes have conferred Al tolerance (Ezaki 2001). However, oxidative stress in roots does not appear to be the primary cause for Al-induced inhibition of root elongation (Yamamoto 2001), because in most cases, it can only be observed after prolonged Al treatment (Liu 2008).

Even though there are such drastic changes in plasma membrane structure and function, there is no evidence that there is a requirement for a severe disruption of the plasma membrane to induce root growth inhibition and callose formation (Horst 1992). It

appears that Al activates signal transduction pathways that lead to the observed symplastic disorders, with a rapid increase in cytosolic Ca^{2+} playing a major role in this effect (Jones 2006). The source of Ca^{2+} is likely from the apoplast due to Al^{3+} liberating bound Ca^{2+} to the cell wall. Al also disrupts the plasma membrane potential, which activates Ca^{2+} channels, allowing for a burst of Ca^{2+} to enter the cell. However, it cannot be ruled out that Al causes a release of Ca^{2+} from symplastic Ca^{2+} pools (Rengel 2003). Increasing Ca^{2+} levels within the cell due to Al exposure can partially explain why callose accumulation and also cytoskeleton disorganization occurs (Rengel 2003). Additionally, Al entering the symplast results in disorganized arrangements of actin filaments in the stele cells of the transition zone of maize roots. Gene expression of actin, as well as profilin are both inhibited by Al exposure. Profilin is an actin-binding protein that regulates the polymerization of actin filaments and plays a role in cell elongation (Zhang 2007). A further effect on the cytoskeleton is the reorientation of microtubles and microfilaments (Blancaflor 1998). This might help explain the swollen root tip due to Al toxicity and halt of mitosis due to abnormal cell plate division and spindle formation (Barceló 2002).

Al is also known to interfere with the production and transport of plant hormones. Ethylene and auxin both have been shown to synergistically affect root growth, and it has been demonstrated that ethylene stimulates auxin biosynthesis and basipetal auxin transport toward the elongation zone causes inhibition of root cell elongation. A recent report has shown a link between ethylene and auxin signaling, indicating that there is a burst of ethylene upon Al treatment, followed by auxin biosynthesis. This suggests that

ethylene serves as a signal to cause downstream changes in auxin distribution in roots by interacting with AUX1 and PIN2 proteins, leading to inhibition of root elongation in the presence of toxic Al^{3+} (Sun 2010). Nitric oxide (NO) production is also negatively effected by Al treatment, which is a signaling molecule for various responses to biotic and environmental stresses. Under normal growing conditions roots express NO at the root cap statocytes, quiescent center and the distal transition zone, but upon Al treatment, NO production is abolished in the distal transition zone only (Illéš 2006). The lack of NO production in Al treated roots, also causes the production of jasmonic acid, a plant signal known to regulate environmental stresses such as ozone, heavy metals and pathogen attack (Xue 2008).

The effects of Al at the nuclear level are also poorly understood and highly debated. Using the fluorescence stain lumogallion, which specifically binds to Al, it was determined that Al^{3+} quickly enters the symplasm and accumulates in the nuclei in the meristematic region of the root tip (Silva 2000). *In vitro* studies have demonstrated that Al binds relatively strongly to DNA at room temperature, and can complex with DNA in different forms ranging from an intrastrand DNA crosslinker to an interstrand DNA crosslinker depending on the pH and status of the DNA (Karlik 1980). Unlike other metals that can bind to DNA, Al does not appear to have a base composition preference, and is most likely driven by ionic forces at the phosphate backbone (Karlik 1989a). Others have shown that Al causes DNA compaction, as well as compaction of chromatin (Karlik 1989b, Lukiw 2010). Al has the astonishing ability, at nanomolar concentrations, to repress specific transcription from A+T-rich DNA templates, normally euchromatin,

which is transcriptionally active. Importantly, many of these gene-silencing effects can be explained due to the extraordinary charge density of the aluminum ion. Aluminum has a particularly high affinity for DNA structures rich in the delocalized electron fields of A+T-rich nucleotides, and these often make up a majority of eukaryotic heterochromatin, which are transcriptionally inactive. Aluminum can bind and repress G+C rich regions but to a lesser extent, possibly because those regions are under the gene silencing effects of epigenetic modifications such as DNA methylation (Lukiw 2010).

CHAPTER THREE

Aluminum Tolerance and Resistance in Plants

Since Al toxic soils are widespread, it is not surprising that they represent some of the most botanically diverse regions due to evolution of effective strategies for coping with Al's toxic effects. Unlike Al toxicity, little is known about Al tolerance and resistance mechanisms in plants. The one mechanism of Al resistance that has been studied in depth and is conserved among many plant species is the excretion of organic acids to the rhizosphere, to limit the internalization of Al through exclusion. Also, another mechanism of Al tolerance that has been studied in depth is where Al is detoxified, internalized and transported as a non-toxic species within the plant. These mechanisms as well as a few others describe our current understanding of plant Al tolerance and resistance and are summarized in Figure 2.

Many plants, especially crop species have developed one major mechanism to protect their root tips from the damaging effects of Al, which involves chelating Al and preventing its uptake into the root. In Al resistant species, there are a variety of genes that have been characterized that are required for Al resistance. It has been determined that usually one or a small handful of these genes are required to confer Al resistance to these plants. This was first identified in an Al resistant wheat cultivar where the roots secrete the organic acid malate into the rhizosphere after Al-exposure (Delhaize 1993). The organic acids chelate Al at the sensitive root growth zone to form nontoxic complexes, which prevents Al related damage to the root tip (Ma 2000a). Since then, a

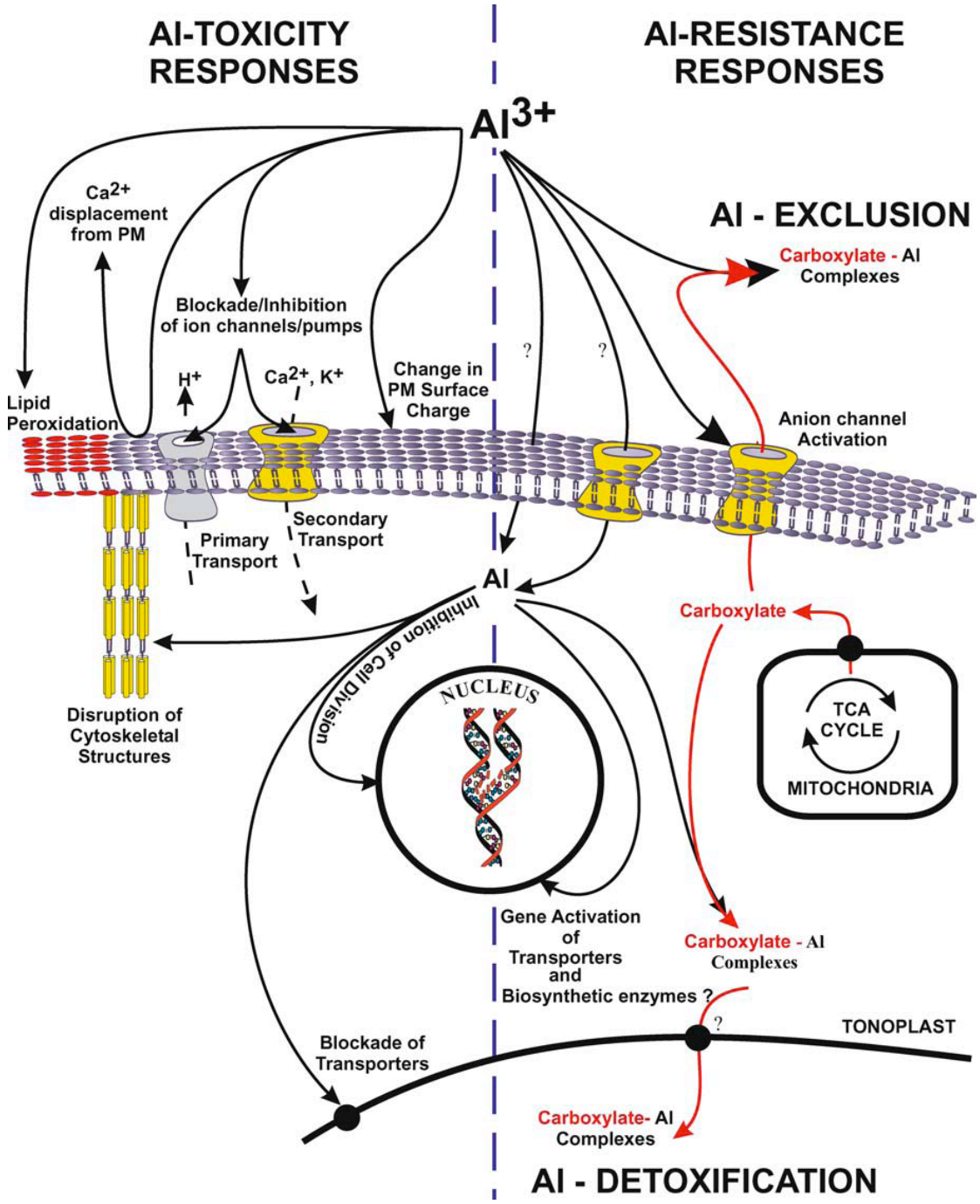

Figure 2. Mechanisms of Al toxicity and Al resistance in plants. Al toxicity targets are described in the text, excluding the interactions of Al with the cell wall, are shown on the left side of the diagram. On the right side, Al-resistance and tolerance mechanisms are shown. Copy by Leon V. Kochian, 2005. Copyright Registration Number 2658940796276.

number of other plant species have been found to employ a similar technique such as malate release by *Arabidopsis*; citrate release by maize, oat, snapbean, sorghum and soybean; buckwheat and taro release oxalate; oat, radish, rapeseed and rye release both citrate and malate (Kochian 1995, Ma 2003, Wong 2003, Kochian 2004). Organic acids were also found to be released from the root apex, but not from the mature root region (Pellet 1995). Of the three organic acids that are secreted from the root apex, citrate is the most common and forms the most stable and non-toxic complex with Al^{3+} since it forms a 1:1 ratio with Al. Oxalate and malate both have less affinity for aluminum since they are both divalent anions (Kochian 2005).

The Al-induced secretion of organic acids can be classified into two patterns depending on the plant species. In Pattern I plants such as Al-tolerant wheat and buckwheat, there is no delay between Al exposure and release of organic acids into the rhizosphere. This pattern suggests that the transporter is not induced by gene activation. There are a variety of proposed mechanisms on how this occurs, including that Al interacts directly with the channel protein, interacts with a specific receptor on the membrane that activates secondary messengers to change the channel activity or Al enters the cytoplasm and alters the channel activity either directly or indirectly (Ma 2000). In contrast, Pattern II plants such as *Cassia tora*, rye and triticale have delayed response to Al suggesting that gene induction may be involved. This pattern probably involves activation of genes that might be related to the metabolism of organic acids, the anion channel on the plasma membrane or transport of organic acids from the mitochondria. Also this pattern is only observed for the secretion of citrate (Ma 2000).

Research on organic acid secretion has lead to the focus of identifying specific transporters that are responsible for the export of organic acids into the rhizosphere. The first Al induced gene responsible for organic ion efflux transport was wheat *ALMT1* (aluminum activated malate transporter). This transporter exports malate and confers Al tolerance to tobacco cells and also barley, which is one of the most Al sensitive cereal crops when it is over-expressed. Tobacco cells with *ALMT1* were able to recover from an 18 hour Al exposure. In addition, over-expressing *ALMT1* in barley conferred increased resistance to Al in both a hydroponic culture and in acidic soils (Sasaki 2004, Delhaize 2004). Since the characterization of wheat *ALMT1*, several active organic acid transporters have been identified such as *Arabidopsis AtALMT1*, sorghum Alt_{SB}, and barley *HvAACT1* (Hoekenga 2006, Magalhaes 2007, Furukawa 2007). While *ALMT1* and *AtALMT1* are novel proteins, the citrate transporter in barley is a member of the multidrug and toxic compound extrusion (MATE) family (Furukawa 2007). This suggests that there could be other, unidentified genes that are encoding anion channels that are important for Al-tolerance (Kochian 2005).

There are other compounds that are capable of chelating Al^{3+} in plants, although it has not been well characterized. Of these compounds, phenolics have been receiving more attention in relation to Al tolerance due to their ability to complex with metals and act as strong antioxidants in response to abiotic stress (Kochian 2004). Phenolics are characterized as organic compounds that have one or more aromatic rings. Two phenolics, the flavenoids catechin and quercetin, are released from maize roots. It was shown that the release of these compounds had a better correlation between the ability of

Al-tolerance in three maize genotypes than with Al-activated oxalate release. The authors suggested that Al stimulated release of phenolics may play an important role in the detoxification of Al at the root tip (Kidd 2001).

Chelation of aluminum as a mechanism of preventing root damage is not limited to the release of organic acids and phenolics into the rhizosphere, since the same mechanism is used to detoxify internalized Al. In Al-tolerant species such as hydrangea, buckwheat, and tea, Al is chelated, internalized and transported as a non-toxic species within the plant. The two extensively studied plant species that utilize this method are hydrangea and buckwheat. When hydrangea is grown in the presence of Al, its sepals change color from red to blue due to the accumulation of the blue colored Al complex. Studies in hydrangea have shown high concentrations of a 1:1 Al-citrate complex in sepals and leaves at levels over 3,000mg kg^{-1}, yet the plant does not show evidence of damage due to Al exposure (Ma 1997). The Al-citrate complex is an incredibly strong complex, since Al binds almost 10^7 times more strongly to ATP than Mg does, which can allow less than nanomolar amounts of Al to compete with Mg for the P sites (Martin 1988). Using ^{27}Al NMR, it was found that the Al-citrate complex is more stable than the Al-ATP complex suggesting that this complex can protect cellular components from the damaging effects of Al (Ma 2000a). In buckwheat, it was found that the plant secretes oxalic acid from the root apex, where it forms a 1:3 Al-oxalate complex. The Al-oxalate complex is then transported through the xylem sap from the roots to the leaves. This allows the plant to accumulate high levels of Al, about 450mg kg^{-1}, in the leaves without showing any evidence of damage due to Al (Ma 2000b). The 1:3 Al-oxalate complex is

also very strong, and also has a higher stability constant that is much higher than Al-ATP, meaning that it also can prevent Al binding to cellular components (Ma 1998). Further research also shows that the Al-oxalate complex in leaves of buckwheat is sequestered to the vacuoles, which may be an additional detoxification step (Shen 2002). Finally, the old leaves of tea can accumulate up to 30,000mg kg^{-1} of Al on a dry-weight basis (Matsumoto 1976). In tea, it has been proposed that Al is transported through the roots to the shoots as an Al-citrate complex (Morita 2004), where Al accumulates at the cell walls of epidermal cells (Matsumoto 1976, Tolrà 2011). By creating complexes with TCA intermediates, these plants can accumulate high concentrations of Al, which represents one mechanism of true Al tolerance.

Until recently, it has been unknown how Al^{3+} enters the cell, which has made it difficult to understand how cells uptake Al for tolerance mechanisms. A transporter, Nrat1 (Nramp aluminum transporter 1) was recently identified in rice. This transporter is specific for Al^{3+} and does not transport any other divalent ions such as iron, manganese and cadmium, or any Al-organic acid complexes. Knockouts of *Nrat1* are hypersensitive to Al but loss of this transporter did not affect the sensitivity to other metals, and causes reduced internalized Al and increased accumulation of Al at the cell wall. It is hypothesized that the increased Al sensitivity is due to the absence of cellular Al detoxification mechanisms with organic acids since the plant is no longer able to transport Al^{3+} into the cell and instead causes accumulation of Al at the cell wall. This mechanism of Al tolerance utilizing Nrat1 for Al^{3+} internalization followed by detoxification is a more effect strategy than allowing Al to accumulate at the root cell

wall because of Al's inhibitory effects to root growth by limiting cell wall elongation (Xia 2010).

Outside of organic acid release as a form of Al tolerance or resistance, an attractive mechanism of Al tolerance is root-mediated alkalinization of the rhizosphere, since Al toxicity is dependent on the pH of the growth environment. Despite the appeal of this process as an Al tolerance mechanism, there is only report that clearly demonstrates this role in Al tolerance. Although it was not demonstrated in an agricultural model system, an Al tolerant mutant line in *Arabidopsis* was shown to release similar amounts of organic acids to wild-type seedlings, indicating that this mutant has a different mechanism of Al tolerance. It was then found that its mechanism of Al tolerance was correlated with an Al-activated root apical H^+ influx. This H^+ influx resulted in an increase in rhizosphere pH at the surface of the root tip, which was significant enough to decrease Al^{3+} activity around the root tip (Degenhardt 1998).

In addition to the various resistance and tolerance mechanisms described, there has been limited evidence that modification of extra- and intracellular anionic sites can have a positive impact on Al resistance. Polyamines are comprised of small aliphatic polycationic molecule that could compete with Al ions for binding sites at the cell wall and membrane to prevent Al from entering the cell (Chen 2008). Plant polyamines are detected in actively growing tissues and under stress conditions. They also have been connected to the control of cell division, embryogenesis, root formation, fruit development and ripening, and responses to biotic and abiotic stresses (Kumar 1997). There are three polyamines, the simplest being putrescine, followed by spermidine, then

spermine. There have been two reports that describe the relationship between Al and polyamines; one report has demonstrated the positive effects of polyamines on Al tolerance, while another has discussed the effects of Al on cellular polyamines. In saffron, 1mM polyamines were able to reduce Al toxicity. Polyamines were also able to decrease H_2O_2 content in the presence of Al as well as Al accumulation at the roots (Chen 2008). In cell cultures of a woody plant *Catharanthus roseus*, it was observed that polyamine levels change upon Al exposure. It was found that spermine levels increased by two- to three-fold after 24 and 48 hours of exposure to Al, and that putrescine levels slightly increased after four hours of exposure, but then sharply decreased (Mincocha 1992). This suggests that even non-chelating molecules can have a significant impact on Al tolerance in plants.

CHAPTER FOUR

Identification and Characterization of *als, alr* and *alt* Mutants in *Arabidopsis*

It has been very difficult to determine other mechanisms of Al tolerance and resistance in agriculturally relevant plants due to issues such as genome size, availability of knockout lines, generation time, and difficulty in creating transgenic lines. The Kochian lab overcame this issue by utilizing the model plant *Arabidopsis thaliana*, which has a smaller diploid genome, an extensive library of knockout lines, and short generation time. Additionally *Arabidopsis* has similar sensitivity to Al in comparison to other crop plants and shows classic signs of Al toxicity (Larsen 1996), making *Arabidopsis* a suitable plant model for Al toxicity for crop species.

In order to find factors that are required for normal plant Al stress response, a genetic approach was taken to identify *Arabidopsis* mutants that exhibit increased Al sensitivity. Mutant lines were generated by treating *Arabidopsis thaliana* ecotype Col-0 wt with EMS. M_2 seedlings were screened for their response to Al by identifying seedlings with normal growth in the absence of Al, but restricted growth on subtoxic levels of Al. The seedlings were grown on a two-layer gel system, with the upper layer consisting of nutrient medium with no added Al and the lower layer consisting of the same nutrient medium equilibrated with a subtoxic level of $AlCl_3$. Any seedlings that could grow normally through the upper layer but could not penetrate the lower layer were isolated. Each of these Al sensitive (*als*) mutants likely represents defects in genes that

are required for mechanisms for Al resistance or tolerance. By using this method, eight unique mutants were isolated that displayed increased sensitivity to $AlCl_3$ (Larsen 1996). Two of these lines, *als1-1* and *als3-1* have been studied in depth. Both of these mutations represent a recessive loss of function mutation that displays greater than wild type root growth inhibition in the presence of low levels of $AlCl_3$.

The first mutant characterized was *als3-1* due to its extreme sensitivity to Al at low levels. When *als3*-1 was grown on Al, there was complete arrest of growth of the primary root and shoots. The roots of Al grown *als3-1* are stunted and have a swollen club shaped root apex, with root hairs at or near the root tip. Also, *als3-1* roots did not initiate any lateral roots, but did produce secondary roots from the base of the hypocotyl. Growth of lateral roots and shoots could resume if *als3-1* plants were removed from an Al environment, but the primary root was irreversibly inhibited by the Al treatment. This response differs from the roots of wild type plants, which were able to fully recover from the Al treatment. The shoot phenotype of *als3-1* when challenged with Al was reduced cotyledon expansion. When *als3-1* plants were removed from the Al stress, leaf expansion was blocked for several days after the transfer. In addition, the first true leaves of *als3-1* developed abnormally following Al treatment. They were severely stunted with very few trichomes, poor leaf expansion, and irregular shaped epidermal cells with a rough leaf surface. The leaves that developed after Al treatment also did not expand but became a disorganized cluster of leaf pegs that eventually expanded without petiole development. Eight days after removal from Al, a second shoot apex formed that developed relatively normally except for a greater number of rosette leaves and some

fused inflorescences. This shoot phenotype was found to only be dependent on *als3-1* plants that were challenged with Al (Larsen 1997).

Since this mutation is completely Al-dependent, it was hypothesized that *als3-1* represents a factor required for Al-tolerance or resistance. This factor was found to be specific for Al tolerance since *als3-1* did not show increased sensitivity to other metals such as copper, nickel, cadmium or lanthanum and does not display any other growth defects in the absence of Al. Staining of *als3-1* roots with hematoxylin and morin, two stains that bind to aluminum, resulted in similar intensity of staining to wild type, suggesting that *als3-1* mutation does not alter the amount of aluminum uptake (Larsen 1997). This was later confirmed using ICP-OES (Larsen 2005). Although there was no difference in the amount of aluminum uptake, when wild type and *als3-1* roots were stained with hematoxylin, wild type plants showed a diffuse pattern of surface bound Al extending from the root apex to the mature region of the root, while *als3-1* roots displayed intense staining just proximal to the root tip (Larsen 2005).

Using map-based cloning, *ALS3* was found to be a phloem and root tip localized putative ATP-binding cassette (ABC) transporter-like protein. The *ALS3* gene product also shows high similarity to a homolog in *E. coli* called *ybbM*, a partial ABC transporter that is required for metal resistance. *ALS3* is a single-copy gene in the *Arabidopsis* genome and is conserved among plant species. Like *ybbM*, *ALS3* lacks an ATPase domain, which may indicate the need for a second factor to complete the transporter.

GUS staining of plants harboring the *ALS3* promoter fused with GUS indicates that *ALS3* expression is localized primarily to the sieve tube elements of the phloem in all

plant organs, and trichoblast cell files and immature root hairs. GUS activity was also found in the epithem tissue of the hydathodes but not in the actual water pore of the tydathode. Since Northern analysis determined that *ALS3* is Al inducible, GUS analysis of Al treated lines resulted in a shift of expression from the root epidermis to the root cortex. From these results, ALS3 was hypothesized to mediate Al transport within the plant, transporting Al from sensitive tissues from the plant such as the root apical meristem in order to sequester it in less sensitive tissues or also to the hydathodes for excretion by guttation. By disrupting this partial ABC transporter, there is inappropriate accumulation of Al^{3+} in the root, leading to severe symptoms of Al toxicity (Larsen 2005).

An ALS3 homolog has also been found in rice, called STAR2. Rice STAR2 interacts with another factor required for rice Al-tolerance called STAR1. The two proteins form a complex that function together as a bacterial-type ABC transporter that transports UDP-glucose. STAR2 contains a transmembrane domain, similar to ALS3 and STAR1, contains a nucleotide-binding domain. Although both ALS3 and STAR2 are both required for plant Al-tolerance, the expression patterns and cellular localization differ. STAR2 is only expressed in the roots and upon Al treatment and it is located in all cell types except for the epidermal cells in the mature root zone. It is currently unclear as to how the transport of UDP-glucose by STAR1-STAR2 enhances the plant's tolerance although it is possible that STAR1-STAR2 might be responsible for transporting UDP-glucose from the cytosol into the vesicles. UDP-glucose or glycoside derived from UDP-glucose would then be released from the vesicles to the apoplast by exocytosis and then

used to modify the cell walls to mask the sites for aluminum binding, resulting in aluminum tolerance in rice (Huang 2009).

After the characterization of *als3-1,* another Al hypersensitive mutant, *als1-1* was also identified by mapped based cloning and subsequently characterized. Similar to *als3-1*, *als1-1* has an extreme increase in Al sensitivity. Map based cloning revealed that the *als1-1* mutation is a single amino acid substitution in a previously uncharacterized half type ABC transporter that has two distinct domains. The N-terminal domain contains at least four predicted transmembrane regions and appears to have a structure typical of the membrane spanning regions of ABC transporters. The C-terminal domain has all the required motifs associated with functional ATPases of ABC transporters. ALS1 also has significant homology to two distinct ABC transporters with different functions. ALS1 is homologous to mammalian TAP-type transporters associated with the endoplasmic reticulum to move short polypeptides for antigen processing. ALS1 is also homologous to yeast mitochrondrial-localized subfamily B ABC transporter, Atm1p and vacuolar localized Ycf1p. Atm1p is an essential component in the mitochondrial export of Fe/S clusters to the cytoplasm, indicating that it is essential for iron homeostasis in yeast. Ycf1p is required for movement of cadmium conjugated with glutathione into the yeast vacuole and loss of Ycf1p results in cadmium hypersensitivity. It is possible that ALS1 functions similarly to Atm1p and Ycf1p, thus transporting a metal complex in *Arabidopsis* (Larsen 2007).

Histochemical staining of plants homozygous for full length *ALS1* fused to GUS was performed. It was determined that ALS1 is primarily limited to vascular tissue in the

roots, leaves, stems and flowers, with high activity throughout the distal portion of the root tip. High GUS activity was also detected in the hydathodes and the area surrounding the water pore. ALS1 was found to be exclusively localized to the vacuolar membrane using *ALS1* fused to GFP (Larsen 2007).

It was proposed that ALS1 is potentially transporting a metal complex from the cytosol to the vacuole of the cell, similar to two yeast homologs Atm1p and Ycf1p. This would allow sequestration of Al into the vacuole and remove interaction of the Al cation within the cytosol. Due to this activity, it is possible that ALS3 loads and unloads Al from the phloem for movement of Al to less sensitive cells, while ALS1 transports intracellular Al from the cytosol to the vacuole for sequestration. Mutation of either of these two factors can lead to inappropriate accumulation of Al in sensitive tissues within the plant (Larsen 2007).

Aluminum resistant (*alr*) mutations have been identified by using EMS mutagenized *Arabidopsis* seedlings that had enhanced root growth on a phytotoxic level of $AlCl_3$. From this screen, five lines were explored further in depth. Four of these lines were mapped to a similar location and all had increased organic acid release of malate and/or citrate. The fourth line did not have enhanced organic acid release, suggesting the resistance is conferred in a manner other than organic acid release, which has already been described previously. Unfortunately, fine scale mapping could not be accomplished due to the difficultly identifying a population that had a clear resistant phenotype (Larsen 1998). Since *als3-1* has such a profound phenotype that is specific to Al challenge, it gave a unique opportunity to use this mutation to help identify factors that confer

increased Al tolerance and/or resistance using a suppressor mutagenesis approach. EMS chemical mutagenesis on *als3-1* was performed and plants that masked *als3*-1 hypersensitivity on low levels of Al were isolated. The *als3-1* suppressor lines represent mutations in factors that confer increased Al resistance and/or tolerance (Gabrielson 2006).

By using this method, 12 strong suppressor mutants were identified, and 3 were initially chosen for further analysis. All three gave similar phenotypes. When crossed with each other they did not give enhanced Al tolerance, and all mapped to the same region. Therefore only one of those lines was studied further, *alt1-1*. When the *alt1-1,als3-1* suppressor mutant was grown in the presence of increasing concentrations of $AlCl_3$, its growth not only reversed $AlCl_3$ hypersensitivity of *als3-1* but it also had increased root growth compared to Col-0 wt in higher levels of $AlCl_3$. It was found that *alt1-1* is a mutation that does not exhibit any enhancement in Al exclusion, due to callose accumulation and Al content of *alt1-1* being similar to wild type (Gabrielson 2006).

Map based cloning of *alt1-1* revealed that it is a single base change in the gene *AtATR* (*ataxia telangiectasia-mutated and Rad3-related*). *AtATR* has previously been shown to be required for the assessment and response to DNA damage and functions to detect single-stranded DNA breaks, DNA crosslinks and blocked replication forks. *atr1-1* without *als3-1* in its background further increased the plant's tolerance to Al, far surpassing wild type growth. Since knockouts of AtATR have previously been shown to be hypersensitive to hydroxyurea (HU), a chemical that causes replication fork blocks, *alt1-1* was tested for HU sensitivity. Like *atr-2*, a previously characterized *AtATR*

mutant, *alt1-1* was hypersensitive to HU suggesting that the toxic effects of HU are distinct from Al toxicity. Due to the link between DNA damage and inhibition of DNA repair by many heavy metals, it was of interest to determine if *alt1-1* plants were tolerant to those as well. Of the heavy metals tested, *alt1-1* plants were tolerant to only nickel and cadmium, suggesting that AtATR is also required for detecting DNA damage caused by these heavy metals (Rounds 2008).

It has been previously shown that AtATR is required for regulating cell cycle progression, with AtATR causing arrest in the G2 phase of the cell cycle after accumulation of DNA damage. A GUS reporter that was fused to the *CycB1;1* promoter and a truncated coding sequence containing a predicted mitotic destruction box was utilized since *CycB1;1* is only expressed during the G2/M transition of the cell cycle and the mitotic destruction box causes the reporter protein to be degraded in cells that have passed mid-M phase. The histochemical activity of this line reports individual mitotic cells (Colon-Carmona 1999). Utilizing this reporter line, it was found that Al-dependent root inhibition arises from ATR-dependent stoppage of the cell cycle due to DNA damage. Additionally, it was found in the Al hypersensitive mutant *als3-1* that high levels of Al forces complete differentiation of the root tip, with the differentiation being the ultimate cause of Al-dependent stoppage of root growth. To verify that terminal differentiation was occurring as a result of Al toxicity, the quiescent center (QC) reporter line QC46 was used, which carries a GUS-based marker that specifically detects the QC. When the QC lines were grown in the presence of toxic levels of Al, wild type and *als3-1*

had a complete loss of staining at the QC, while *alt1-1* plants displayed normal GUS activity and maintenance of the QC (Rounds 2008).

The role of the cell cycle is to check the integrity of the DNA before mitotic cells enter cell division. If damage is detected, there is arrest of the cell cycle until repair occurs. Work was attempted to identify the type of DNA damage caused by Al. Utilizing the Comet assay, it was found that Al treatment causes an increase of double stranded and single stranded DNA fragmentation, but *alt1-1* does not prevent accumulation of DNA fragmentation. This suggests that the increased capability to grown on an Al-toxic environment for *alt1-1* is from a failure to detect and respond to Al-dependent DNA damage. It was determined that AtATR is required for blockage of the cell cycle and terminal differentiation due to loss of the quiescent center following Al treatment. The *alt1-1* mutation prevents detection of DNA damage, therefore allowing maintenance of the quiescent center and sustained growth in an Al-toxic environment (Rounds 2008). To date, there has been no *in vivo* or genetic evidence as to what specific type of DNA damage is occurring due to Al toxicity since DNA fragmentation can result from DNA crosslinking, replication fork blocks, ROS, nucleotide excision repair, and a variety of other stressors.

RESULTS

CHAPTER FIVE

Identification and Characterization of *als7-1*

als7-1 is hypersensitive to $AlCl_3$

In a previous study, *Arabidopsis* mutants that are hypersensitive to aluminum were isolated (Larsen 1996). One of these, *als7-1*, was studied further to determine the nature of its increase in Al sensitivity. Col-0 wt and *als7-1* were grown in a gel-soaked environment for 10 days on increasing concentrations of $AlCl_3$ to quantify the sensitivity of *als7-1* to $AlCl_3$. As shown in Figure 3, after 10 days of growth of Col-0 wt and *als7-1* on increasing concentrations of $AlCl_3$, root lengths were measured (A). When the lengths of *als7-1* were compared to Col-0 wt (B), there was a dramatic increase in sensitivity of *als7-1* roots to $AlCl_3$ that only slightly inhibited root growth of Col-0. Visually after 10 days of growth, roots of *als7-1* have a drastic reduction of growth on 0.75mM $AlCl_3$ (Figure 4). These data show that *als7-1* is hypersensitive to $AlCl_3$ at normally subtoxic levels. In addition, the root length of *als7-1* is only slightly inhibited in the absence of $AlCl_3$, which suggests that the *als7-1* mutation is in a factor that is required for Al tolerance or resistance.

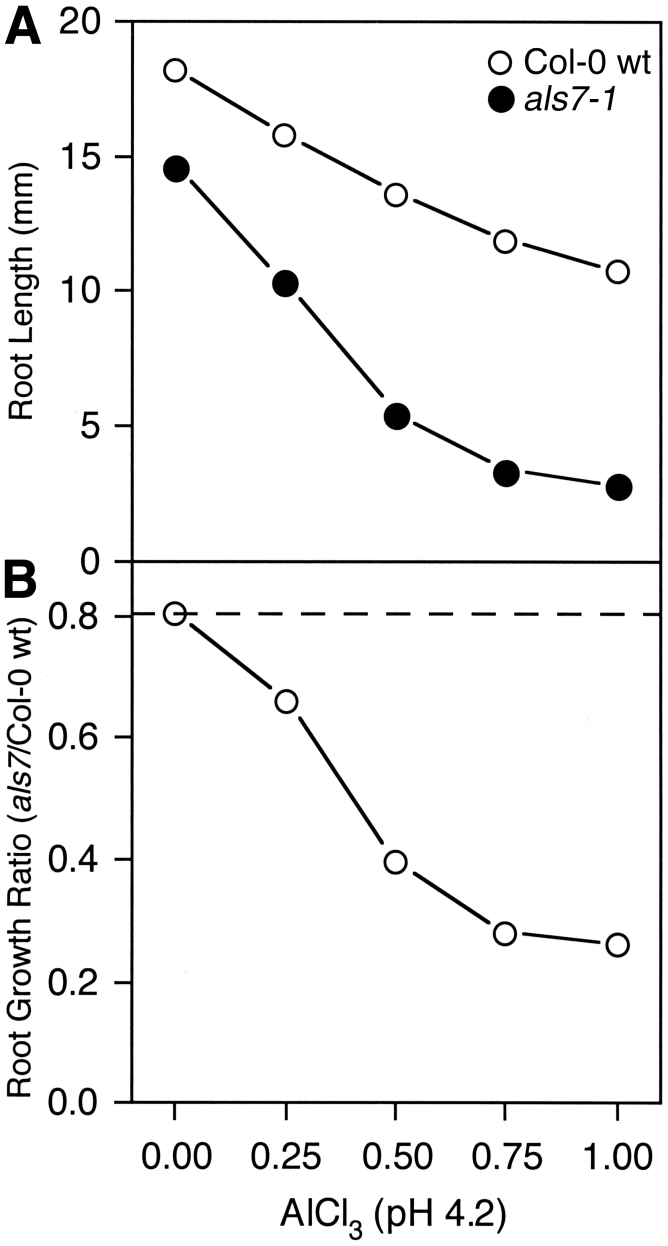

Figure 3. Growth of *als7-1* in an Al toxic environment. (A) Col-0 wt and *als7-1* grown for ten days on nutrient media (pH 4.2) with either no or increasing concentrations of $AlCl_3$ ranging from 0.25mM to 1.0mM. Following growth, root lengths were measured, with mean ±SE values determined from 30 roots of each. (B) *als7-1*/Col-0 root length ratio following ten days of growth on nutrient media supplemented with increasing concentrations of $AlCl_3$.

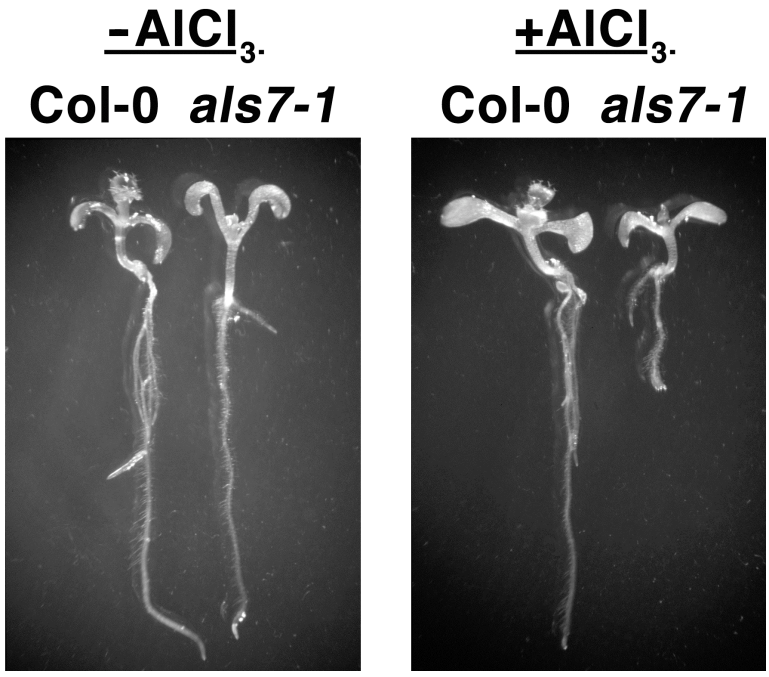

Figure 4. *als7-1* in an Al toxic environment. Col-0 wt and *als7-1* seedlings following ten days of growth on solid nutrient media supplemented with 0 and 0.75mM $AlCl_3$.

als7-1 has increased stress response to $AlCl_3$

There are several indicators of Al-responsive stress including callose accumulation and expression of Al-induced genes. By testing these indicators, it is possible to assess if *als7-1* mutant phenotype is due to altered Al uptake. Callose is a polysaccharide that accumulates in response to damage caused to the root due to pathogens, Al challenge or other stressors. Previous work on *als7-1* suggested that the roots of *als7-1* had reduced levels of Al-induced callose accumulation (Larsen 1996), which created a contradiction when considering *als7-1*'s hypersensitivity to Al. Therefore, roots of Col-0 wt and *als7-1* seedlings were stained for callose (Figure 5). Unlike the previous report, both Col-0 wt and *als7-1* show similar callose accumulation in the presence of $AlCl_3$.

There are several transporters that have been previously described that transport Al to less sensitive areas of the plant, such as ALS3 and ALS1. Therefore it was necessary to determine if the total Al content of *als7-1* was altered. Previously *als7-1* roots were stained with morin and hematoxylin, two stains that are used as a means to detect the presence of Al in plant tissue. That report suggested that *als7-1* has a reduced Al uptake using a qualitative manner. Based on that previous report, it was important to determine total Al content using ICP-OES to establish if there was a change in accumulation of Al in *als7-1* to Col-0 wt (Figure 6). Unlike the other *als* mutants that have been previously characterized, *als7-1* has increased Al accumulation in the presence of Al compared to Col-0 wt.

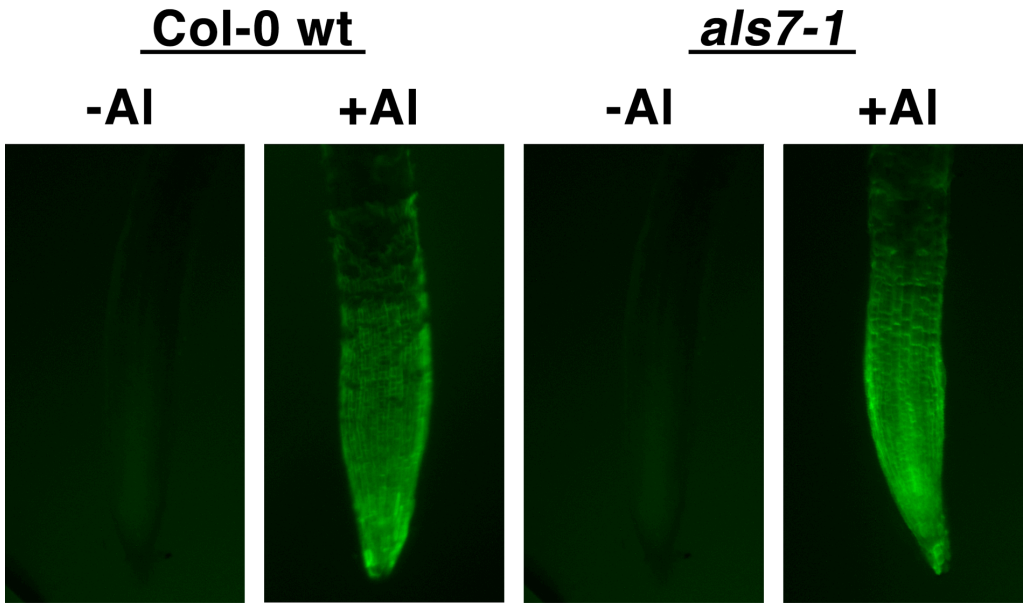

Figure 5. Callose accumulation in *als7* in the presence of $AlCl_3$. Col-0 wt and *als7-1* were grown hydroponically for 7 days after which they were transferred to nutrient media supplemented with 25μM $AlCl_3$ (pH 4.2) for 24 hours. Seedlings were fixed and stained with 0.1% aniline blue. Callose was visualized using an epifluorescent-dissecting microscope.

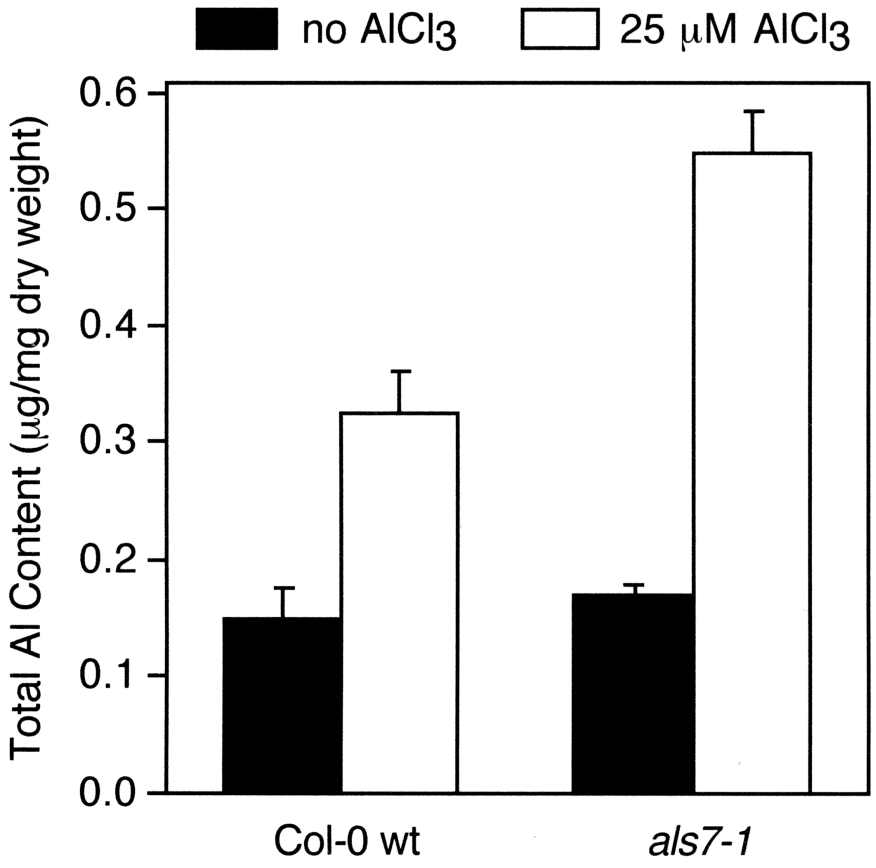

Figure 6. Total Al content in *als7-1* roots following Al treatment. Col-0 and *als7-1* were grown hydroponically for 10 days after which they were transferred to nutrient media supplemented with 0μM or 25μM $AlCl_3$ (pH 4.2) for 48 hours. Root tissue was harvested, dried, weighed, ashed in nitric acid and analyzed for total Al content using ICP-OES.

There are also several Al-inducible genes that have been previously identified, one of which is *AtALMT1*. *AtALMT1*, which encodes a malate transporter and it is associated with Al resistance and tolerance (Figure 7). *als7-1* shows greater than wild type expression of *AtALMT1*, which indicates that increased stress response to internalized Al is not sufficient to overcome the loss of the ALS7-mediated mechanism of Al tolerance. These studies suggest that the *als7-1* mutation has a defect in Al exclusion since *als7-1* is hyper accumulating Al, and has increased *AtALMT1* expression compared to Col-0 wt.

The *als7-1* mutation results in an altered splice site in Slow Walker2

A map-based cloning approach was used to identify the *als7-1* mutation using a mapping population that was created by crossing *als7-1* (Col-0) to wild type (Ws-0). The F_2 population was then screened for lines that exhibited extreme sensitivity to subtoxic levels of $AlCl_3$ in a gel soaked environment. Tight linkage was localized to chromosome 1 upstream of *At1g72480* and the polymorphic marker *nga111* (Figure 8). Mutations consistent with those generated by EMS treatment were sought, with these being a single base pair change from a G:A pair to a C:T pair. Examination of this mapping area revealed a single base pair change in the gene *At1g72440*, which is a previously characterized factor called *Slow Walker2* (Li 2009). High fidelity PCR amplification and sequencing was performed, revealing the mutation in *als7-1* results in a change from a G to a T at the splicing site of the fifth exon and fifth intron (Figure 8). This unusual mutation for an EMS-mutagenized population was the only one found in the mapping

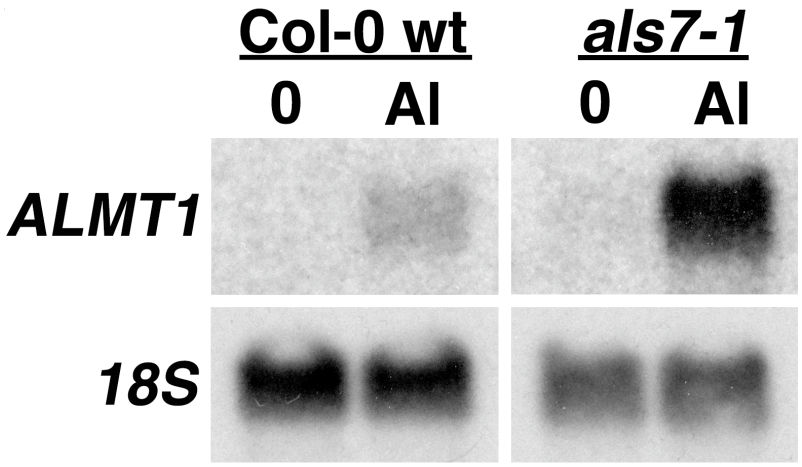

Figure 7. Al-dependent induction of *AtALMT1* in *als7-1*. RNA extracted from roots and 10μg of total RNA was loaded in each lane. Northern analysis was performed using *AtALMT1* as a probe. Tomato *18S* rDNA was used for comparison of loading.

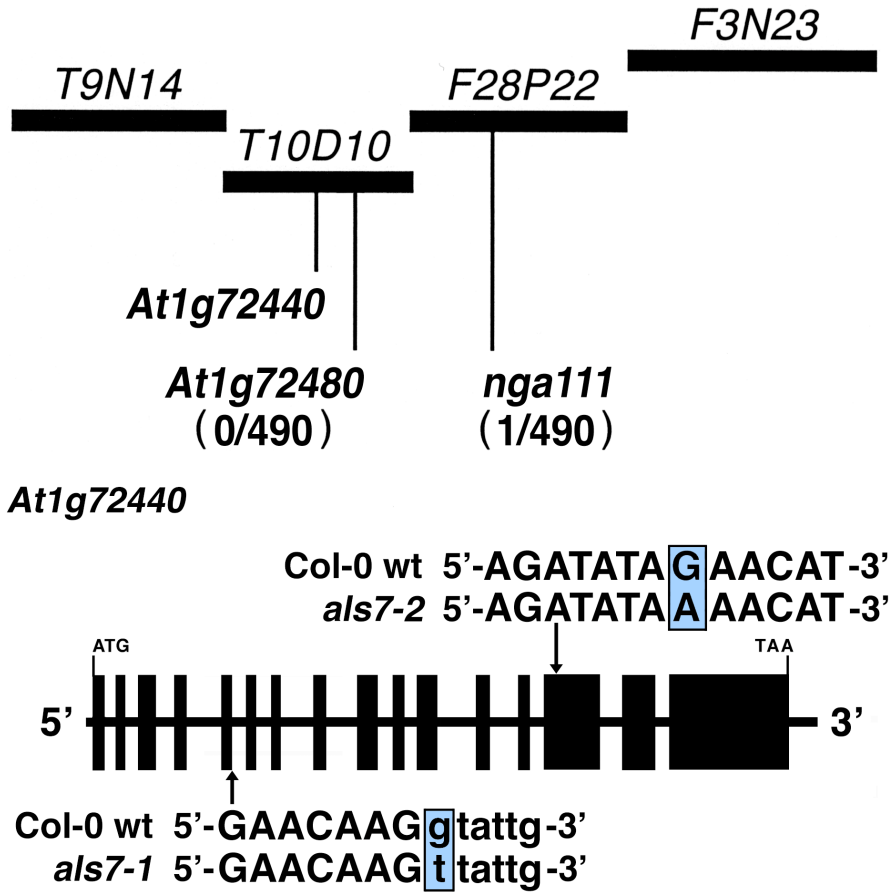

Figure 8. Physical mapping of *als7-1*. The *als7-1* mutation was located on chromosome 1 between markers *At1g72480* and *nga111*. Thick bars represent the order of bacterial artificial chromosomes from chromosome 1 where *als7-1* is located. Mutations in *als7-1* and *als7-2* are indicated on the gene structure of *At1g72440*. The *als7-1* mutation is a G to T base substitution at the splicing junction between exons 5 and 6, while the *als7-2* mutation is a G to A base substitution in exon 14.

window for *als7-1* and probably results in improper mRNA processing for *At1g72440*, ultimately causing reduced Slow Walker2 (SWA2) function.

Since the *als7-1* mutation occurs at a splicing site and all homozygous T-DNA insertion alleles are embryonic lethal, an allele was found by using a TILLING approach to identify additional non-lethal loss-of-function alleles of *swa2*. TILLING gives the advantage of finding mutations in genes that represent single base changes in an allelic manner (Colbert 2001, Henikoff 2004). The *als7-2* mutation is a change from a G to an A in the 14th exon resulting in a change from a glutamic acid to a lysine at position 634 (Figures 8, 9 and 10). Seeds of Col-0 wt, *als7-1* and *als7-2* were grown in a gel-soaked environment in the presence of Al to verify that the *als7-2* phenotype is similar to *als7-1*. As shown in Figure 9, there is no observable difference between *als7-1* and *als7-2* in the absence and presence of Al.

Protein sequence analysis of ALS7/SWA2 utilizing BLAST, Interpro Scan (Zdobnov 2001) and The *Arabidopsis* Information Resource database (www.arabidopsis.org) was performed (Figure 10). The blue highlighted region including the black highlighted region represents an armadillo (ARM)-like fold that binds to large substrates such as nucleic acids and proteins. The black highlighted region is a CCAAT-Box Binding Factor (CBF) domain that has been described to stimulate transcription from the HSP70 promoter. The red lettering at the C-terminus represents the predicted nuclear localization signal. The mutation identified for *als7-2* is depicted as a box within the CBF domain. Utilizing BLAST, it was found that ALS7 has similarity

Figure 9. Analysis of *als7-2*. Col-0, *als7-1* and *als7-2* were grown in gel soaked environment that contained 0mM or 0.75mM $AlCl_3$ (pH 4.2). After 10 days of growth photographs were taken.

ALS7

MSKIKPLSKSSQDLSLLTSDIASFASSIGLASALPSSGFNDT
DFRKPAKSKTQKRKKPKKDQQHKDEDEEGEPKSNIGNEKGKD
FGARKQNKDAPVKQTLQPKPKPGFLSIDDESTGYKKKRFDEF
KSLPKLPLVKASLLSSEWYNDAAEFEEKVFGGRKVAVANKED
FKGVVEKKRELGERLMWQYAEDFATSKGKGGDMKMVISAQKS
GTVADKITAFEIMVGENPIANMRSLDALLGMVTSKVGKRFAF
KGLKALSEILIRLLPDRKLKSLLQRPLNIIPENKDGYSLLLF
WYWEDCLKQRYERFVTALDESSKDMLPELKDKALKTIYFMLT
SKSEQERKLLVSLVNKLGDPQNKSASNADYHLTNLLADHPNM
KAVVIDEVDSFLFRPHLGLRAKYHAVNFLSQIRLSHKGEDPK
VAKRLIDVYFALFKVLTTEANRKQGADDKGAADKKKSNPKDT
KQEVSTDSPIELDSRILSALLTGVNRAFPYVSTDEADDIIES
QTPVLFKLVHSANFNVGVQSLMLLDKISSKNKIVSDRFYRAL
YSKLLLPSAMNSSKAEMFIGLLLRAMKNDINIKRVAAFSKRV
LQVALQQPPQYACGCLFLLSEVLKSRPPLWKMVVQRESVEEE
EDIEHFEDVIEGDDVDPNKKAENDENVVEVDHDGVEKSSRDG
DSSSDDEEALAIRLSDEEDDNASDDSEELIRNETPQLEEVME
VSNDMEKRSQPPMRPSSLPGGYDPRHREPSYCNADRASWWEL
GVLSKHAHPSVATMAGTLLSGTNIVYNGNPLNDLSLTAFLDK
FMEKKPKQNTWHGGSQIEPSKKLDMSNRVIGAEILSLAEGDV
APEDLVFHKFYVNKMTSTKQSKKKKKKKLPEEEAAEELYDVN
DGDGGENYDSDVEFEAGDESDNEEIENMLDDVDDNAVEEEGG
EYDYDDLDGVAGEDDEELVADVSDAEMDTDMDMDLIDDEDDN
NVDDDGTGDGGDDDSDGDDGRSKKKKKEKRKRKSPFASLEEY
KHLIDQDEKEDSKTKRKATSEPTKKKKKKKSKASE

Figure 10. Predicted protein sequence of ALS7. Blue highlighted region is a predicted ARM-like fold, black highlighted region is a predicted CBF domain and red lettering is a nuclear localization signal. *als7-2* mutation is indicated as a white box within the predicted CBF domain.

to the CCAAT/enhancer binding protein zeta from rat, human and mouse with each having 33% identity and 51% similarity to *Arabidopsis* ALS7/SWA2. The human CBF (hCBF) has been described to work in conjunction with proteins such as p53 to control transcription of a growth regulated hsp70 gene in HeLa cells. Since SLOW WALKER2 was proposed to be involved in ribosome biogenesis, yet homologs such as hCBF are directly involved in transcription, it is currently unclear as to what role ALS7/SWA2 plays in the nucleolus.

To confirm that the *als7-1* phenotype is caused by a single base change in *At1g72440*, a functional complementation approach was taken by creating a wild type genomic construct containing the 5' UTR, coding sequence, and 3' UTR of *ALS7* and this was introduced into *als7-1* via *Agrobacterium*-mediated transformation (Figure 11). The functional complementation of *als7-1* with *At1g72440* restored wild type growth in the presence of Al confirming that *als7-1* does represent a mutation within *At1g72440*.

Northern analysis was performed to determine the *ALS7/SWA2* expression pattern in Col-0 wt and *als7-1* and to determine if it is Al-inducible (Figure 12). Col-0 and *als7-1* seedlings were grown in a hydroponic environment for 7 days and then treated with or without $AlCl_3$ for 24 hours. Root tissue was collected for RNA extraction and Northern analysis. There was no change in expression in root tissue when both Col-0 and *als7-1* were exposed to Al (Figure 12, upper panel). Surprisingly, Northern analysis of *als7-1* shows increased transcript levels of *ALS7*. The stability of the transcript in *als7-1* could be increased due to the mutation at the splice site. In addition, tissue from 4-week-old

Figure 11. Functional complementation of *als7-1*. Col-0, *als7-1* and *als7-1* with *ALS7* were grown on a gel soaked environment containing 0.75mM $AlCl_3$ (pH 4.2). After 10 days of growth, photographs were taken.

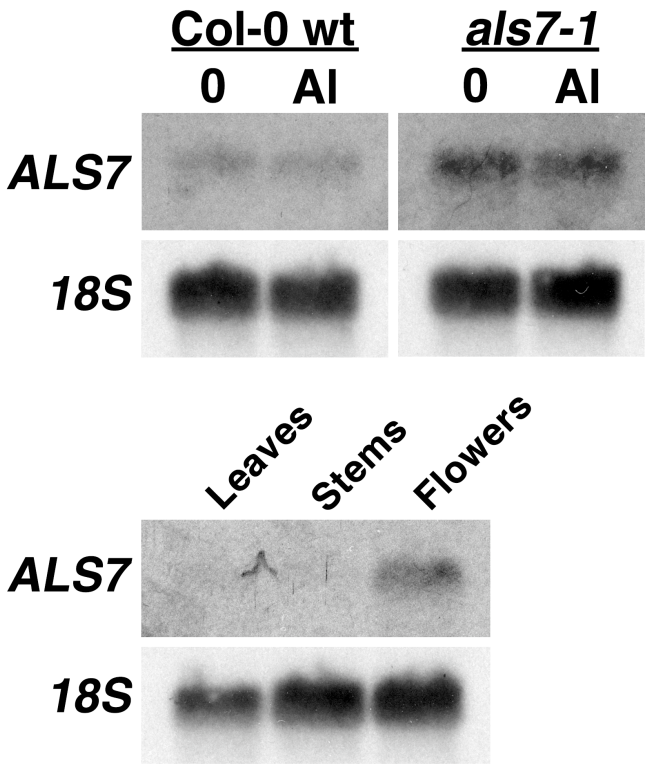

Figure 12. Northern analysis of *ALS7* Al-inducibility and tissue expression. RNA extracted from roots, leaves, stems, flowers from Col-0 wt and *als7-1*. For Northern analysis, 10μg of total RNA for each sample was loaded in each lane. Tomato *18S* rDNA was used for comparison of loading.

Col-0 wt plants were taken from leaves, stems and flowers that were not challenged with $AlCl_3$ to determine the expression pattern in different organs. Leaves and stems showed low levels of expression, while flowers had high levels of expression, which is consistent with its role in female gametophyte development (Figure 12, lower panel).

ALS7:GFP localizes to the nucleolus in developing root tissues

An *ALS7:GFP* fusion was introduced into Col-0 wt to determine the subcellular localization of ALS7. For a factor to be involved in Al tolerance, it is expected that it should be expressed at or near the root tip. The ALS7:GFP fusion accumulates in the cell nucleolus solely in the root tip of primary and lateral roots, which is consistent with the prediction that ALS7 is a factor required for Al tolerance (Figure 13 A, B, D). Transgenic plants were treated with or without $AlCl_3$ to determine if expression pattern is altered upon Al challenge. There was no change in expression pattern with treatment of $AlCl_3$, but the root tip did show altered root architecture due to the Al challenge (Figure 13 B and C). GFP studies also show that *ALS7* expression appears to be coincident with lateral root initiation as indicated by the arrows (Figure 13 E-H). It is possible that ALS7 is required for lateral root initiation and that it is regulating genes that are required for rapidly dividing cells that are found within the root tip.

als7-1 causes altered expression levels of *AtARD3* and *At4g10500*

The strict nucleolar localization pattern of ALS7/SWA2, its accumulation in areas of rapidly dividing cells and its similarity to hCBF suggests that it has a role related to

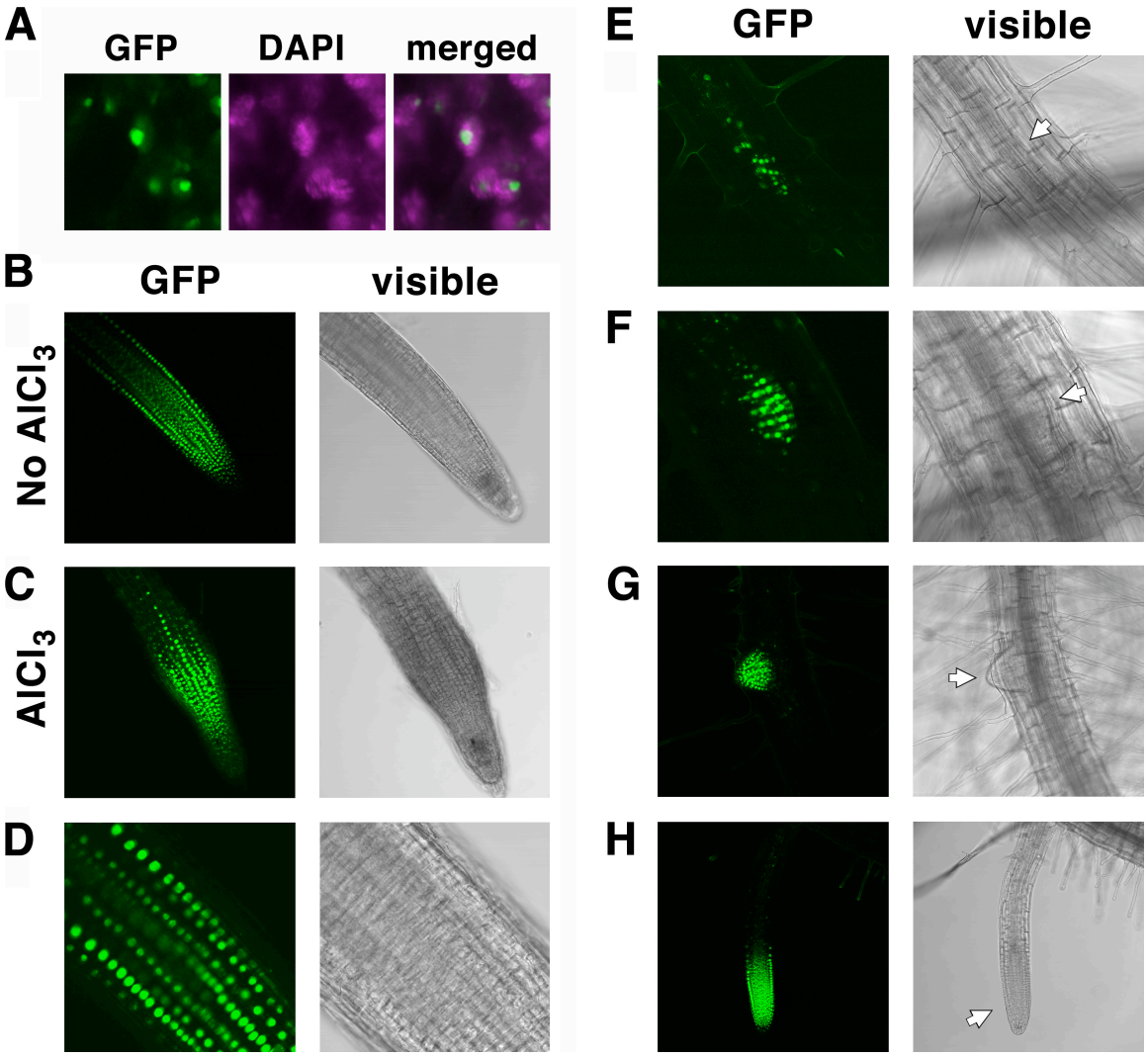

Figure 13. Localization of ALS7:GFP. Transgenic *Arabidopsis* T2 plants expressing an *ALS7:GFP* fusion under the control of *ALS7* promoter. (A) Analysis of subcellular location of ALS7:GFP. Cells were counterstained with DAPI to allow for nuclei visualization. (B-C) Analysis of ALS7:GFP accumulation in roots exposed to 0μM or 25μM $AlCl_3$. (D) Close up view of ALS7:GFP accumulation in (C) the root tip. (E-H) Analysis of ALS7:GFP accumulation in lateral roots at various stages of lateral root initiation.

gene expression. It was of interest to determine which gene(s) have altered expression patterns in *als7-1* compared to Col-0 wt, so seedlings were challenged with $AlCl_3$ and cDNA was synthesized from the root tissue. Affymetrix *Arabidopsis* ATH1 genome array, which represents approximately 24,000 genes, was used to analyze which transcripts have altered expression patterns in the mutant. From the preliminary GeneChip data, a variety of genes involved with oxidative stress were identified as having altered expression patterns. Transcripts from those genes were then analyzed using qPCR to confirm the results observed on the GeneChip and the data were analyzed by the REST2009 software (Pfaffl 2002). Two genes, *At4g10500* and *At2g26400* were found to have reduced expression patterns in *als7-1* compared to Col-0 wt when grown in the presence of $AlCl_3$ (Figure 14). *At4g10500* is an uncharacterized member of the 2OG-Fe(II) oxygenase superfamily of oxidoreductases. These enzymes reduce molecular oxygen at the Fe(II) ion, where it reacts with 2-oxogluterate and a specific substrate and one atom of oxygen is then incorporated in each compound. *At2g26400* is an acireductone dioxygenase (*AtARD3*) that is required for methionine recycling.

Northern analysis was performed to confirm the qPCR results for *At4g10500* and *AtARD3* expression (Figure 15). In Col-0 wt, there is slight induction of *AtARD3* upon $AlCl_3$ challenge. When the expression of *AtARD3* was analyzed in *als7-1* there is similar expression pattern to Col-0 wt in the absence of Al. On the other hand, in *als7-1* there is little to no expression of *AtARD3* upon $AlCl_3$ challenge. This suggests that *AtARD3* expression in the presence of $AlCl_3$ is dependent on *ALS7*. When *At4g10500* expression patterns were observed, there was a slight induction of gene expression in Col-0 wt upon

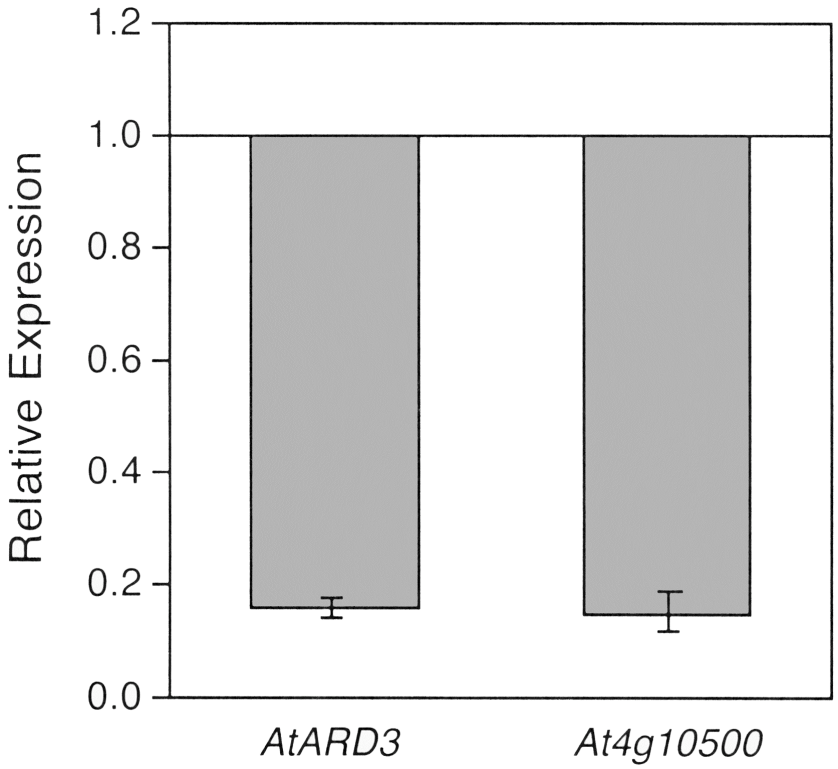

Figure 14. Analysis of expression patterns of *AtARD3* and *At4g10500*. Col-0 wt and *als7-1* were grown hydroponically for 7 days after which they were transferred to nutrient media supplemented with 25μM $AlCl_3$ (pH 4.2) for 24 hours. RNA was extracted from roots and cDNA was synthesized from 1μg of RNA. qPCR analysis was performed using 2μL of a 1:5 dilution of the cDNA. qPCR analysis of *AtARD3* and *At4g10500* comparing expression levels in Col-0 wt to *als7-1*. Relative expression was calculated using REST2009 software.

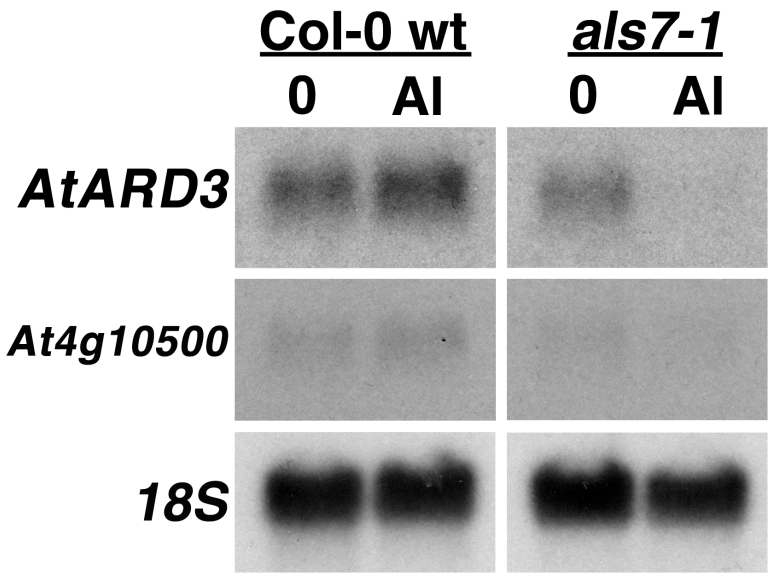

Figure 15. Northern analyses of *AtARD3* and *At4g10500*. Col-0 wt and *als7-1* were grown hydroponically for 7 days after which they were transferred to nutrient media supplemented with 25μM $AlCl_3$ (pH 4.2) for 24 hours. RNA was extracted from roots and 10μg of RNA was loaded for each sample. Tomato *18S* rDNA was used for comparison of loading.

Al challenge. In *als7-1*, there is reduced expression of *At4g10500* and it does not show any Al inducibility. Since both genes display lower expression levels based on GeneChip, qPCR and Northern analysis in *als7-1* plants compared to Col-0 wt, T-DNA knockout mutations of each gene were obtained. When these lines were grown in the absence and presence of $AlCl_3$ there was no observable difference in growth compared to wild type.

Addition of methionine increases root growth in the presence of $AlCl_3$

Acireductone dioxygenases have been previously described to be members of the methionine (Met) cycle (Figure 16). The pathway recycles methylthioadenosine (MTA) to Met. MTA is created after decarboxylated S-adenosylmethionine (AdoMet) is utilized for biosynthetic reactions such as in ethylene, polyamine or phytosiderophore biosyntheses by donating its aminopropyl group. Since ALS7 has been shown to be required for *AtARD3* expression in the presence of Al, it is possible that the roots of *als7-1* plants are unable to recycle MTA back to Met and therefore have reduced levels of available Met in the presence of Al. Since AtARD3 represents a step in Met recycling prior to the production of Met, it was tested what effect addition of exogenous Met would have on growth of *als7-1* roots. Col-0 wt and *als7-1* were both grown in the absence and presence of subtoxic levels of $AlCl_3$ that are highly inhibitory to *als7-1* in a gel soaked environment either with or without supplementation of 10μM Met to test if *als7-1* can be rescued using Met supplementation (Figure 17). *als7-1* displayed increased root growth with Met supplementation in the presence of $AlCl_3$ showing that they could be lacking

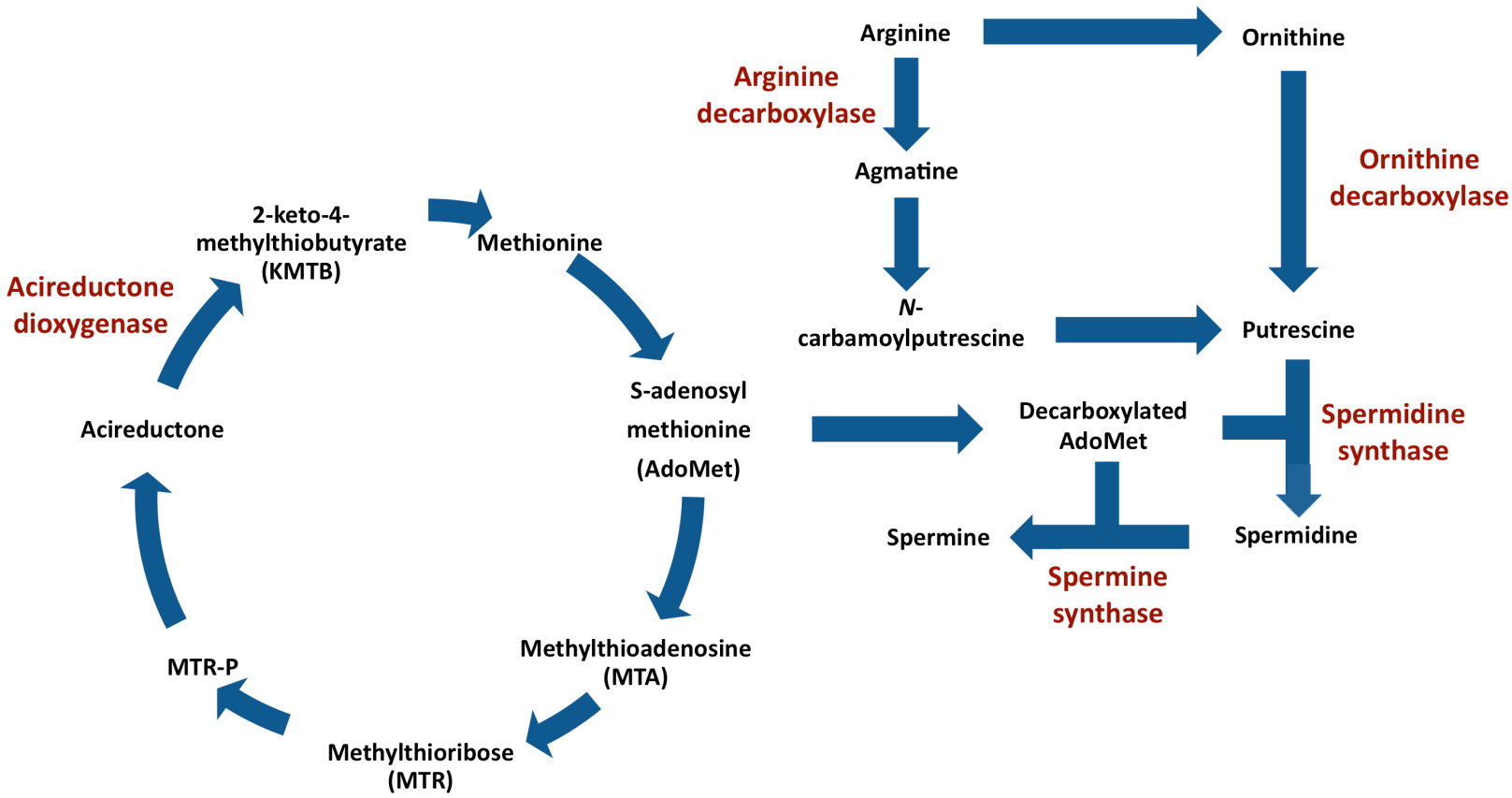

Figure 16. The methionine cycle is linked to polyamine biosynthesis. Met cycling pathway, including polyamine biosynthetic pathway. Enzymes that are mentioned within this report are marked in red.

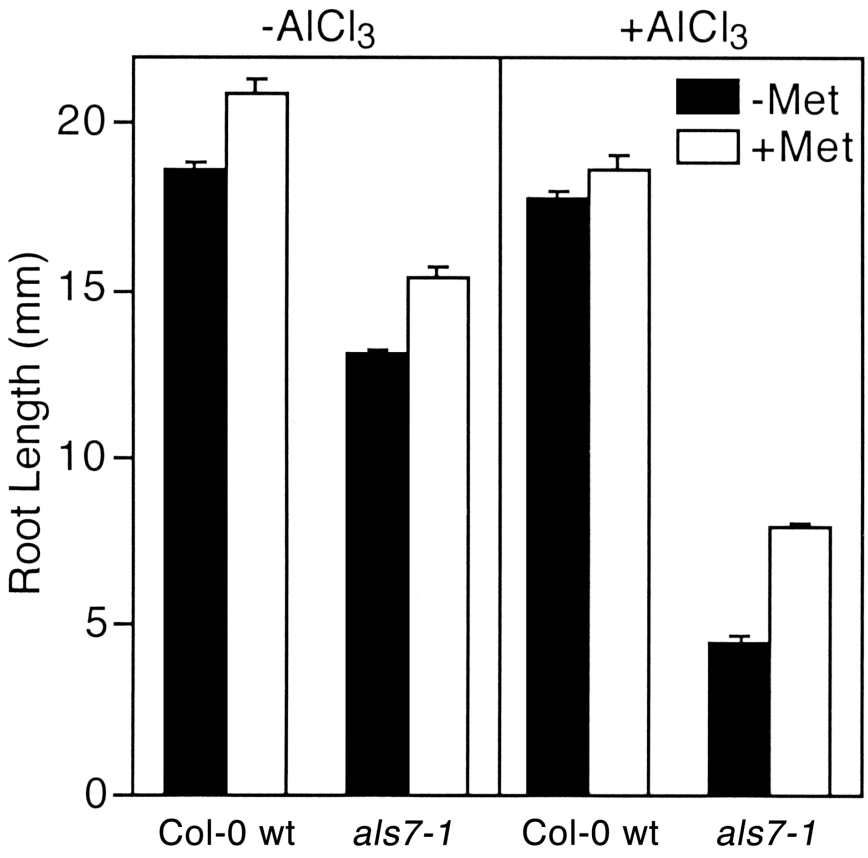

Figure 17. Root growth is increased upon methionine supplementation. Col-0 wt and *als7-1* grown on nutrient media (pH 4.2) for 10 days with 0mM or 0.75mM $AlCl_3$ supplemented with 0μM or 10μM Met. After growth, root lengths were measured, with mean ±SE values determined from 30 roots of each.

free Met in their cells, and possibly that AdoMet deficiency may contribute to the Al hypersensitivity of *als7-1*.

als7-1 Al hypersensitivity is correlated with reduced spermine levels

Given that there was almost a 50% increase in root length with *als7-1* when treated with Met, it was highly likely that there are low levels of biomolecules that require Met in *als7-1*. Met is required for the production of S-adenosylmethionine (AdoMet), which can then be decarboxylated and used to produce the polyamines spermidine and spermine. Polyamines represent a class of small aliphatic polycatonic molecules that are found in almost all organisms that have a multitude of functions including maintenance of DNA structure, promotion of RNA processing, stabilization of membranes, and scavenging reactive oxygen species. Spermine is a common polyamine that is synthesized in a manner directly dependent on available pools of AdoMet (Takahashi 2010). Col-0 wt and *als7-1* were grown in hydroponics supplemented with spermine or spermidine in the presence or absence of $AlCl_3$. It was found that supplementation with these polyamines rescued the Al-dependant root growth inhibition in both Col-0 wt and *als7-1* (Figure 18). When both Col-0 and *als7-1* were treated with 50μM $AlCl_3$ and treated with spermine, there was a dramatic increase in root growth, upwards of a 6-fold increase in root growth for *als7-1* (Figure 19). In contrast, after the addition of 1.5mM difluoromethylornithine (DFMO), an inhibitor of the enzyme ornithine decarboxylase that catalyzes the conversion of ornithine to putrescine, the

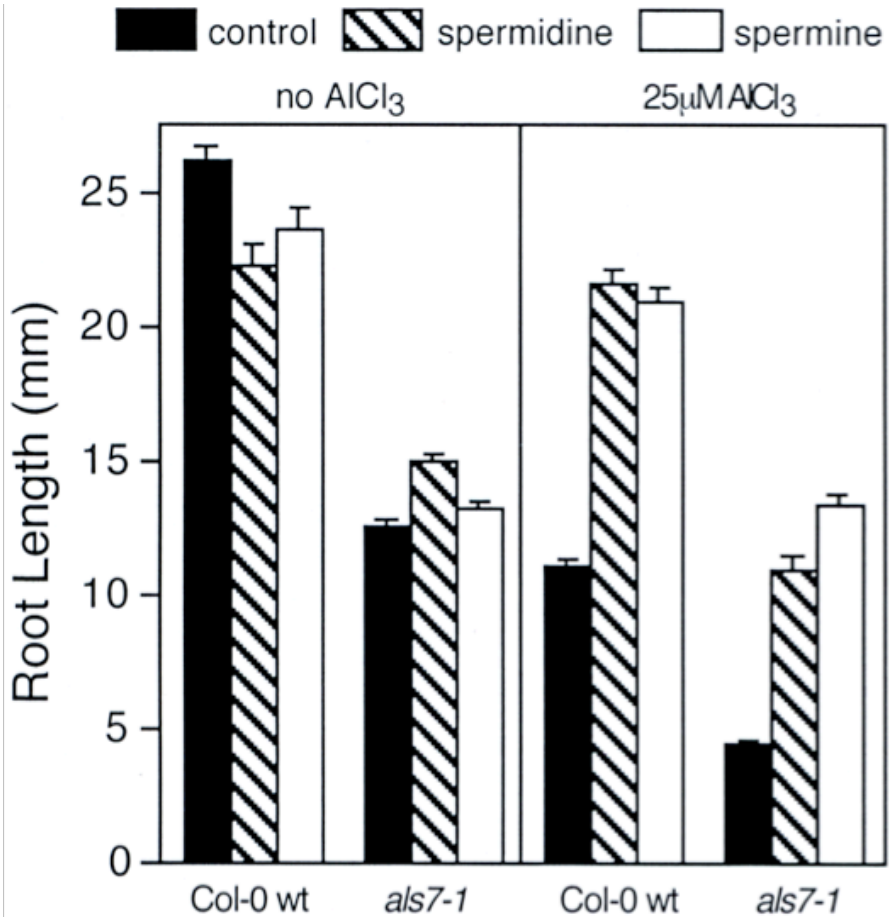

Figure 18. Polyamines increase root length of Col-0 wt and *als7-1* in the presence of $AlCl_3$. Col-0 wt and *als7-1* grown for 7 days in hydroponics with 0μM or 25μM $AlCl_3$ (pH 4.2) and supplemented with 0μM or 25μM spermidine or spermine. After growth, root lengths were measured, with mean ±SE values determined from 30 roots of each.

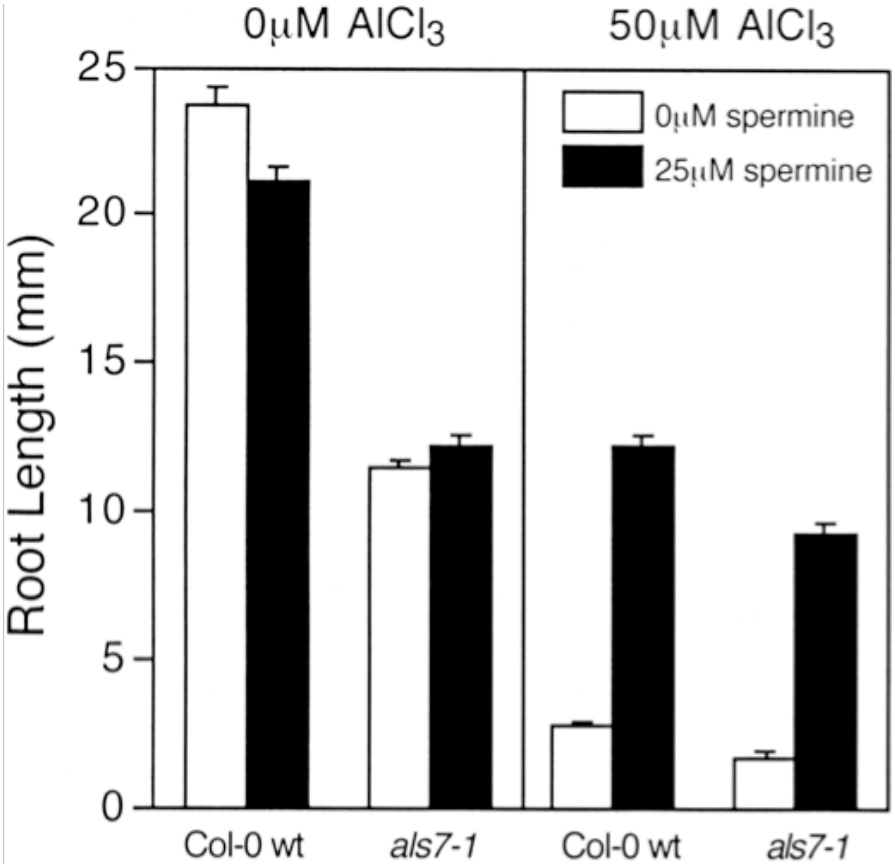

Figure 19. Spermine increases root length of Col-0 wt and *als7-1* in the presence of high levels of $AlCl_3$. Col-0 wt and *als7-1* grown for 7 days in hydroponics with 0μM or 50μM $AlCl_3$ supplemented with 0μM or 25μM spermine. After growth, root lengths were measured, with mean ±SE values determined from 30 roots of each.

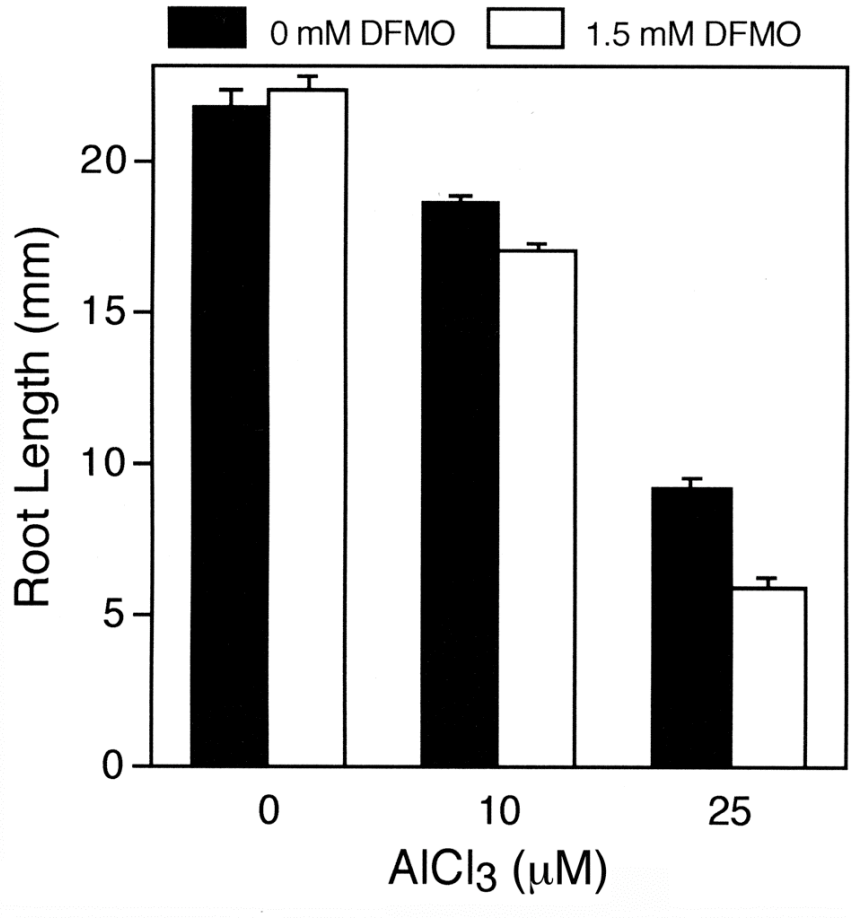

Figure 20. The inhibitor of ornithine decarboxylase, DFMO reduces root growth in the presence of Al. Seedlings of Col-0 wt were grown either in the absence or presence of 1.5mM DFMO in a hydroponic environment supplemented with increasing concentrations of $AlCl_3$ (pH 4.2). After 7 days of growth, root length was measured for all treatments, with mean ±SE values determined from 30 roots of each.

precursor to polyamines spermidine and spermine, resulted in a measureable decrease in root length in Col-0 wt roots in the presence of Al (Figure 20).

Since polyamines promote root growth in the presence of Al, it was important to determine if polyamines are playing a role in Al tolerance or resistance. Al tolerance would indicate that there would be increased capability to cope with internalized Al, while resistance would indicate there is enhanced exclusion of Al. Col-0 wt seedlings were grown with or without 25μM spermine for six days, and treated for 48 hours in the presence of 0 or 25μM $AlCl_3$. Al accumulation was measured using ICP-OES in Col-0 wt plants. From this analysis, there was a significant reduction in Al accumulation in the roots that were treated with spermine (Figure 21). This indicates that spermine enhances the plant's resistance to Al.

To further confirm that polyamines are playing a role in Al resistance mechanisms, the total spermine content of Col-0 wt and *als7-1* was analyzed (Figure 22). From this analysis, *als7-1* roots have a significant reduction in spermine content compared to Col-0 wt. Although there is no increase in spermine content in Col-0 wt upon Al treatment, the reduction of spermine in *als7-1* indicates that this polyamine is essential for proper growth of *als7-1*. In addition to this finding, *als7-1* roots have an increase in Al accumulation that is correlated with reduced spermine content. From this, it is likely that endogenous polyamines are required to limit the amount of Al that is internalized by competing for binding to extra- and intracellular anionic sites at the root tip.

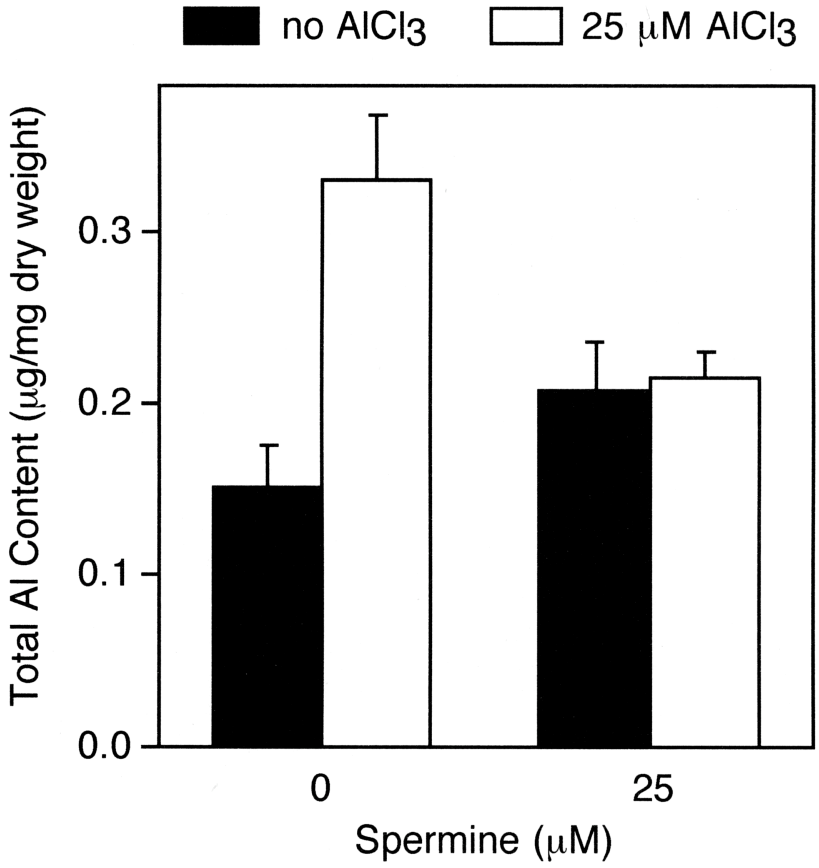

Figure 21. Treatment with spermine reduces total Al content in Col-0 wt roots. Col-0 wt was grown in hydroponics in the absence of Al, supplemented with 0μM or 25μM spermine. After six days they were transferred to nutrient media supplemented with 0μM or 25μM $AlCl_3$ (pH 4.2), with 0μM or 25μM spermine for 48 hours. Root tissue was harvested, dried, weighed, ashed in nitric acid and analyzed for total Al content using ICP-OES.

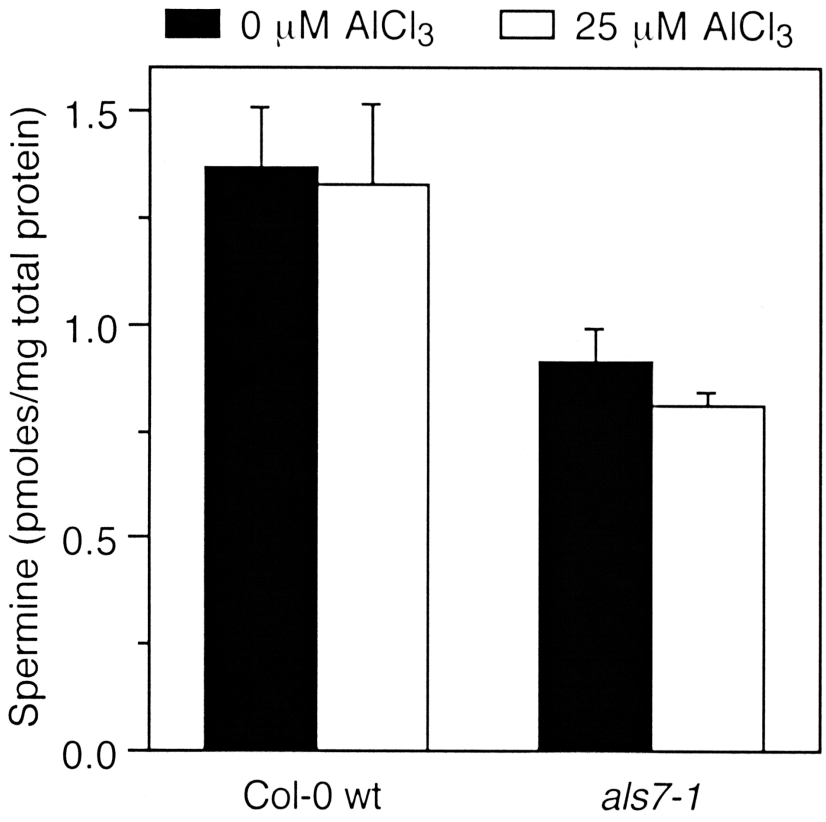

Figure 22. *als7-1* roots have reduced spermine content. Col-0 wt and *als7-1* were grown for 10 days in hydroponics supplemented with 0μM or 25μM $AlCl_3$. After growth, roots were harvested, ground and digested in 0.2N percholoric acid. The supernatant was used for HPLC analysis for spermine levels. The pellet was neutralized and then used to determine total protein content.

CHAPTER SIX

Identification and Characterization of *alt2-1*

alt2-1;als3-1 is tolerant to $AlCl_3$

Previously, seeds of *Arabidopsis als3-1* were treated with EMS. M_2 seedlings were grown on a gel soaked environment with levels of $AlCl_3$ that are highly inhibitory to *als3-1* to identify mutants that suppress the *als3-1* phenotype. From this screen, one was found to be a strong recessive suppressor mutation and represents a second locus that confers increased Al tolerance (*alt2-1)*. In order to determine how well *alt2-1* grows in the presence $AlCl_3$, Col-0 wt, *als3-1*, and *alt2-1*;*als3-1* were grown in a gel soaked environment for 7 days on increasing concentrations of $AlCl_3$. It was found that *alt2-1* not only completely suppresses the *als3-1* phenotype, but also provides greater than wild type growth in concentrations of Al that inhibit wt root growth (Figure 23A). Visually after 7 days of growth, roots of *alt2-1;als3-1* have a drastic increase on growth on 0.75mM $AlCl_3$, and greater than wild type growth on 1.5mM $AlCl_3$ (Figure 23B).

alt2-1;als3-1 has increased stress response to $AlCl_3$

To determine if the phenotype caused by *alt2-1* mutation was due to altered $AlCl_3$ uptake or exclusion mechanisms, several physiological studies were done similar to the studies done for *als7-1*. The roots of Col-0 wt, *als3-1* and *alt2-1;als3-1* were stained for callose in the presence of $AlCl_3$. There was no observable difference in the staining

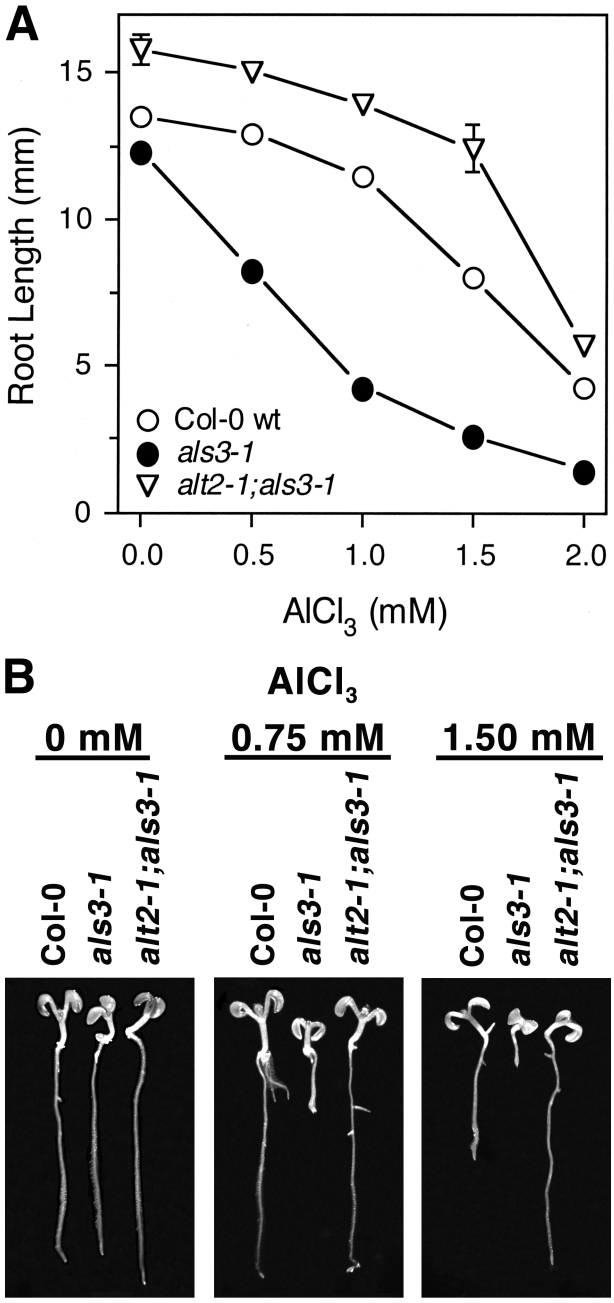

Figure 23. Growth of *alt2-1;als3-1* in an Al toxic environment. (A) Col-0, *als3-1* and *alt2-1;als3-1* were grown for seven days on nutrient media (pH 4.2) supplemented with increasing levels of $AlCl_3$, ranging from 0.5mM to 2.0mM. Following growth, root lengths were measured, with mean ±SE values determined from 30 roots of each.

patterns of all three lines (Figure 24).

There are several transporters that have been described that transport Al, and as seen in the *als7-1* project, anions and cations such as polyamines can alter Al accumulation. Al accumulation was measured using ICP-OES in Col-0, *als3-1* and *alt2-1;als3-1* to determine if Al exclusion was impacted. From this analysis it was found that there was no significant difference in Al accumulation of *alt2-1;als3-1* compared to *als3-1* and Col-0 wt (Figure 25).

To confirm that the mutation in *alt2-1* is not affecting Al-inducible genes, the transcript of *AtALMT1* was measured. Northern analysis was performed using root tissue from Col-0 wt, *als3-1* and *alt2-1;als3-1* grown for 7 days and then treated for 24h in the absence or presence of $AlCl_3$. The *AtALMT1* transcript was increased in all three lines after $AlCl_3$ treatment, but showed the greatest increase with *alt2-1;als3-1* (Figure 26). This indicates that *alt2-1;als3-1* plants are still responding to internalized Al and the mutation is not affecting exclusion mechanisms. These sets of data suggest that *alt2-1;als3-1* plants are responding normally to $AlCl_3$ stress, but show increased expression of Al-stress related genes. These data indicate that *alt2-1* has increased Al tolerance since Al is entering the tissue and exclusion is not affected.

The *alt2-1* mutation results in a single amino acid change in a WD40 protein

A mapped based cloning approach was used to identify the *alt2-1* mutation. In order to create a mapping population, a T-DNA insertion mutation of *als3* in La-0 (*als3-4)* was used to cross to *alt2-1*. The F_2 progeny were grown on 0.75mM $AlCl_3$ in a gel

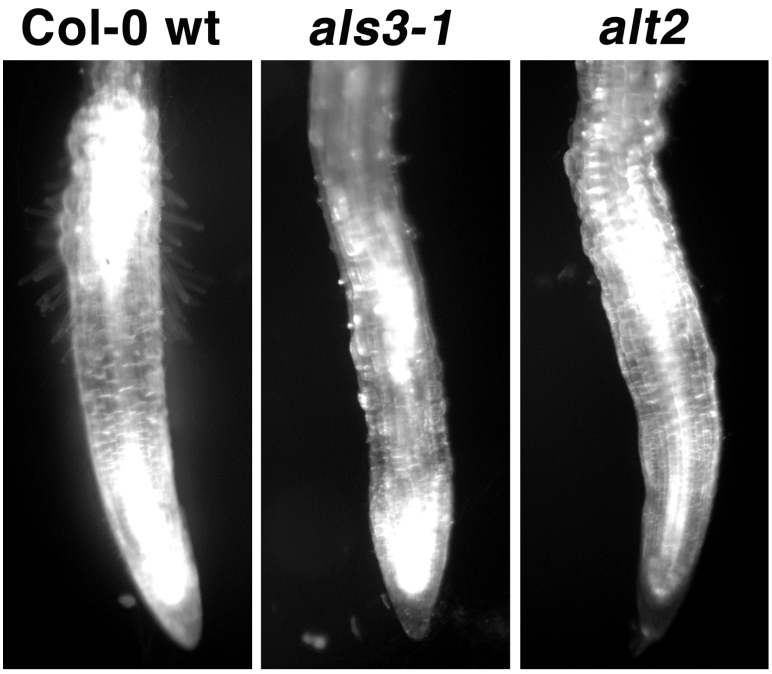

Figure 24. Callose accumulation in *alt2-1;als3-1* in the presence of AlCl3. Col-0 wt, *als3-1* and *alt2-1;als3-1* were grown hydroponically for 7 days after which they were transferred to nutrient media supplemented with 25μM $AlCl_3$ (pH 4.2) for 24 hours. Seedlings were fixed and stained with aniline blue. Callose was visualized using an epifluorescent-dissecting microscope.

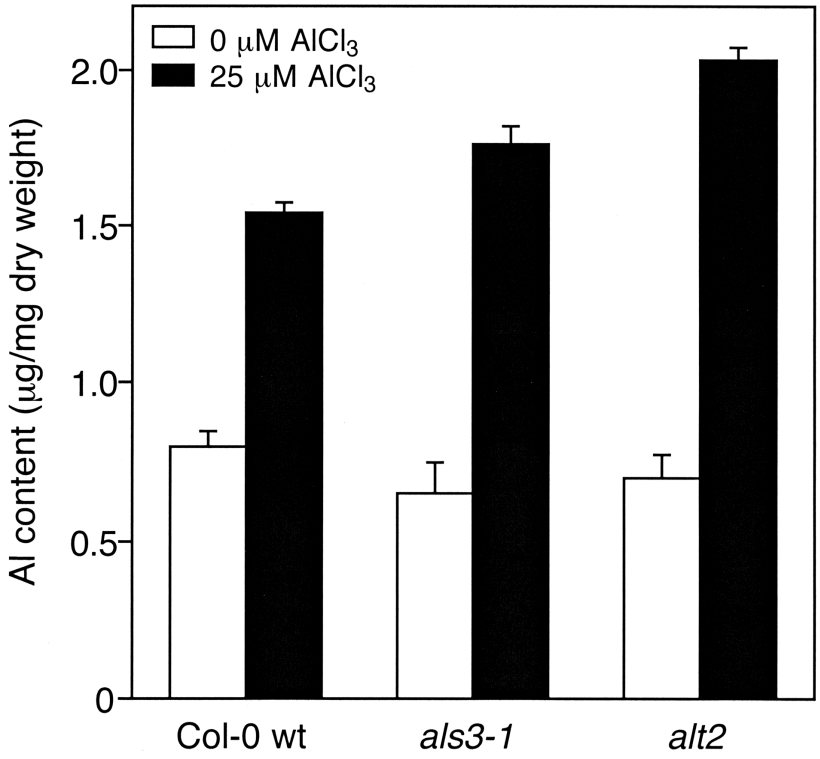

Figure 25. Total Al content in *alt2-1;als3-1* roots following Al treatment. Col-0 wt, *als3-1*, and *alt2-1;als3-1* were grown for 6 days in hydroponics after which they were transferred to nutrient media supplemented with 0μM or 25μM $AlCl_3$ (pH 4.2) for 48 hours. Root tissue was harvested, dried, weighed, ashed in nitric acid and analyzed for total Al content using ICP-OES.

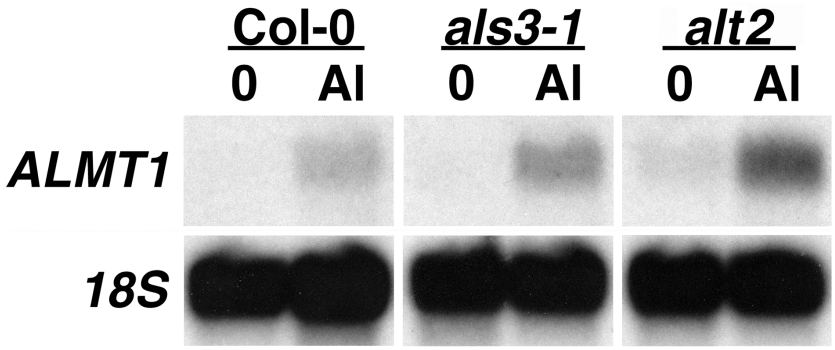

Figure 26. Al-dependent induction of *AtALMT1* in *alt2-1;als3-1*. Col-0 wt, *als3-1* and *alt2-1* were grown hydroponically for 7 days after which they were transferred to nutrient media supplemented with 0μM or 25μM $AlCl_3$ (pH 4.2) for 24 hours. RNA extracted from roots and 10μg of total RNA was loaded in each lane. Northern analysis was performed using *AtALMT1* as a probe. Tomato *18S* rDNA was used for comparison of loading.

soaked environment and screened for seedlings that displayed the *alt2* phenotype since *alt2-1* is a recessive mutation. By utilizing map-based cloning, the *alt2-1* mutation was localized to the bottom of chromosome 4, just upstream of the CAPS marker PRNA. Potential genes that included those that are expressed in the root, implicated in DNA damage response pathways or the response to toxic agents were sequenced. Each candidate gene was amplified by PCR from *alt2-1;als3-1* genomic DNA, sequenced and compared to the published Col-0 wt sequence. The *alt2-1* mutation was identified as a single base change from a G to an A in the 12th exon in a previously identified WD40 repeat protein *At4g29860* (Figure 27). Utilizing BLAST it was found that *ALT2* is a single copy gene in *Arabidopsis* and there are homologs in many plant species such as rice, maize, barley, grape vine and castor oil plant that also exist as single copies.

Since homozygous T-DNA insertion alleles are embryonic lethal, a TILLING approach to identify additional non-lethal loss-of-function alleles of *alt2*. The *alt2-2* mutation was a change from a G to an A in the 7th exon (Figure 27). Seeds of Col-0 wt, *alt2-1* and *alt2-2* were grown in a gel-soaked environment in the presence of Al to verify that the *alt2-2* phenotype is similar to *alt2-1*. As shown in Figure 28, there is no observable difference between *alt2-1* and *alt2-2* in the absence and presence of Al.

Protein sequence analysis of ALT2 utilizing BLAST, Interpro Scan (Zdobnov 2001) and The *Arabidopsis* Information Resource database was performed (Figure 29).

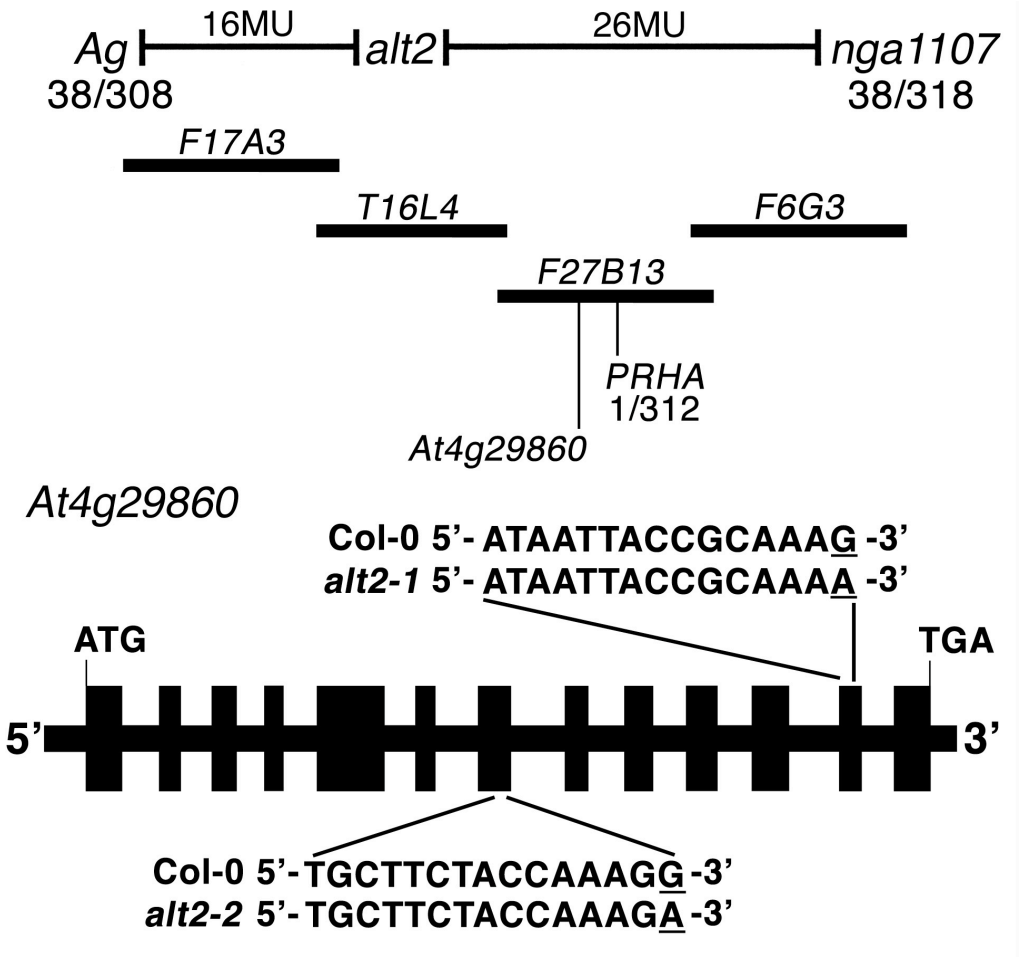

Figure 27. Physical mapping of *alt2-1*. The *alt2-1* mutation was located on chromosome 4 between markers *Ag* and *PRHA*. Thick bars represent the order of bacterial artificial chromosomes from chromosome 4 where *alt2-1* is located. Mutations in *alt2-1* and *alt2-2* are indicated on the gene structure of *At4g29860*. The *alt2-1* mutation is a G to A base substitution within exon 12, while the *alt2-2* mutation is a G to A base substitution in exon 7.

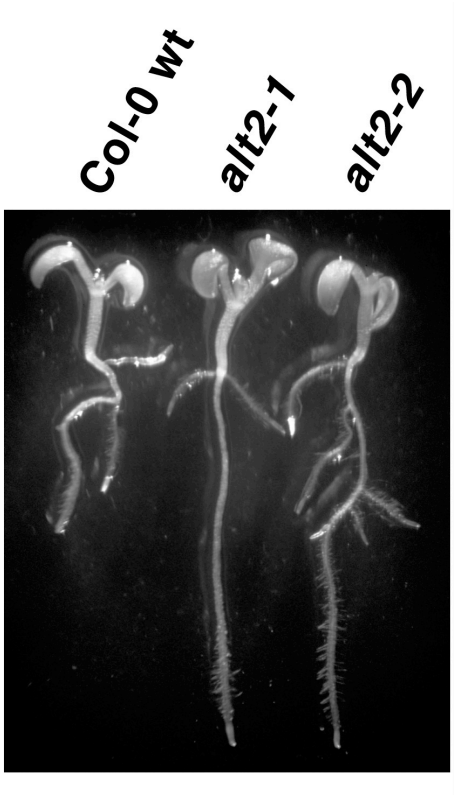

Figure 28. Analysis of *alt2-2*. Col-0 wt, *alt2-1* and *alt2-2* were grown in a gel soaked environment containing 0 and 1.5mM $AlCl_3$ (pH 4.2) for 7 days. After growth, photographs of representatives of the population of each line were taken.

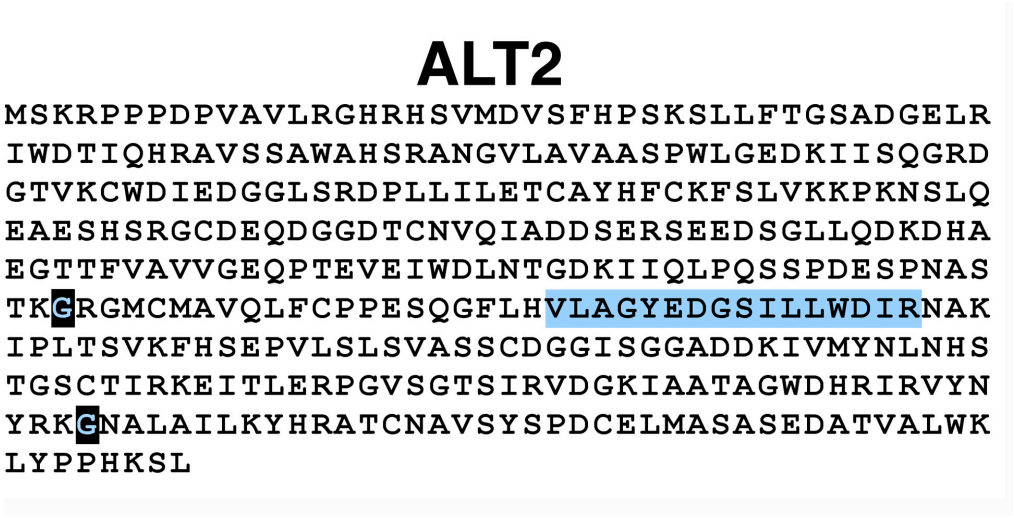

Figure 29. Predicted protein sequence of ALT2. The entire ALT2 protein is a WD40 repeat protein. The blue highlighted region represents the predicted 16 amino acid DWD domain (DDB1 binding WD40). The *alt2-1* and *alt2-2* mutations are depicted as black boxes. The *alt2-1* mutation is closer to the C-terminal end of the protein, and the *alt2-2* mutation is just upstream of the DWD domain.

ALT2 is a member of a family of proteins called WD40 repeat proteins that contain a DDB1 binding WD40 (DWD) domain. The blue highlighted region is a putative 16 amino acid conserved DWD domain with four highly conserved residues Asp-7 (or Glu), Trp-13 (or Tyr), Asp-14 (or Glu), and Arg-16 (or Lys) (Lee 2008). Utilizing Interpro Scan, ALT2 contains 5 predicted WD40 domains, which is in contrast to the initial characterization of ALT2 performed by Yamagishi, et al in 2005, who predicted that ALT2 contained 7 WD40 domains. ALT2 also shows limited similarity to other DWD proteins such as AtCSA. The *alt2-1* mutation results in replacement of a glycine with an arginine at amino acid residue 340, which occurs between the 6^{th} and 7^{th} WD40 repeat of ALT2. The *alt2-2* mutation results in a replacement of a glycine with a glutamic acid at amino acid residue 213, which occurs at the beginning of the 4^{th} WD40 repeat of ALT2 and upstream of the DWD domain. Both of these mutations cause an introduction of a charged large side chain in the place of a glycine.

To determine if the *alt2-1* phenotype is due to this mutation, a functional complementation approach was utilized. A wild type genomic construct of *At4g29860*, including 1 Kb of the promoter region, the 5'-UTR, all exons and introns and the 3'-UTR was introduced into *alt2-1* with *als3-1* in its background. The functional complementation was grown in the presence of 0.75mM $AlCl_3$ and resulted in full restoration of the *als3-1* phenotype confirming that the *alt2-1* phenotype is due to a mutation in *At4g29860* (Figure 30).

Northern analysis was performed to determine the *ALT2* expression pattern in Col-0 wt and *alt2-1* and to determine if it is Al-inducible (Figure 31). Col-0 and *alt2-1*

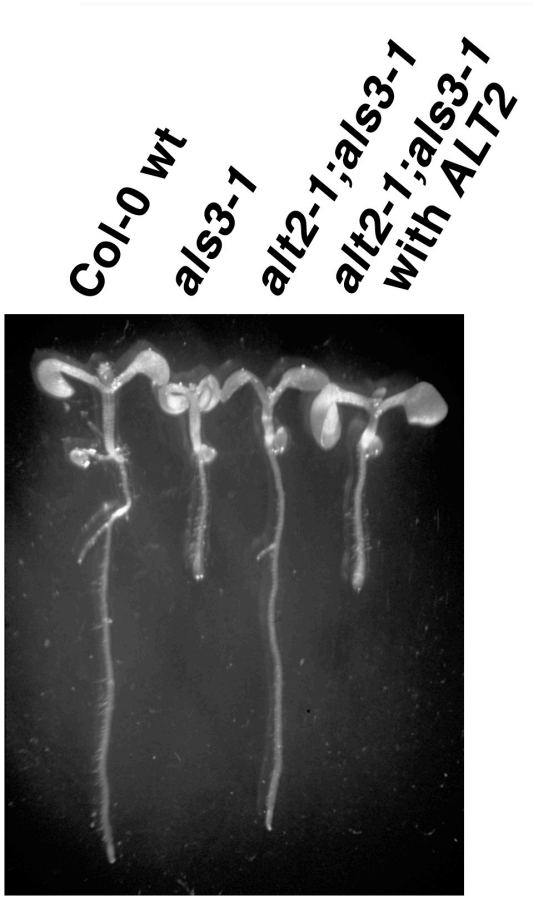

Figure 30. Functional complementation of *alt2-1*. Col-0 wt, *als3-1*, *alt2-1;als3-1* and *alt2-1;als3-1* with *ALT2* were grown in a gel soaked environment containing 0 and 0.75mM $AlCl_3$ (pH 4.2) for 7 days. After growth, photographs of representatives of the population of each line were taken.

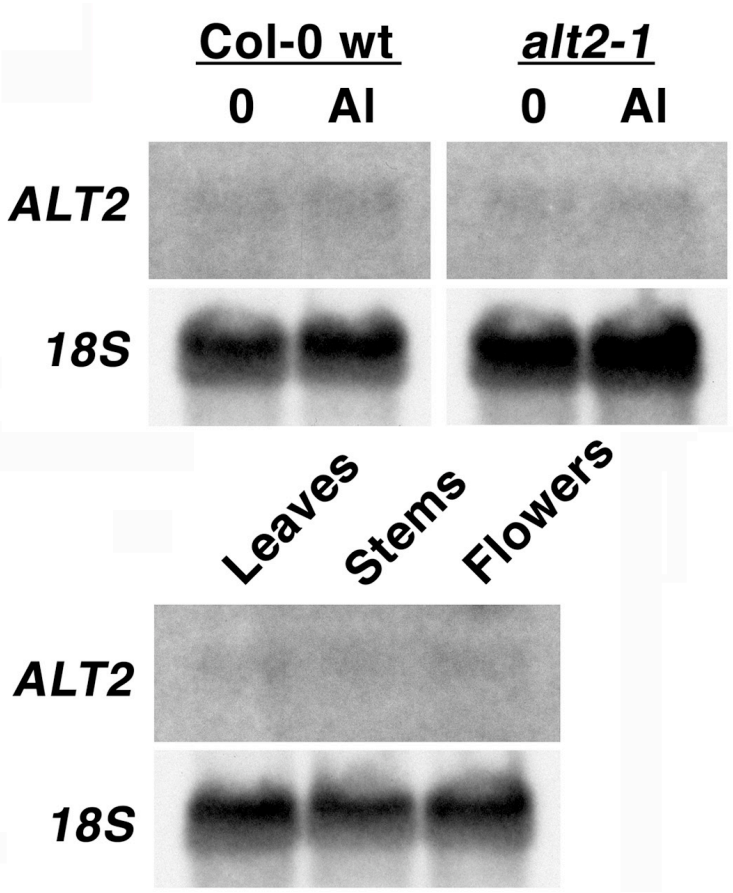

Figure 31. Northern analysis of *ALT2* Al-inducibility and tissue expression. RNA was extracted form leaves, stems, and flowers from Col-0 wt and roots from both Col-0 wt and *alt2-1*. For Northern analysis, 10µg of total RNA for each sample was loaded in each lane. The *ALT2* cDNA was used as a probe. Tomato *18S* rDNA was used for comparison of loading.

seedlings were grown in a hydroponic environment for 7 days and then treated with or without $AlCl_3$ for 24 hours. Root tissue was collected for RNA extraction and Northern analysis. *ALT2* is a weakly transcribed transcript that does not change in root tissue when both Col-0 and *alt2-1* were exposed to Al (Figure 12, upper panel). Northern analysis of *alt2-1* does not show altered transcript levels of *ALT2*, which is not surprising since the base pair change in *alt2-1* does not alter a splice site or result in a stop codon. In addition, tissue from 4-week-old Col-0 wt plants was taken from leaves, stems and flowers that were not challenged with $AlCl_3$ to determine the expression pattern in different organs. Leaves, stems and flowers all displayed low transcript levels of *ALT2*, similar to the levels in the roots.

ALT2:GFP fusion changes localization upon Al treatment

An *ALT2:GFP* fusion was introduced into *alt2-1;als3-1* to determine the subcellular localization of ALT2. Initial attempts were made to introduce the *ALT2:GFP* fusion into Col-0 wt, but due to the low transcript levels, the protein was also weakly expressed so it was difficult to screen for transformants that had detectable levels of ALT2:GFP. Instead a functional complementation approach was taken to identify transgenic GFP lines. Any transgenic lines in the *alt2-1;als3-1* background that were grown in the presence of 0.75mM $AlCl_3$ that displayed the *als3-1* phenotype were chosen for imaging, since they represent lines that have functioning ALT2:GFP. In the absence of Al, the ALT2:GFP fusion accumulates in the cell cytoplasm throughout the root

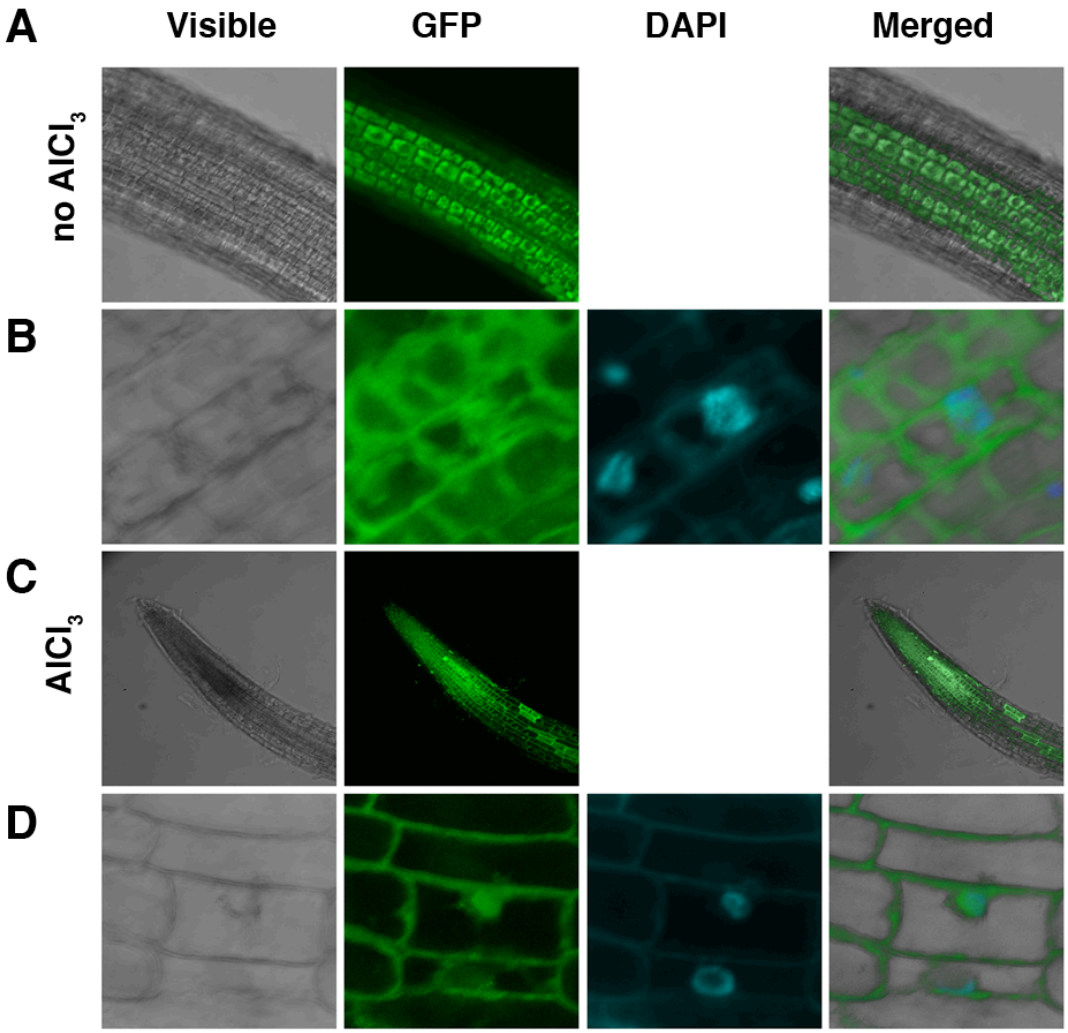

Figure 32. Localization of ALT2:GFP. Transgenic *Arabidopsis* T2 *alt2-1;als3-1* plants expressing an *ALT2:GFP* fusion under the control of *ALT2* promoter. (A) Analysis of tissue location of ALT2:GFP in the absence of Al. (B) Analysis of ALT2:GFP subcellular localization in the absence of Al. Cells were counterstained with DAPI to allow for nuclei visualization. (C) Analysis of tissue localization of ALT2:GFP after treatment for 48 hours with 25µM $AlCl_3$. (D) Analysis of ALT2:GFP subcellular localization after treatment for 48 hours with 25µM $AlCl_3$. Cells were counterstained with DAPI to allow for nuclei visualization.

(Figure 32 A and B). The transgenic GFP plants were treated with $AlCl_3$ to determine if expression pattern was altered upon Al challenge. Upon Al challenge, the ALT2:GFP fusion changed localization from the cytoplasm to the nucleus (Figure 32 C and D). This suggests that ALT2 is required for Al-stress response and it is dependent on its localization to the nucleus where it could act in response to DNA damage.

Growth analyses of *alt2-1* and *alt1-1*

Since *alt2-1* contains *alt3-1* in its background, it was important to determine if the Al hypersensitive mutant *als3-1* adds any deleterious effects to the Al tolerance of *alt2-1*. The *als3-1* mutation was crossed out of the *alt2-1;als3-1* line by crossing it with Col-wt. The *alt2-1* line was tested for aluminum tolerance by growth on 0 and 1.5mM $AlC1_3$ gel soaked plates. The *alt2-1* line was found to be very tolerant to high levels of Al, barely being inhibited by 1.5mM $AlCl_3$, while Col-0 was severely inhibited (Figure 33). The growth of *alt2-1* was greater than the *alt2-1;als3-1* double mutant, suggesting that the presence of the *als3-1* mutation is harmful, even in an Al tolerant line.

It was previously described that *alt1-1* was extremely tolerant to Al, so it was of interest to determine if an *alt1-1;alt2-1* double mutant would be able to confer even greater Al tolerance. The *alt2-1* line was crossed with *alt1-1*, F_2 seeds were obtained and screened for plants homozygous for both mutations with wild type *ALS3*. Col-0 wt, *alt1-1*, *alt2-1* and *alt1-1;alt2-1* were grown in the presence of 0 and 1.25mM $AlCl_3$ in a gel soaked environment. The double mutation had no increased tolerance to Al compared to the single mutations *alt1-1* and *alt2-1*. This indicates that both ALT1 (AtATR) and

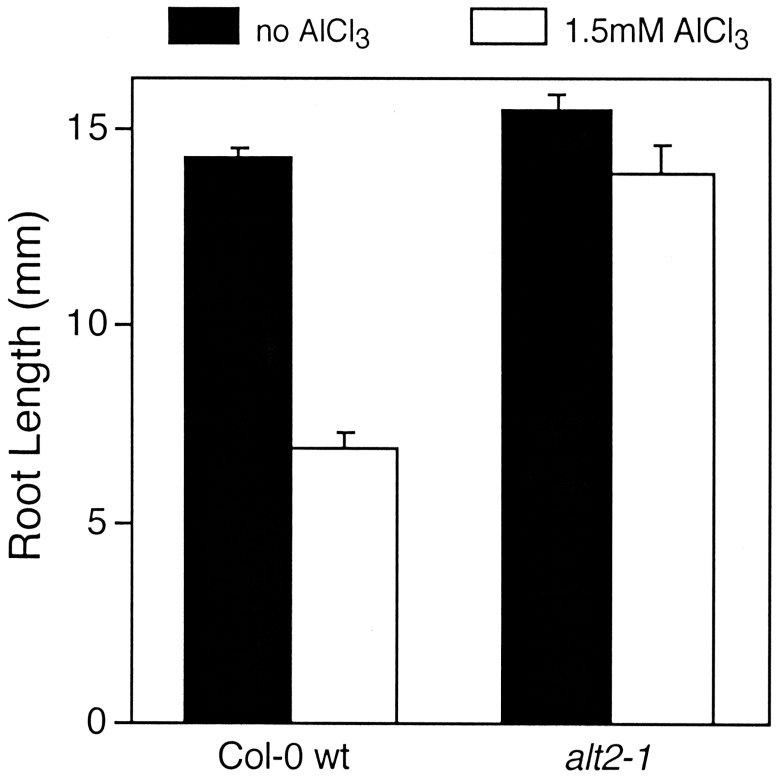

Figure 33. Growth of *alt2-1* without *als3-1*. Col-0 and *alt2-1* were grown on a gel soaked environment with 0 or 1.5mM $AlCl_3$ (pH 4.2). After 7 days of growth, root length was measured, with mean ±SE values determined from 30 roots of each.

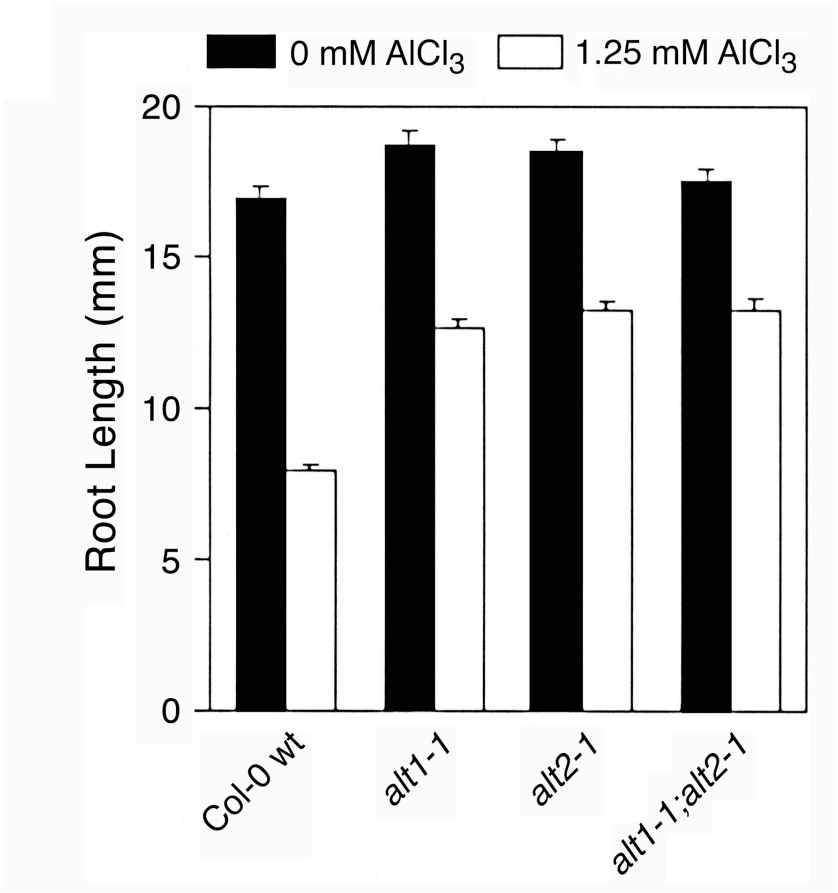

Figure 34. *alt1-1;alt2-1* double mutation does not have enhanced Al tolerance. Col-0, *alt1-1*, *alt2-1*, and *alt1-1;alt2-1* were grown on a gel soaked environment with 0 or 1.25mM $AlCl_3$ (pH 4.2). After 7 days of growth, root length was measured, with mean ±SE values determined from 30 roots of each.

ALT2 are participating in the same pathway that is required for Al-dependent root growth inhibition. Since AtATR has been implicated in the DNA damage response pathway in *Arabidopsis* and other organisms, it is likely that ALT2 is also playing a role in the same DNA damage response pathway.

ALT2's role as a DWD protein

Based on homology, ALT2 is predicted to be a member of a family of 85 WD40 proteins that contain a DWD domain in *Arabidopsis*. The DWD proteins in *Arabidopsis* were further divided into five subgroups in a phylogenetic tree (Lee 2008). ALT2 is found in the A1 subgroup of the *Arabidopsis* DWD proteins, the same subgroup that contains *AtCSA*, a factor required for UV-B tolerance and genome integrity and also *DDB2*, a factor that was originally identified as a factor that interacts with *DDB1*, that is required for DNA repair in response to UV stress. The DWD proteins are also classified based on the location of the WD40 repeats and other motifs they may contain. ALT2 is a type D DWD protein, whose proteins are solely the WD40 repeats. AtCSA is also a type D DWD protein, while DDB2 is a type B DWD protein, whose WD40 repeats are in the middle of the protein, with undefined C and N terminal domains.

It was of interest to determine if a knockout in AtCSA results in altered Al response due to AtCSA's limited sequence similarity to ALT2, as well as being in the same group of the phylogenetic tree and same type as ALT2. Col-0 wt, *alt2-1* and *atcsa-1,1* were grown on increasing concentrations of Al (Figure 35). *atcsa-1,1* had no

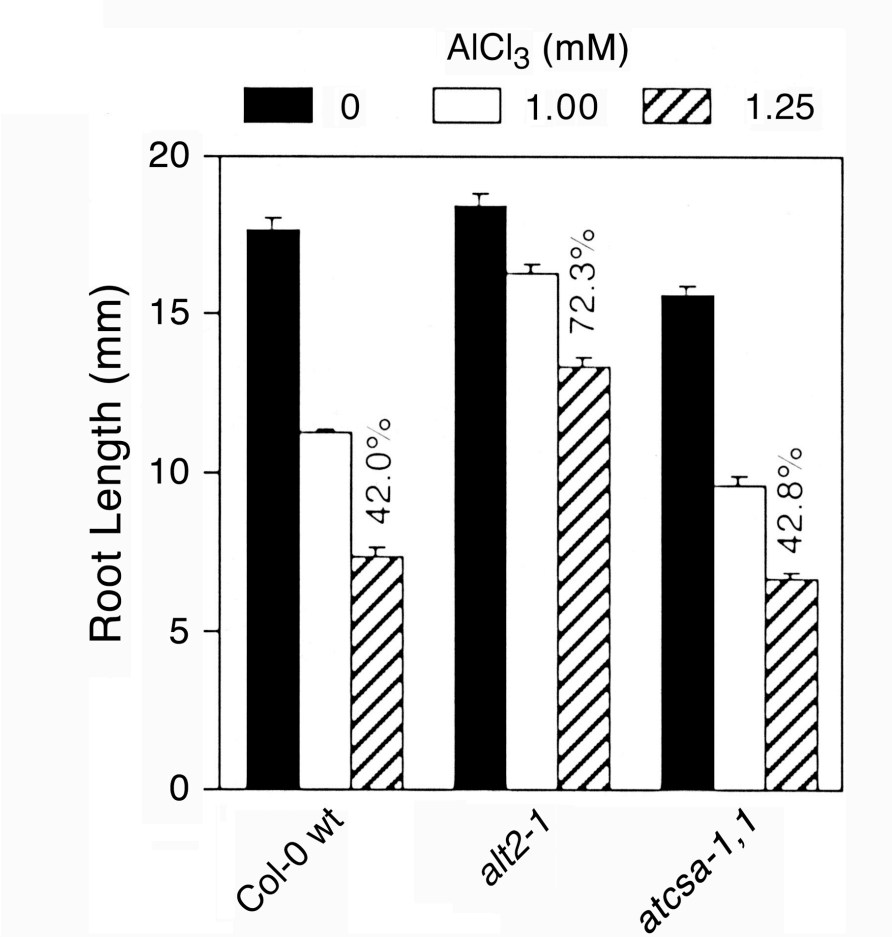

Figure 35. *AtCSA* does not have an altered growth response to Al. Col-0, *alt2-1*, and *atcsa-1,1* were grown on a gel soaked environment with 0mM, 1.0mM or 1.5mM $AlCl_3$ (pH 4.2). After 7 days of growth, root lengths were measured, with mean ±SE values determined from 30 roots of each.

difference in Al tolerance or sensitivity and grew just as well as wild type on all concentrations of Al tested.

As a member of the DWD proteins, ALT2 should interact with DDB1. In *Arabidopsis* there are two highly similar copies of DDB1, DDB1A and DDB1B. T-DNA insertion knockouts of DDB1A and DDB1B were grown on increasing concentrations of Al. DDB1A grew similar to wild type on increasing concentrations of Al, while DDB1B displayed slight Al tolerance (Figure 36A). In addition it was important to confirm that ALT2 can interact with DDB1, since the DWD motif is required for interaction with DDB1. Yeast two-hybrid analysis was performed with ALT2, DDB1A and DDB1B, which resulted in no interaction. *In vitro* pulldowns were also performed since yeast two-hybrids are dependent on a functional protein in yeast and it is possible that any of the proteins tests were improperly folded in the yeast. The *in vitro* pulldowns resulted in a very weak positive interaction between ALT2 and DDB1B, but no interaction was seen between ALT2 and DDB1A. The *alt2-1* mutation was also tested and a positive interaction was also seen between DDB1B and *alt2-1* (Figure 36B). This is not surprising since the *alt2-1* mutation does not occur within the DWD domain and it is possible that this mutation is altering an interaction with another protein or possibly the DNA.

DDB2 was also tested for Al tolerance due to its similarity to ALT2, by growing *ddb2* in the presence of increasing concentrations of Al. *ddb2* had an interesting phenotype on Al, since it displayed no change in root length when grown on increasing

Figure 36. *ddb1b* is slightly tolerant to Al and weakly interacts with ALT2. (A) Ws-2 wt and *ddb1b* were grown on a gel soaked environment with increasing concentrations of $AlCl_3$ ranging from 0mM to 1.25mM $AlCl_3$ (pH 4.2). After 7 days of growth, root lengths were measured, with mean ±SE values determined from 30 roots of each. To confirm that *ddb1b* represents a knockout in DDB1B, cDNA was synthesized from total RNA of Ws-2 wt and *ddb1b*. PCR was performed using the cDNA as a template for amplification of *DDB1B*. *ACT2* was used as a positive control. (B) DDB1B weakly interacts with ALT2. *In vitro* binding assay with the association of the bacterially produced MBP and MBP:ALT2 or MBP:ALT2^{G340R} fusion proteins with *in vitro* radiolabeled ([^{35}S] methionine) DDB1B protein. MBP alone was used as a negative control. No binding association was observed using 5µl of *in vitro* translated DDB1B protein.

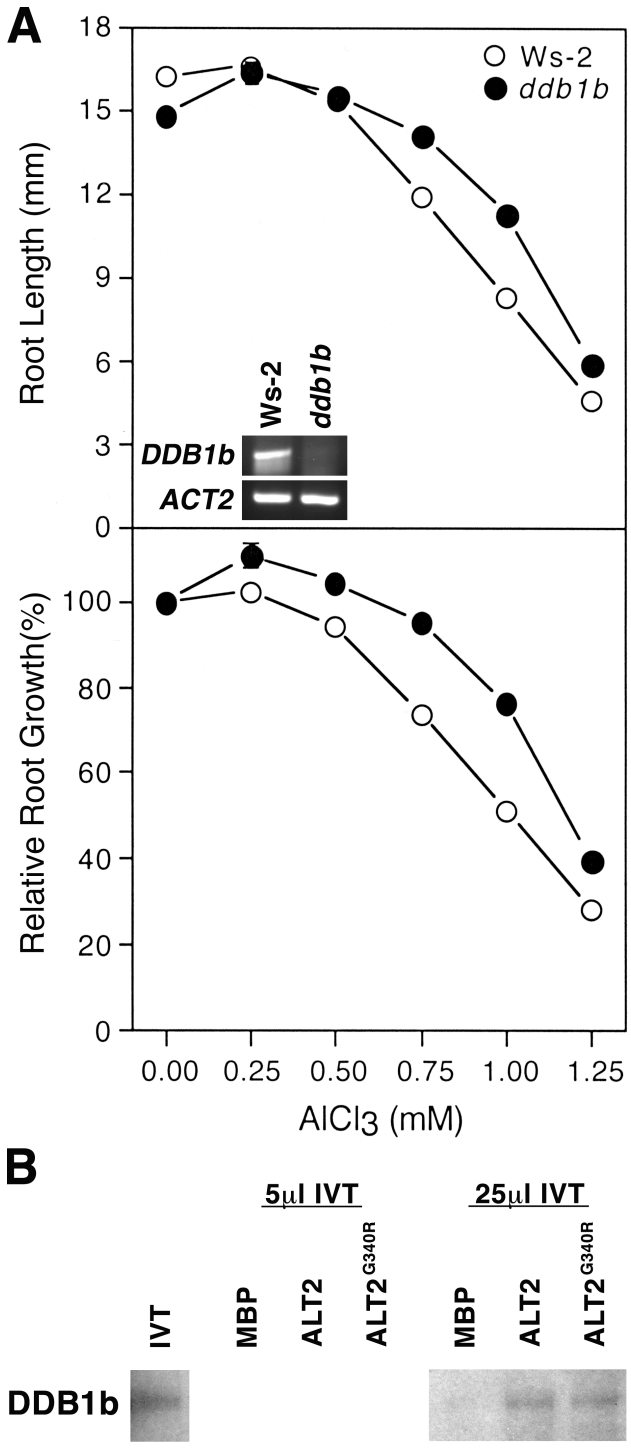
A
Root Length (mm)
Ws-2
ddb1b
Ws-2
ddb1b
DDB1b
ACT2
Relative Root Growth(%)
AlCl3 (mM)
B
5μl IVT
25μl IVT
IVT
MBP
ALT2
ALT2G340R
MBP
ALT2
ALT2G340R
DDB1b

concentrations of Al (Figure 37A). *ddb2* also had a severe growth defect, even when grown in the absence of Al so it is difficult to determine if *ddb2* is truly Al tolerant. Yeast two-hybrid analysis was also performed between DDB2 and ALT2 to determine if these two proteins could interact. The yeast two-hybrid analysis resulted in no interaction between DDB2 and ALT2. To confirm this result, *in vitro* pulldowns were performed with ALT2 and DDB2. A weak interaction, but one that was stronger than the ALT2-DDB1b interaction was observed between ALT2 and DDB2 (Figure 37B). DDB2 plays a role in nucleotide excision repair in response to UV stress. These data taken together suggest that Al-mediated DNA damage is not similar to the DNA damage caused by UV stress.

ALT2 is slightly tolerant to heavy metals

Many heavy metals have been shown to inhibit DNA repair, promote DNA damage and also alteration of gene expression due to DNA hypermethylation and histone hypoacetylation (Kasprzak 2003, Waisberg 2003). Previous work has shown that *alt1-1* has increased nickel and cadmium resistance (Rounds 2008). To test to see if *alt2-1* responds similarly, *alt2-1* was grown in the presence of nickel and cadmium in a hydroponic environment. When Col-0 wt and *alt2-1* were treated with 10μM $NiCl_2$, there was a 23% reduction of growth observed with *alt2-1* but 47% reduction in Col-0 wt. When $NiCl_2$ concentration was increased to 20μM, *alt2-1* no longer had any increased tolerance to $NiCl_2$ compared to Col-0 wt (Figure 38). This is in contrast to *alt1-1*, which was very tolerant to $NiCl_2$, even at 20μM (Rounds 2008).

Figure 37. *ddb2* is unaffected by Al treatment and weakly interacts with ALT2. (A) No-0 wt and *ddb2* were grown on a gel soaked environment with increasing concentrations of $AlCl_3$ ranging from 0mM to 1.25mM $AlCl_3$ (pH 4.2). After 7 days of growth, root lengths were measured, with mean ±SE values determined from 30 roots of each. To confirm that *ddb2* represents a knockout in DDB2, cDNA was synthesized from total RNA of No-0 wt and *ddb2*. PCR was performed using the cDNA as a template for amplification of *DDB2*. *ACT2* was used as a positive control. (B) DDB2 weakly interacts with ALT2. *In vitro* binding assay with the association of the bacterially produced MBP and MBP:ALT2 or MBP:$ALT2^{G340R}$ fusion proteins with *in vitro* radiolabeled ([^{35}S] methionine) DDB2 protein. MBP alone was used as a negative control. Binding associations were observed using both 5µl and 25µl of *in vitro* translated DDB2 protein.

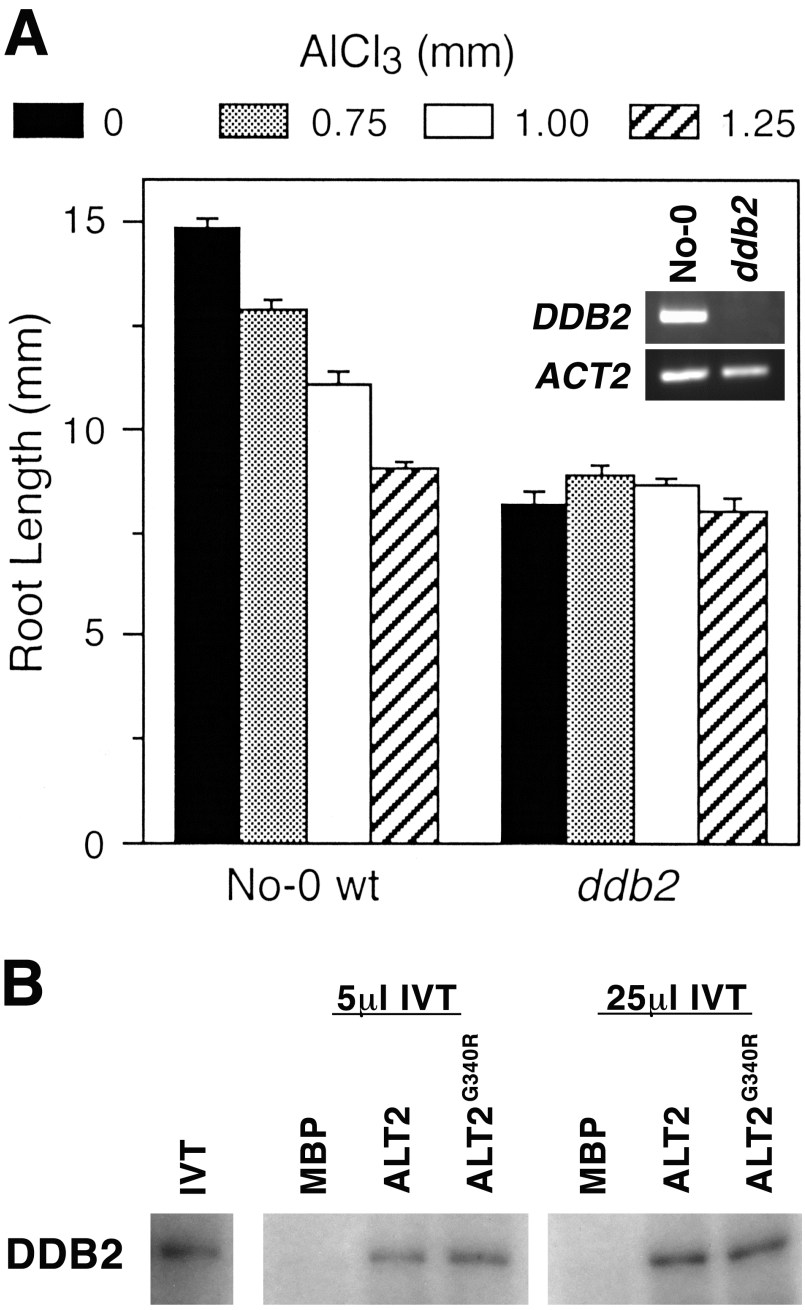
A
AlCl3 (mm)
0
0.75
1.00
1.25
Root Length (mm)
15
10
5
0
No-0
ddb2
DDB2
ACT2
No-0 wt
ddb2
B
5µl IVT
25µl IVT
IVT
MBP
ALT2
ALT2G340R
MBP
ALT2
ALT2G340R
DDB2

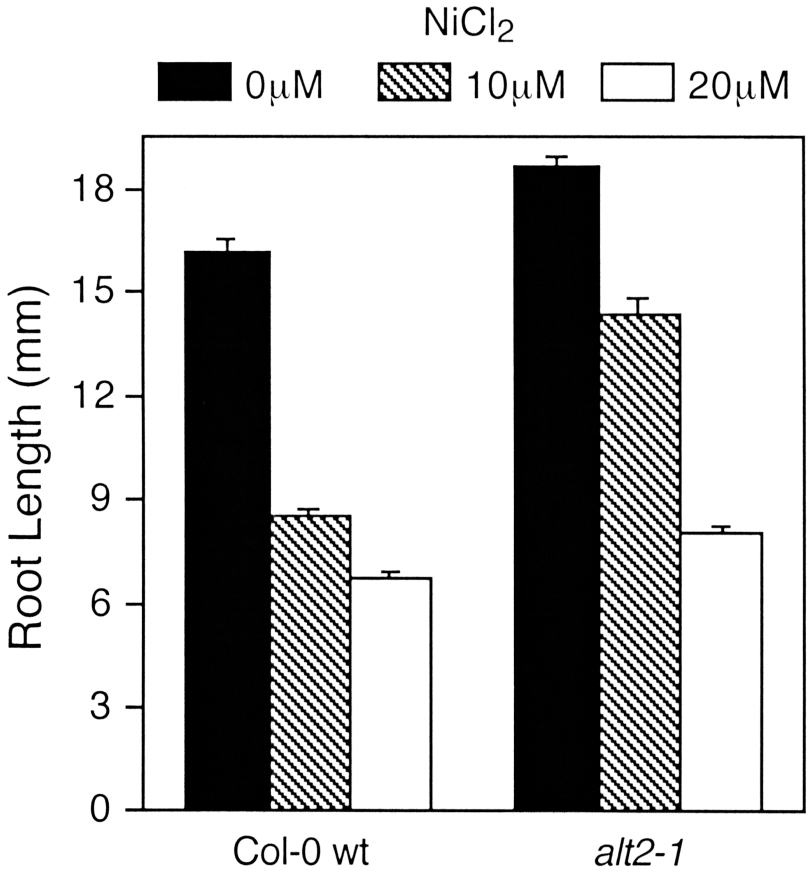

Figure 38. *alt2-1* roots are slightly tolerant to nickel. Col-0 wt and *alt2-1* were grown hydroponically either 0μM, 10μM or 20μM $NiCl_2$ (pH 5.5) for seven days. After growth, root lengths were measured, with mean ±SE values determined from 30 roots of each.

Col-0 and *alt2-1* were also challenged with 10μM and 20μM $CdCl_2$. At both concentrations *alt2-1* displayed slight tolerance compared to Col-0 wt (Figure 39). This result was similar to the response of *alt1-1* to $CdCl_2$, which resulted in slight tolerance to 10μM $CdCl_2$. Although both *alt1-1* and *alt2-1* both show increased tolerance to the heavy metals nickel and cadmium, but *alt1-1* appears to have an additional role in the plant's response to nickel.

ALT2 fails to induce stoppage of the cell cycle upon Al treatment

Previous research on *alt1-1* displayed that Al treatment induces stoppage of the cell cycle upon Al treatment (Rounds 2008). Utilizing a *CyclinB1;1*:GUS reporter construct it is possible to visualize cell cycle progression in plants treated with genotoxic agents. Like all *Arabidopsis* cyclin B genes, *CyclinB1;1* is upregulated during the G2/M phase of the cell cycle. In the reporter line, a truncated version of *CyclinB1;1* was fused to a mitotic destruction box which causes its degradation during mitosis. The construct also contains the β-glucuronidase gene that catalyzes the formation of a blue color when treated with X-Gluc, which makes it possible to identify individual cells that have arrested in the G2/M phase of the cell cycle (Colón-Carmona 1999).

In order to determine if the checkpoint activation function is affected by the *alt2-1* mutation, Col-0 wt plants containing the *CyclinB1;1*:GUS (*CycB1;1*) construct were crossed with *alt2-1*. F_2 seeds were collected and screened for the *alt2-1* mutation and the presence of GUS staining. Col-0;*CycB1;1* and *alt2-1*;*CycB1;1* were grown in the presence of 0, 0.75 and 1.5mM $AlCl_3$ in a gel soaked environment for seven days, after

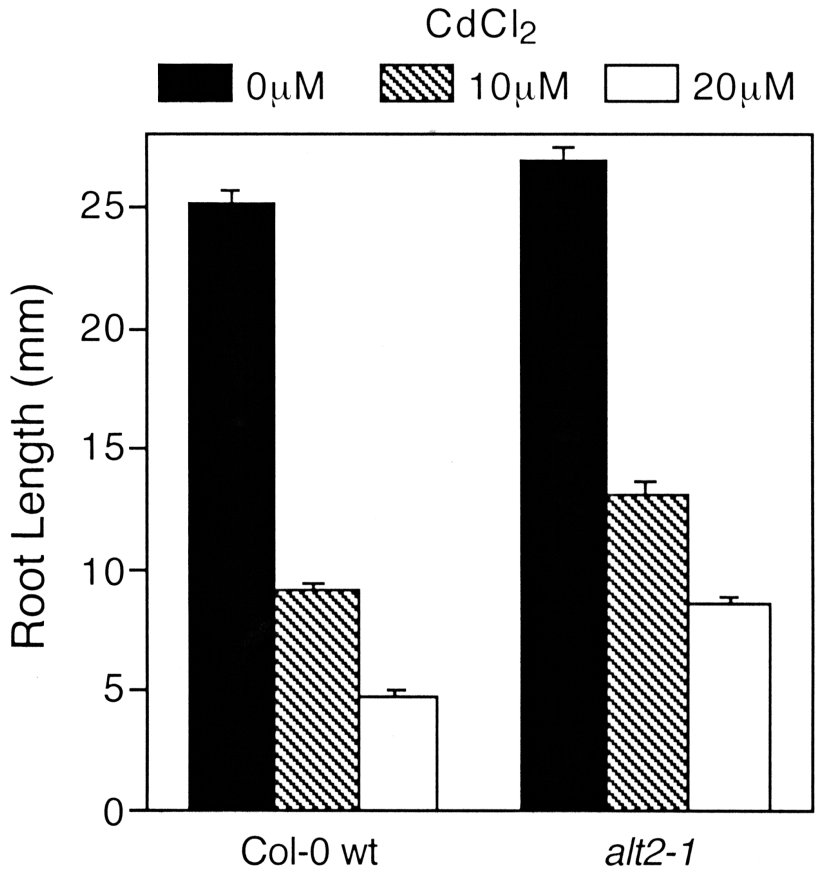

Figure 39. *alt2-1* roots are slightly tolerant to cadmium. Col-0 wt and *alt2-1* were grown hydroponically either 0μM, 10μM or 20μM $CdCl_2$ (pH 5.5) for seven days. After growth, root lengths were measured, with mean ±SE values determined from 30 roots of each.

which the roots were stained for GUS activity. After the development of blue color, the seedlings were observed and photographed. At 0.75mM $AlCl_3$, there was upregulation and stabilization of the *CycB1;1*:GUS in Col-0 wt background (Figure 40A). When *CycB1;1*:GUS was grown on 1.5mM $AlCl_3$, the toxic effects of Al can be seen, which causes the inhibited roots to become differentiated closer to the root tip with root hairs closer to the apex, and had cells that were highly vacuolated. In contrast, the *alt2-1* roots failed to develop any GUS stain, even at 1.5mM $AlCl_3$. The roots also did not display any of the effects of Al toxicity that were seen in Col-0 wt roots. These results indicate that Al exposure leads to upregulation of *CycB1;1* in Col-0 wt but not in *alt2-1*. This indicates that Al causes a type of damage to the cells that triggers the G2/M checkpoint, and the *alt2-1* mutation affects some ability of the plant to detect the toxic effects of Al.

The dramatic root phenotype of Al-treated Col-0, and also previous work on *alt1-1* raised the question if *alt2-1* roots also maintained the quiescent center and had not terminally differentiated. The promoter trap line, QC46, which expresses the GUS gene in the quiescent center was used. The quiescent center is a subset of slow dividing cells in the root meristem that are responsible for replacing damaged cells in the meristem and maintaining pluripotency of the stem cells.

In order to determine if the quiescent center is maintained by the *alt2-1* mutation, Col-0 wt plants containing the *QC46* gene trap line were crossed with *alt2-1*. F_2 seeds were collected and screened for the *alt2-1* mutation and the presence of GUS staining. Col-0;*CycB1;1* and *alt2-1*;*CycB1;1* were grown in the presence of 0 and 1.5mM $AlCl_3$ in a gel soaked environment for seven days, after which the roots were stained for GUS

Figure 40. *alt2-1* maintains cell-cycle progression and the quiescent center in the presence of Al. (A) *alt2-1* maintains the cell-cycle progression in the presence of Al. The *CyclinB1;1*:GUS construct was crossed into *alt2-1* plants. F_2 homozygous lines were grown on a gel soaked enivornment with 0mM, 0.75mM or 1.5mM $AlCl_3$ (pH 4.2). After 7 days of growth, seedlings were harvested, stained for GUS and photographed. (B) *alt2-1* maintains the QC in the presence of Al. The QC promoter trap line in the Col-0 wt background was crossed with *alt2-1*. F_2 double homozyotes were grown on a gel soaked environment with 0 or 1.5mM $AlCl_3$ (pH 4.2). After 7 days of growth, seedlings were harvested, stained for GUS and photographed. (C) The observed staining with the reporter lines is not due to cell death. Col-0 wt and *alt2-1* were grown on a gel soaked environment with 0mM, 0.75mM or 1.5mM $AlCl_3$. After 7 days of growth, seedlings were harvested and stained with propidium iodide. Fluorsecent images were immediately taken after staining.

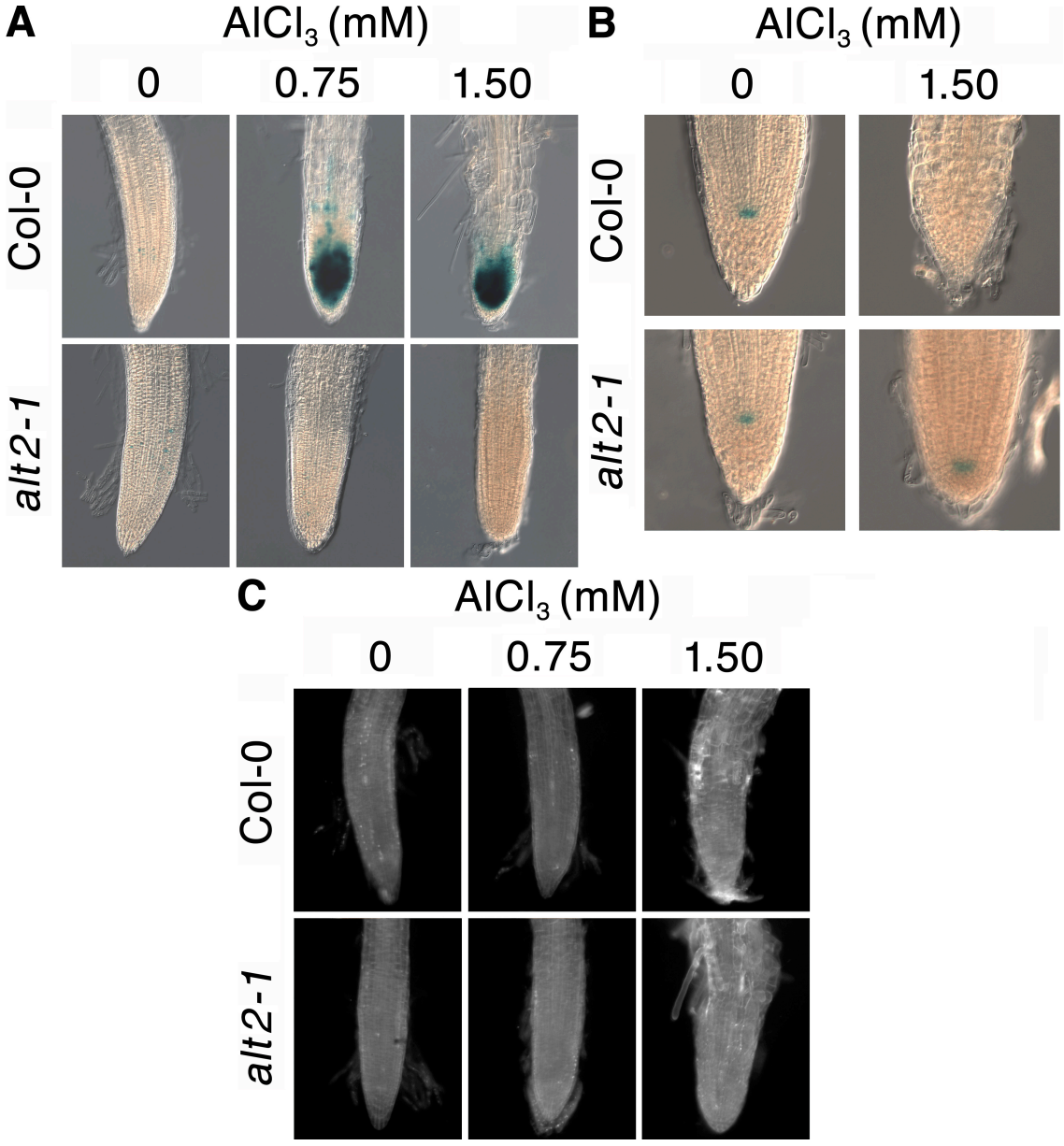
A
AlCl3 (mM)
0
0.75
1.50
Col-0
alt2-1
B
AlCl3 (mM)
0
1.50
Col-0
alt2-1
C
AlCl3 (mM)
0
0.75
1.50
Col-0
alt2-1

activity. After development of blue color, the seedlings were observed and photographed. Both lines displayed normal staining of the quiescent center when grown without $AlCl_3$ (Figure 40B). However, treatment with Al resulted in complete loss of staining in the Col-0 wt line, while *alt2-1*;QC46 retained the GUS staining. Interestingly in the *alt2-1*;QC46 line, the quiescent center shifts downwards. This could be due to some limited toxic effects of Al on *alt2-1* roots, which could be causing the root apex to condense and causing differentiated cells to occur closer to the root apex. These data show that like *alt1-1*, *alt2-1* plants are able to maintain the quiescent center, even in high levels of Al, which allows the roots to be Al tolerant.

To determine if the lack of GUS staining in Col-0;QC46 was not due to cell death but to cell differentiation, propidium iodide (PI) staining was used. PI cannot permeate the membrane, so it is generally excluded from viable cells. Therefore PI can be used to identify dead cells. Col-0 and *alt2-1* seedlings were grown on 0, 0.75 and 1.5mM $AlCl_3$ in a gel soaked environment for 7 days. Seedlings were harvested and stained with PI and immediately photographed. On 1.5mM $AlCl_3$ there was very little PI staining observed in either Col-0 wt or *alt2-1*, and on all other concentrations there was no PI staining (Figure 40C). These results rule out that the lack of staining seen in QC46 was due to cell death and is instead due to terminal differentiation of the root tip.

ALT2 is not responsible for detecting DNA fragmentation

With the overwhelming evidence that *alt2-1* may play a role in detecting DNA damage due to Al, it was of interest to determine what type of DNA damage is occurring

due to Al treatment. Since *alt1-1* and *alt2-1* display a similar phenotype when grown in the presence of $AlCl_3$ and because both are predicted to be involved in detection of DNA damage, *alt2-1* was grown in hydroxyurea (HU). HU is an inhibitor of ribonucleotide reductase by scavenging free radicals that are used for the reduction of ribonucleotides. This stalls the replication fork due to depletion of deoxyribonucelotides. ATR functions to detect replication fork blocks and single stranded DNA breaks, so mutants like *alt1-1* are hypersensitive to HU (Rounds 2008). Col-0 and *alt2-1* were grown for 4 days in hydroponic media, when approximately a quarter of the roots were measured. The remaining seedlings were transferred to hydroponics plates containing 0 or 1mM HU and were allowed to grow for an additional three days before they were measured. The average length of the roots prior to transfer was subtracted from the average length of control and treatment plates following transfer to determine the amount of growth on HU. Relative root growth was determined separately for each by comparing treated values to untreated. It was found that *alt2-1* roots are not hypersensitive to short term HU treatment and were only mildly inhibited by HU, similar to wild type (Figure 41).

To confirm that the root growth inhibition observed by HU treatment was due to arrest of the G2/M phase of the cell cycle, the *CycB1;1*:GUS reporter line was used. Col-0 wt and *alt2-1* carrying *CycB1;1*:GUS reporter gene. Both Col-0 wt and *alt2-1* were grown for 7 days in 0 or 1mM HU in hydroponics. After growth, seedlings were harvested and stained for GUS activity. In the presence of HU, Col-0 displayed upregulation and stabilization of the *CycB1;1*:GUS staining, while *alt2-1* had a reduced capacity to induce *CycB1;1*:GUS upregulation and stabilization (Figure 42). Since HU

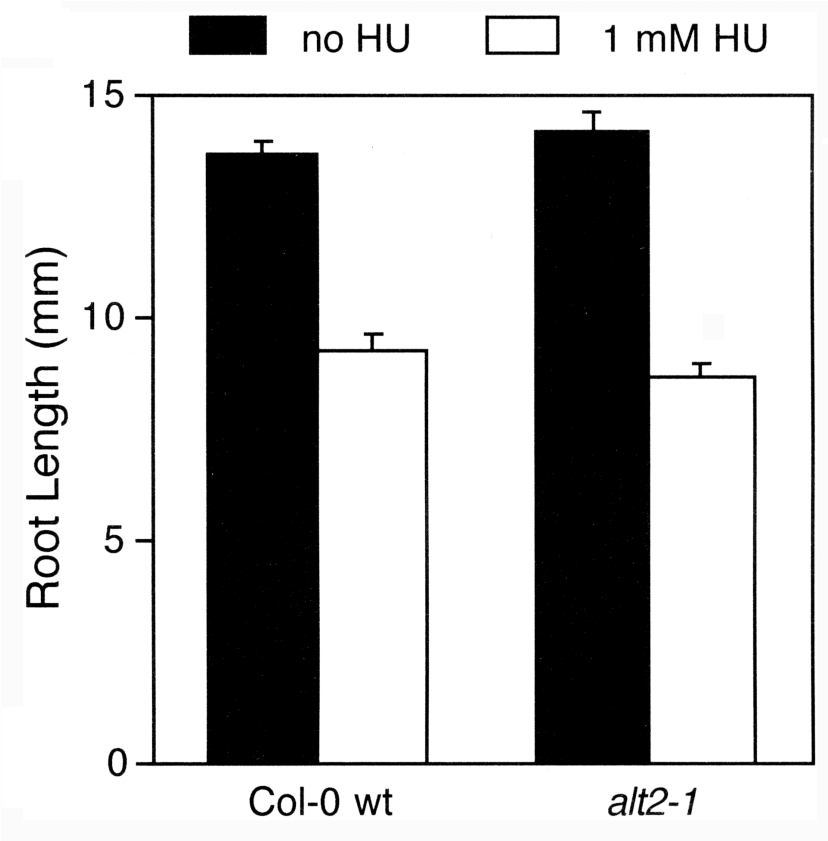

Figure 41. *alt2-1* roots are not hypersensitive to short-term hydroxyurea treatment. Col-0 wt and *alt2-1* were grown hydroponically for four days and then exposed to 0mM or 1mM HU for an additional three days. Following growth, root lengths were measured, with mean ±SE values determined from 30 roots of each.

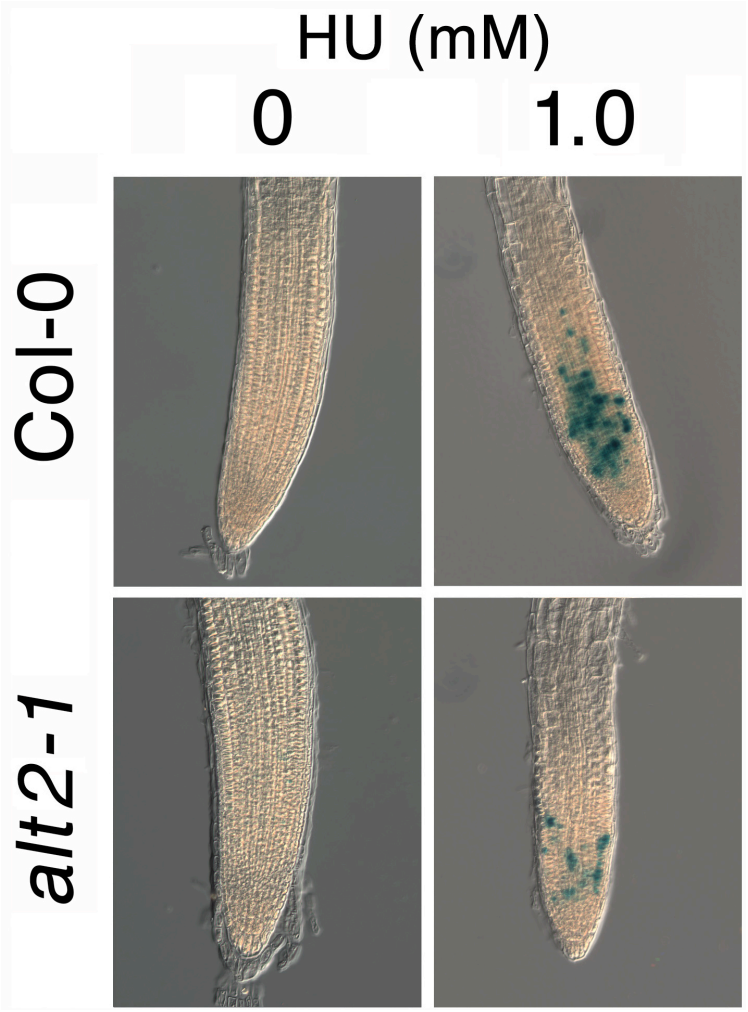

Figure 42. *alt2-1* has a reduced capacity to arrest the cell cycle in the presence of HU. *CycB1;1*:GUS plants in Col-0 wt or *alt2-1* background were grown in hydroponics in the presence of 0mM or 1mM HU for 7 days. After growth, seedlings were harvested, stained for GUS and photographed.

causes stalled replication forks, and also single stranded DNA breaks, it is possible that *alt2-1* might be required to respond to single stranded DNA breaks. These results rule out the possibility that Al treatment generates replication fork blocks, as *alt2-1* is not hypersensitive to short term HU treatment and is able to induce *CycB1;1* expression.

Seeing as *alt2-1* is not hypersensitive to short term HU treatment, but *alt1-1* is, it was of interest to determine if there were any other differences between the two factors in their role of detecting or responding to DNA damage. For *Arabidopsis*, the only established means of assessing DNA strand breaks is the Comet assay. This procedure involves the isolation of plant nuclei, followed by embedding in low melting agarose on a glass slide. The nuclei are subjected to gentle electrophoresis, dried, stained and imaged. Damaged DNA will be unwound during the procedure and trail out behind the intact DNA during electrophoresis, producing a comet-like figure. The size of the tail is directly proportional to the amount of damage incurred by the nucleus (Wang 2006).

Col-0 wt and *alt2-1* were grown on 0 and 1.5mM $AlCl_3$ in a gel soaked environment for 7 days. Roots were collected and nuclei were isolated by chopping the roots in ice-cold 1xPBS, then filtering out the cellular debris using a 40μM filter. The nuclei were then used for the Comet assay, and the slides were scored for DNA damage by measuring the percent of DNA in the comet tail with the CometScore software. From this analysis, there is increased DNA fragmentation resulting from both double stranded and single stranded DNA breakage (Figure 43). The amount of fragmentation does not change between Col-0 wt and *alt2-1* suggesting that although Al is causing increased DNA fragmentation, this is not the type of damage that is detected by ALT2.

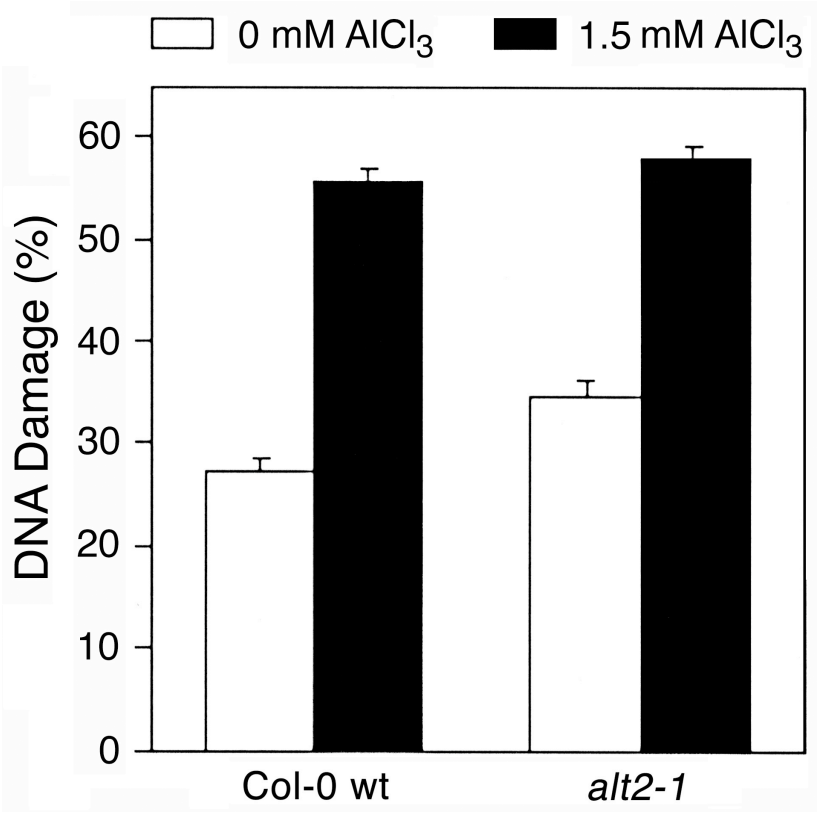

Figure 43. Al-mediated DNA fragmentation is not altered by the *alt2-1* mutation. Seedlings of Col-0 wt and *alt2-1* were grown on a gel soaked environment with 0mM or 1.5mM $AlCl_3$ (pH 4.2) for 7 days. Nuclei were harvested from the roots, embedded in low-melting agarose on glass slides and subjected to electrophoresis. Slides were stained with SYBR Green and individual nuclei were analyzed for DNA damage, represented as the percent of DNA located in the tail of the comet. The tails of 150 comets were analyzed utilizing CometScore software.

Given that *alt2-1* displays increased Al tolerance, but shows no difference in DNA fragmentation compared to wild type in the presence of Al, it was of interest to determine the type of DNA damage that ALT2 is detecting in the presence of Al. Initially T-DNA insertion lines that were previously characterized as members of DNA checkpoint factors and repair pathways were analyzed for Al tolerance or hypersensitivity. The first gene of interest was *UVH1* (*RAD1*), which is a 5' repair endonuclease that has been previously shown to be involved in repair of DNA damage by UV-B, UV-C and ionizing radiation. The repair for double strand breakage is mediated by homologous recombination, and also excises dimers by nucleotide excision repair (Liu 2000, Fidantsef 2000).

To determine if *uvh1-1* has an altered response to Al, it was grown on increasing concentrations of $AlCl_3$ for 7 days, after root lengths were measured. It was found that *uvh1-1* is slightly hypersensitive to Al, but was just as sensitive to Col-0 wt at 1.25mM $AlCl_3$ (Figure 44). Additionally the phenotype observed of *uvh1-1* is much different than what has previously been published. When *uvh1-1* is exposed to gamma irradiation, or UV stress, the plants will not survive the stress. This could indicate that a minor type of DNA damage is caused by Al is repaired in an UVH1-dependent manner, but the function of UVH1 is not required for repair of the majority of the DNA damage caused by Al. It is likely that the double stranded DNA breaks that were observed from the Comet assay are being repaired in an UVH1-dependent manner. This further suggests that DNA fragmentation is not the type of DNA damage caused by Al that ALT2 is detecting.

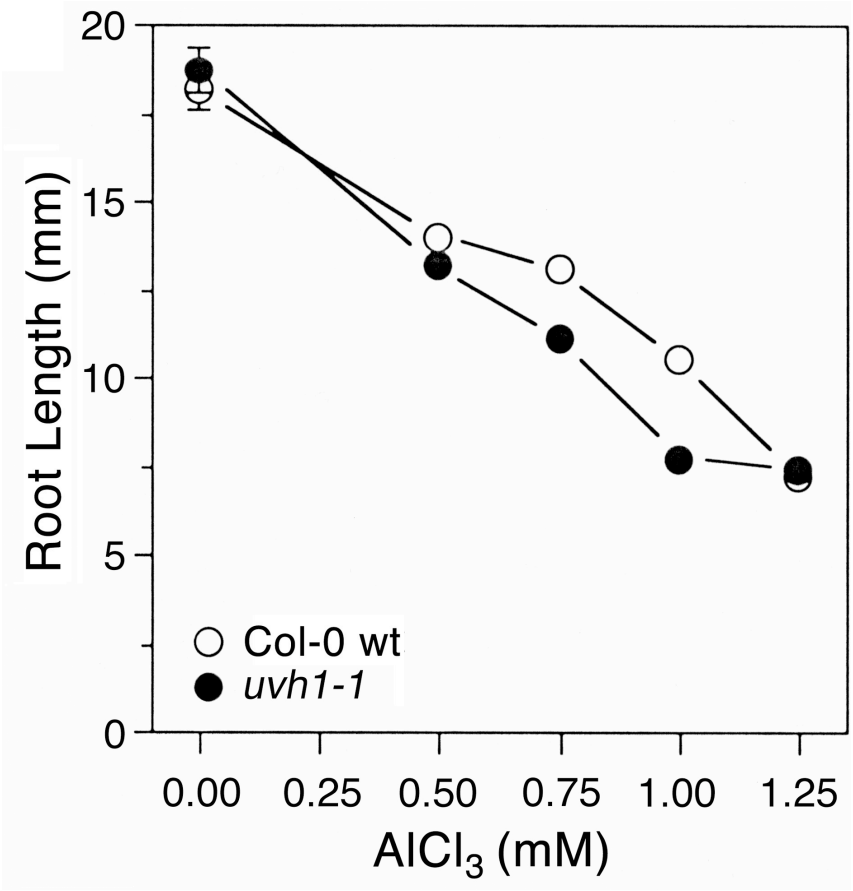

Figure 44. *uvh1-1* is slightly sensitive to $AlCl_3$. Col-0 wt and *uvh1-1* were grown in a gel soaked environment with increasing concentrations of $AlCl_3$ (pH 4.2) ranging from 0mM to 1.25mM $AlCl_3$. After 7 days of growth, root lengths were measured, with mean ±SE values determined from 30 roots of each.

Another DNA checkpoint factor is RAD17, which shows sequence homology to the replication factor C and acts as a proliferating cell nuclear antigen (PCNA) clamp loader. This protein also is part of the yeast RAD1/Hus1/RAD9-checkpoint complex (9-1-1 complex) and seems to function at the beginning of the cell cycle checkpoint signal cascade. RAD17 regulates the 9-1-1 complex's association with chromatin after treatment with DNA-damaging agents. *RAD1*, *RAD9*, *HUS1* and *RAD17* are all necessary for S phase and G2/M arrest in response to both DNA damage and stalled DNA replication. The *rad17-1* mutants have delayed repair of double stranded DNA breaks. Also, homologous recombination is increased in the mutant background, indicating that the *rad17-1* mutation does not lead to a general defect in DNA repair but mainly to a deficiency in non-homologous recombination (Heitzeberg 2004).

Since RAD17 plays a different role in DNA repair, the T-DNA insertion mutation *rad17-1* was grown on increasing concentrations of $AlCl_3$ for 7 days on a gel soaked environment. At all concentrations of Al, *rad17-1* displayed greater than wild type sensitivity to Al (Figure 45). This suggests that the DNA damage caused by Al is triggering repair in a RAD17 dependent manner. Although there is not extreme hypersensitivity of Al, it still indicates that this factor is required for Al tolerance. Additionally, *rad17-1* mutants are also hypersensitive to the genotoxic agents bleomycin and mitomycin C (MMC), and also hypersensitive to telomere lengthening. Previous work on *alt1-1* indicates that Al does not affect telomere length (Rounds 2008). Therefore, is it possible that Al-mediated DNA damage could be similar to the DNA

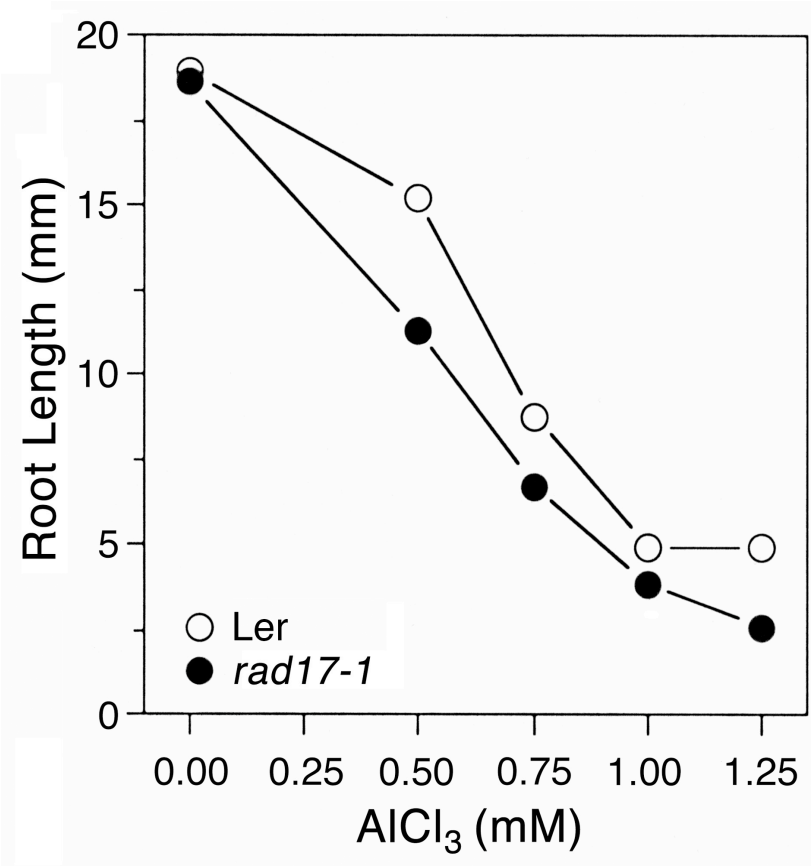

Figure 45. *rad17-1* is slightly sensitive to $AlCl_3$. Ler wt and *rad17-1* were grown in a gel soaked environment with increasing concentrations of $AlCl_3$ (pH 4.2) ranging from 0mM to 1.25mM $AlCl_3$. After 7 days of growth, root lengths were measured, with mean ±SE values determined from 30 roots of each.

damage caused by bleomycin and/or MMC.

Bleomycin is a true radiomimeticum, or an agent that imitates the effects of radiation. Bleomycin is a glycopeptide antibiotic that is produced by the bacterium *Streptomces verticilus* that acts by inducing DNA strand breaks by chelating iron, which produces ROS, which in turn cleaves the DNA (Dorr 1992). To test if *alt2-1* has an altered phenotype when grown on bleomycin, Col-0 wt and *alt2-1* were grown with 0 and 0.1μg/mL bleomycin on plant nutrient medium plus sucrose (PNS) for 7 days. The root lengths were measured after the 7 days of growth and it was found that *alt2-1* does not have any enhanced sensitivity or tolerance to bleomycin (Figure 46). This was not surprising since the Comet assay had already revealed that Al is causing DNA fragmentation, yet the *alt2-1* mutation does not alter the pattern of DNA fragmentation but is extremely tolerant to Al.

alt2-1 is hypersensitive to crosslinking agents

Mitomycin C (MMC) is an aziridine-containing antibiotic isolated from *Streptomyces caepitosus*. MMC itself does not react with DNA, but once it becomes reduced by quinone, the aziridine opens and allows MMC to attack the DNA. This reaction forms crosslinks across the complementary strands of the DNA double helix, or interstrand crosslinks (Tomasz 1995). To test if *alt2-1* had an altered response when grown on MMC, Col-0 wt and *alt2-1* and *atr-2* were grown with 0 and 15μg/mL MMC on PNS for 7 days and after growth, the root lengths were measured. Additionally, the

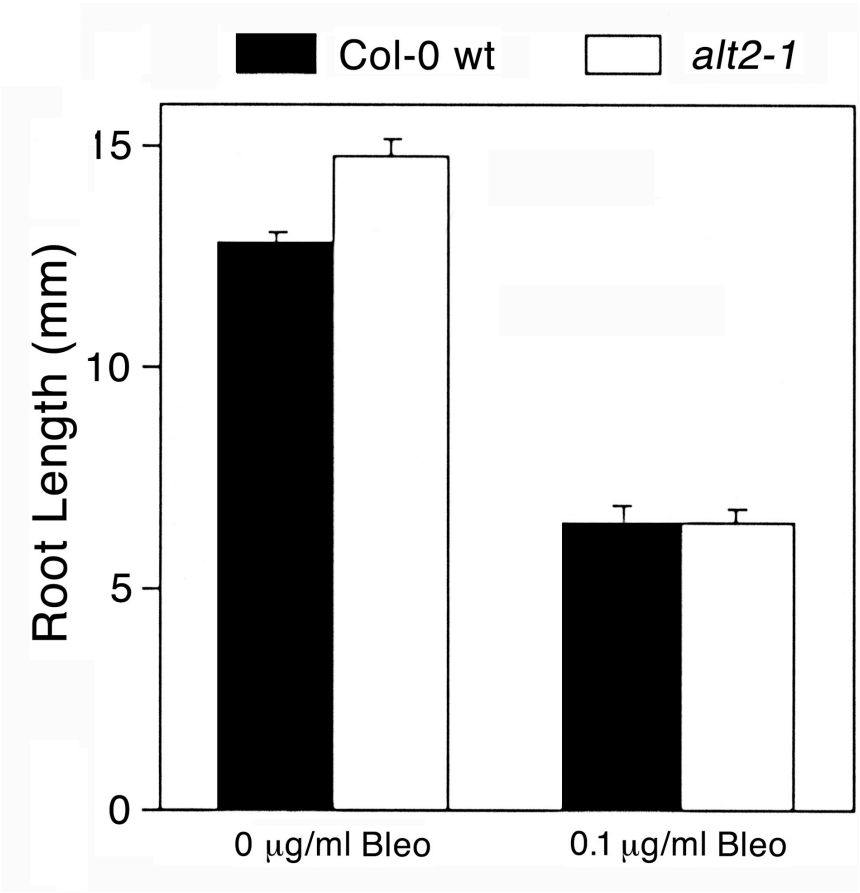

Figure 46. *alt2-1* is not hypersensitive to bleomycin. Col-0 wt and *alt2-1* were grown on plant nutrient media plus sucrose supplemented with 0μg/mL or 0.1μg/mL bleomycin. After 7 days of growth, root lengths were measured, with mean ±SE values determined from 30 roots of each.

atr-2 mutation was included in this growth experiment. Since previous results indicate that ALT2 and AtATR are working in the same pathway to detect Al-mediated DNA damage (Figure 34), it was important to confirm that the *atr-2* mutation had a similar phenotype on MMC to verify this type of DNA damage detected by both proteins. The *atr-2* mutation was used instead of *alt1-1* because *atr-2* has been already verified to be a complete knockout of AtATR, while the *alt1-1* mutation only partially knocks out the function of AtATR (Rounds 2008). Unlike every other chemical treatment *alt2-1* was subjected to, *alt2-1* was severely hypersensitive to MMC and *atr-2* mutation was also very hypersensitive to MMC (Figure 47A). Visually, the *alt2-1* line displayed a phenotype that was very similar to the *als3-1* phenotype when grown on high levels of Al (Figure 47B).

It was of interest to determine if the root growth inhibition seen by *alt2-1* was mediated by stoppage of the cell cycle in the G2/M phase by *CycB1;1*. The same *CycB1;1*:GUS lines that were used for analysis of the cell cycle in the presence of Al were used to monitor the cell cycle. Both Col-0 wt and *alt2-1* that contained the *CycB1;1*:GUS reporter were grown for 7 days in 0 or 15µg/mL MMC on PNS. After growth the seedlings were harvested, stained for GUS activity and photographed. In the presence of 15µg/mL MMC, Col-0 wt had upregulation and stabilization of the *CycB1;1*:GUS staining, while *alt2-1* had no *CycB1;1*:GUS staining (Figure 48, upper panel). The *alt2-1* roots were vacuolated and had a large amount of root hairs near the root apex, which is very similar to the toxic effects of Al. The lack of staining in the

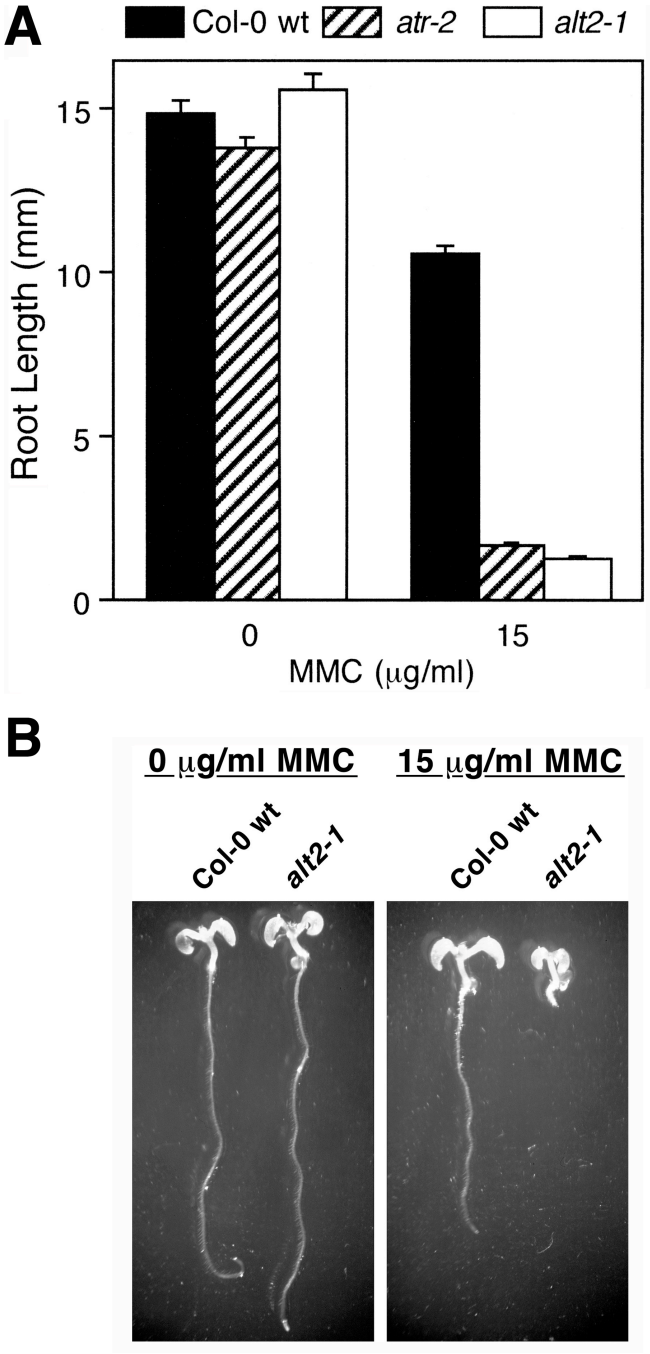

Figure 47. *alt2-1* is hypersensitive to mitomycin C. Col-0 wt, *atr-2* and *alt2-1* were grown on plant nutrient media plus sucrose supplemented with 0μg/mL or 15μg/mL mitomycin C. (A) After 7 days of growth, root lengths were measured, with mean ±SE values determined from 30 roots of each.with mean ±SE values determined from 30 roots of (B) Photographs were taken of representatives from each treatment of Col-0 wt and *alt2-1*.

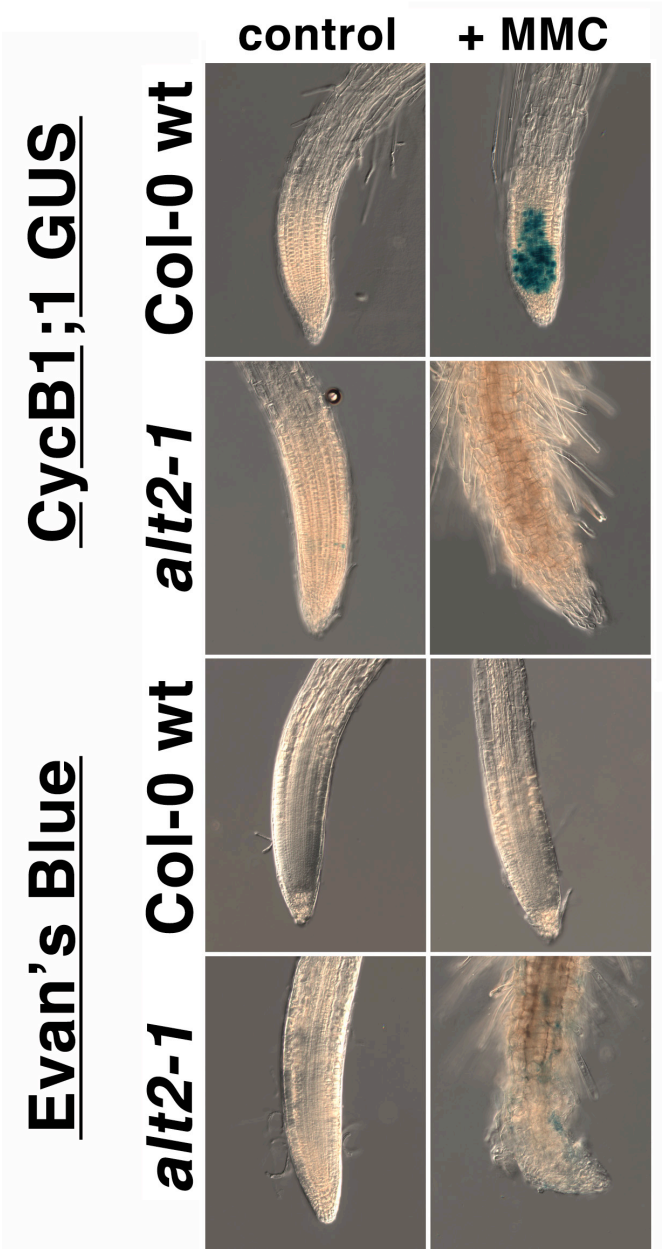

Figure 48. *alt2-1* fails to arrest the cell cycle in the presence of mitomycin C. The *CyclinB1;1*:GUS construct was crossed into *alt2-1* plants. F_2 homozygous lines were grown on plant nutrient medium supplemented with 0µg/mL or 15µg/mL MMC. After 7 days of growth, seedlings were harvested, stained for GUS and photographed. To confirm that the observed staining with the reporter lines was not due to cell death, Col-0 wt and *alt2-1* were grown on a gel soaked environment with 0µg/mL and 15µg/mL MMC. After 7 days of growth, seedlings were harvested and stained with the vital stain Evan's Blue. Photographs were immediately taken after staining.

alt2-1 roots treated with MMC may indicate that the cells of the root tip have differentiated and lost their pluripotency, or that the MMC treatment caused cell death. To verify cell viability, the vital stain Evan's blue was used. Similar to PI, Evan's blue is unable to permeate the plasma membrane, so living cells remain their natural color, while damaged or dead cells stain deep blue. Col-0 wt and *alt2-1* were grown in 0 and 15μg/mL MMC on PNS for 7 days. The seedlings were harvested, stained with Evan's blue dye, washed and photographed. Despite the severe growth phenotype in *alt2-1*, there was very little staining observed with MMC treatment, except for a few cells scattered throughout the root tip (Figure 48, lower panel). These results rule out the possibility that the lack of *CycB1;1*:GUS staining in *alt2-1* is due to widespread death and instead is likely due to terminal differentiation of the root tip.

DNA crosslinking can also occur between adjacent bases, called intrastrand DNA crosslinking. The chemotherapy drug cisplatin (CDDP) is a platinum-containing drug that is a neutral molecule until it is activated through a series of spontaneous aquation reactions, which involve the sequential replacement of the *cis*-chloro ligands of cisplatin with water molecules. When the aquation event occurs, this allows the platinum atom to bind to DNA, preferentially guanine bases, which forms DNA–protein and DNA–DNA interstrand and intrastrand crosslinks with 1,2-intrastrand ApG and GpG crosslinks as the major forms of DNA crosslinks, accounting for 85–90% of the total lesions (Siddik 2003). The *alt2-1* and *atr-2* mutants were also tested for hypersensitivity to CDDP since CDDP also acts as a DNA crosslinker. Col-0 wt and *alt2-1* were grown for 7 days with 0 or 5μM CDDP on PNS, and root lengths were measured after growth. Similar to the

MMC result, *alt2-1* and *atr-2* are both hypersensitive to CDDP, while Col-0 wt was barely affected by the treatment (Figure 49). This shows that both ALT2 and AtATR are required for the detection of intrastrand DNA crosslinking.

Similar to the MMC treatment, it was important to determine if the root growth inhibition seen by *alt2-1* was mediated by stoppage of the cell cycle in the G2/M phase by *CycB1;1*. Both Col-0 wt and *alt2-1* that contained the *CycB1;1*:GUS reporter were grown for 7 days in 0 or 5μM CDDP on PNS. After growth the seedlings were harvested, stained for GUS activity and photographed. In the presence of 5μM CDDP, Col-0 wt had modest upregulation and stabilization of the *CycB1;1*:GUS staining, while *alt2-1* had no *CycB1;1*:GUS staining (Figure 50, upper panel). The *alt2-1* roots were vacuolated and had a large amount of root hairs near the root apex, similar to the phenotype seen with the MMC treatment. Comparable to the MMC treatment, the lack of staining in the *alt2-1* roots treated with CDDP may indicate that the cells of the root tip have differentiated and lost their pluripotency, or that the CDDP treatment caused cell death. To verify cell viability, the vital stain Evan's blue was used. Col-0 wt and *alt2-1* were grown in 0 and 5μM CDDP on PNS for 7 days. The seedlings were harvested, stained with Evan's blue dye, washed and photographed. Despite the severe growth phenotype in *alt2-1*, there was very little staining observed with CDDP treatment, except for a few cells scattered throughout the root tip (Figure 50, lower panel). These results also rule out the possibility that the lack of *CycB1;1*:GUS staining in *alt2-1* is due to widespread death due to CDDP and instead is likely due to terminal differentiation of the root tip. These results indicate that both ALT2 and AtATR are essential for detection of

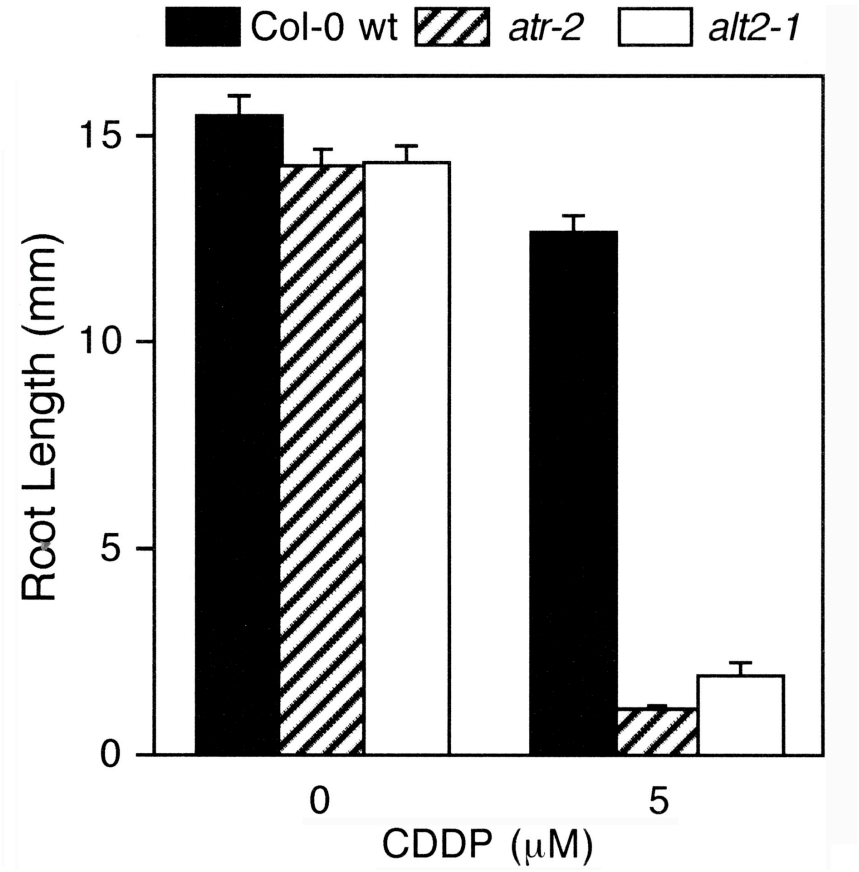

Figure 49. *alt2-1* is hypersensitive to cisplatin. Col-0 wt, *atr-2* and *alt2-1* were grown on plant nutrient media plus sucrose supplemented with 0μM or 5μM CDDP. After 7 days of growth, root lengths were measured, with mean ±SE values determined from 30 roots of each.

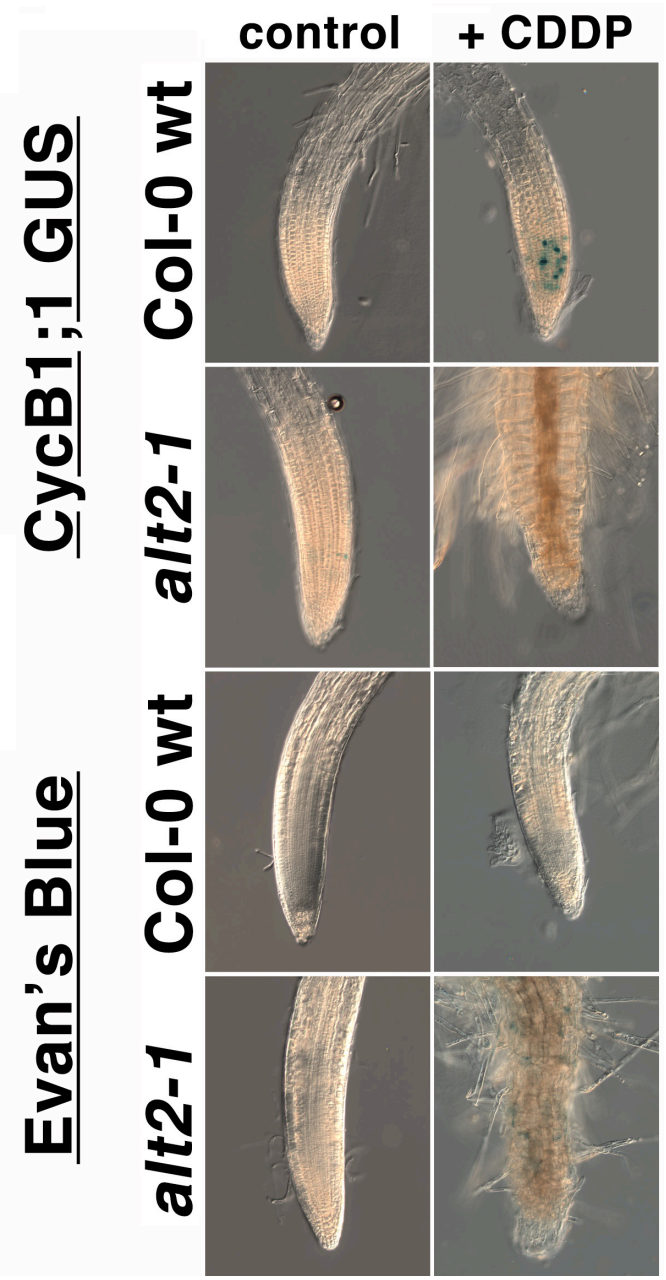

Figure 50. *alt2-1* fails to arrest the cell cycle in the presence of cisplatin. The *CyclinB1;1*:GUS construct was crossed into *alt2-1* plants. F_2 homozygous lines were grown on plant nutrient medium supplemented with 0μM or 15μM CDDP. After 7 days of growth, seedlings were harvested, stained for GUS and photographed. To confirm that the observed staining with the reporter lines was not due to cell death, Col-0 wt and *alt2-1* were grown on a gel soaked environment with 0μM and 5μM CDDP. After 7 days of growth, seedlings were harvested and stained with the vital stain Evan's Blue. Photographs were immediately taken after staining.

DNA crosslinks and loss of these factors cause severe hypersensitivity to DNA crosslinkers.

ALT2:GFP fusion accumulates in the nucleus after treatment with crosslinking agents

With the overwhelming evidence that ALT2 is required for the detection of DNA crosslinks, it was important to determine if ALT2 also localizes to the nucleus in response to DNA crosslinkers, similar to Al. The same *ALT2:GFP* fusion within *alt2-1;als3-1* to determine the subcellular localization of ALT2. The *ALT2:GFP* lines were grown for 5 days in hydroponics in the absence of any DNA damaging agent. The seedlings were transferred either no DNA damaging agents, 25μM $AlCl_3$, 15μg/mL MMC or 5μM CDDP for 48 hours. Before imaging, the seedlings were counterstained with DAPI to visualize the nucleus. In the absence of any chemical treatment, the ALT2:GFP fusion is enriched in the cytoplasm, but upon treatment with $AlCl_3$, the ALT2:GFP fusion accumulates in the nucleus. When the GFP lines were treated with MMC or CDDP, the ALT2:GFP fusion also accumulates in the nucleus (Figure 51). This further confirms that ALT2 translocation into the nucleus is required for response to DNA crosslinkers.

Al is a weak DNA crosslinker *in vivo*

In order to determine if Al is causing DNA crosslinking *in vivo*, a modified protocol of the Comet assay was performed. DNA that contains interstand crosslinks is unable to separate under denaturing conditions and can be exploited in the Comet assay.

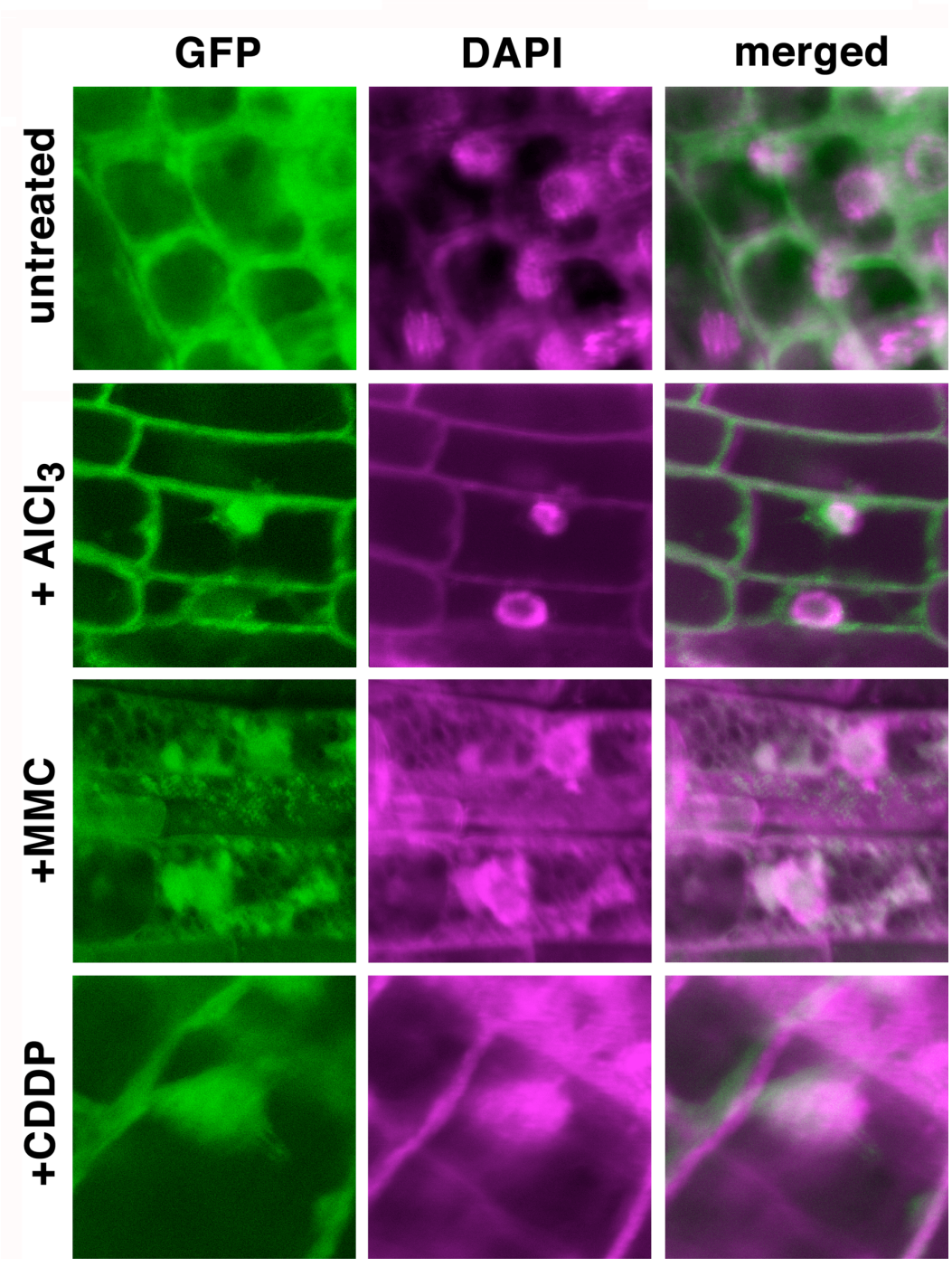

Figure 51. Crosslinking agents cause ALT2 to accumulate to the nucleus. Transgenic *Arabidopsis* T2 *alt2-1;als3-1* plants expressing an *ALT2:GFP* fusion under the control of *ALT2* promoter. Roots were treated for 48 hours with 0, 25µM Al, 15µg/mL MMC, or 5µM CDDP and cells were counterstained with DAPI to allow for nuclei visualization.

To detect the crosslinks, the plants are either irradiated immediately prior to analysis or treated long term with an agent that causes fragmentation, such as bleomycin to deliver a fixed level of random strand breaks to the genome. Col-0 wt was grown in hydroponics and treated for three days with no chemicals, 0.1μg/mL bleomycin, 0.1μg/mL bleomycin with 20μg/mL MMC or 0.1μg/mL bleomycin with 100μM $AlCl_3$. Root tips were collected and nuclei were isolated by chopping the roots in ice-cold 1xPBS, and then filtering out the cellular debris using a 40μM filter. The nuclei were then used for the modified Comet assay, and Olive tail moments of 200 nuclei for each sample were calculated utilizing the Comet Assay IV software. During electrophoresis any relaxed or broken DNA will migrate faster than the undamaged, supercoiled DNA, creating a comet-like image. The presence of interstrand DNA crosslinks slows down the migration of the irradiated DNA during electrophoresis compared to the irradiated non-crosslinked control due to the crosslinks physically holding the fragments of DNA together. The extent of retardation is therefore proportional to the amount of DNA interstrand crosslinking. From this analysis, there is a 93.0±0.04% decrease in the tail moment of the MMC treated nuclei and 38.8±0.06% decrease in the tail moment of the Al treated nuclei (Figure 52). It was expected that MMC would reduce the tail moment, since it is a potent interstrand crosslinker, but treatment with Al also reduced the tail moment. The decrease in tail moment upon treatment with Al suggests that Al is a weak DNA interstrand crosslinker.

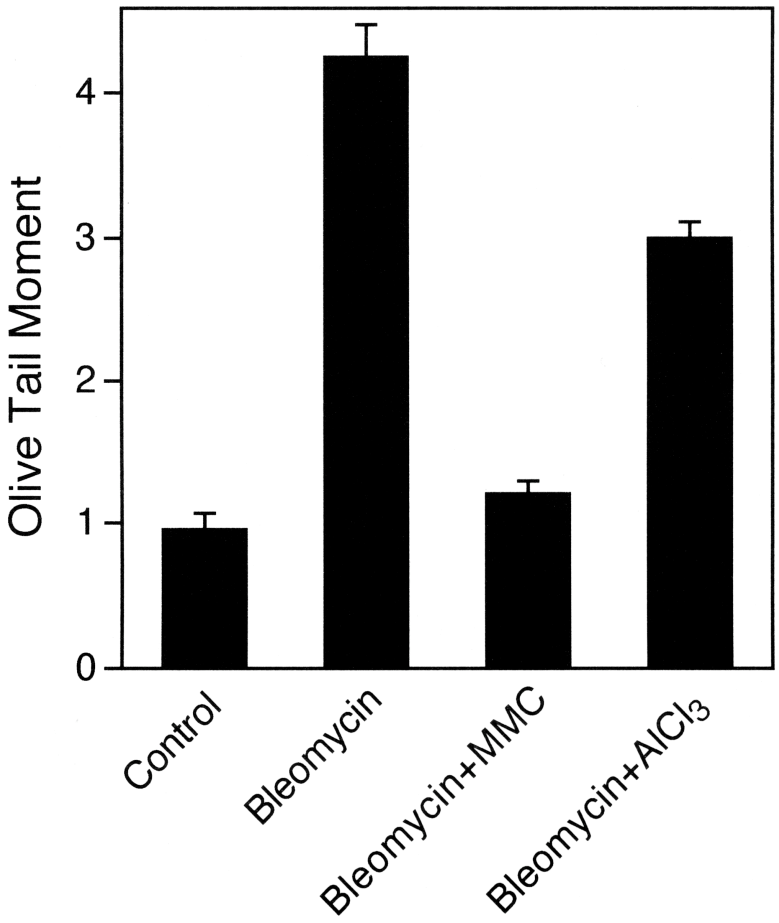

Figure 52. Al is a weak DNA crosslinker *in vivo*. Col-0 wt plants were grown in hydroponics for 5 days, and were subsequently treated for 3 days with no chemicals, 0.1µg/mL bleomycin, 0.1µg/mL bleomycin with 20µg/mL MMC or 0.1µg/mL bleomycin with 100µM $AlCl_3$. Nuclei were harvested from the root tips, embedded in low-melting agarose on glass slides and subjected to alkaline electrophoresis. Slides were stained with SYBR Green and individual nuclei were analyzed. Olive tail moments of 200 nuclei were analyzed utilizing the Comet Assay IV software. The decrease in Olive tail moment in the bleomycin treated samples is proportional to the level of interstrand crosslinking.

Discussion

CHAPTER SEVEN

ALS7 Provides the First Genetic Evidence for a Requirement of Polyamines for Al Resistance

Aluminum toxicity in acidic acids is a global agricultural problem that can inhibit root elongation within hours of exposure, affecting approximately one third of the world's potentially arable lands. Most of the research revolves around understanding the physiological effects of Al toxicity but there has been increased interest in understanding mechanisms of tolerance to find ways to confer greater tolerance in Al sensitive plants. The major advancement in understanding Al resistance focuses on the release of organic acids from the root to the rhizosphere to chelate Al and transport it as a nontoxic compound (Ma 1997, Ma 2000). Further studies were completed to find the transporter that is required for malate release in wheat, *ALMT1*, which confers greater Al resistance (Sasaki 2004, Delhaize 2004). In order to identify other factors that are required for plant Al response, *Arabidopsis* mutants that exhibited Al hypersensitivity were isolated (Larsen 1996). From this study, *ALS3*, which encodes an ABC transporter-like protein and *ALS1*, which encodes a half type ABC transporter were isolated and characterized (Larsen 2005, Larsen 2007), which have both helped our understanding on Al tolerance in *Arabidopsis*.

als7-1, another loss of function mutation was isolated from the same screen that produced *als3* and *als1*. Unlike the preliminary study that was completed on *als7-1* (Larsen 1996), *als7-1* is able to accumulate callose in the presence of Al stress, induce an Al-stress response gene and also accumulate Al. Using map-based cloning, *als7-1* was identified as *At1g72440,* a single based change in *SLOW WALKER2* (*SWA2*), a NOC1/MAK21 homolog that is required for cell cycle progression during female gametophyte development and ribosome biogenesis (Li 2009). Studies on SWA2 have only been done on a heterozygous mutant population, since homozygous mutant seeds arrest in embryo development just prior to the globular stage. It was proposed that SWA2 is a nucleolar protein required for ribosome biogenesis during female gametophyte development due to 31% identity and 53% similarity to yeast NOC1. Attempts were made to functionally complement a yeast *noc1/mak21* mutant with *SWA2* but these were not successful (Li 2009). Additionally, the human homolog CBF could not functionally complement the *noc1* yeast mutant (Edskes 1998). Even though there may be limited sequence similarity, it is most likely that they are functionally and structurally different.

Based on this current study, there is a different hypothesis for the function of *ALS7*. Sequence analysis of *ALS7* of the predicted cDNA of *At1g72440* reveals that it contains a CBF domain, a predicted nuclear localization signal and an ARM-like fold using BLAST and Interpro Scan. CBFs have been shown to be transcription factors in a variety of eukaryotes that bind to a variety of CCAAT boxes with different levels of specificity. Putative CCAAT-box motifs have been identified in a variety of plant genes

and a protein complex has been identified in *Arabidopsis* that binds to the CCAAT motif (Edwards 1998). However, CBFs do not only exist as complexes, but can bind to DNA without any accessory proteins. Utilizing BLAST, it was found that ALS7 has similarity to the CCAAT/enhancer binding protein zeta from rat, human and mouse with each having 33% identity and 51% similarity to *Arabidopsis* ALS7. ALS7 also has 31% identity and 53% similarity to yeast NOC1, but this similarity only covers 61% of ALS7. Additionally, the human CBF (hCBF) covers 88% of the ALS7 gene, indicating there is high similarity between ALS7 and hCBF. The hCBF works in conjunction with proteins such as p53 to control the expression of *hsp70* gene and is growth regulated in HeLa cells. It has been hypothesized that hCBF controls a set of genes that are required for the G1/S stage of the cell cycle (Lum 1990). Since SLOW WALKER2 has been proposed to be involved in ribosome biogenesis yet homologs such as hCBF are directly involved in transcription, it is currently unclear as to what role SWA2 plays in the nucleolus. Northern analyses displayed an abundance of *ALS7* transcript in the flowers and ALS7:GFP fusion had accumulation in the nucleus of root tips. These are the locations of the floral meristem and root meristem that contain actively dividing cells. These features suggest that *At1g72440* is a transcription factor, similar to hCBF that is required not only for stress response but also for plant development. Even though ALS7 may be required for proper development, loss of this factor also increases the sensitivity of the plant to $AlCl_3$.

Based on this knowledge a preliminary GeneChip analysis was performed on Col-0 and *als7-1* to determine which genes might require *ALS7* for proper expression. From

this analysis two genes, *At4g10500* and *At2g26400* were found to have very low expression levels in the GeneChip, qRT-PCR and Northern analyses. However, knockout mutations of both of these factors did not result in a change of phenotype in the presence of $AlCl_3$. *At4g10500* is an uncharacterized member of the 2-oxoglutarate and Fe(II)-dependent oxygenase superfamily that could scavenge reactive oxygen species (ROS) in response to $AlCl_3$ exposure. It has been shown that $AlCl_3$ exposure instantly and continuously induces a massive production of ROS. Over expression of a variety of factors in the antioxidant pathway have resulted in increased Al tolerance in *Arabidopsis* such as glutathione S-transferase and peroxidase (Ma 2008). A phenotype in *At4g10500* knockout was probably not observed due to *Arabidopsis* having multiple factors that are required for the antioxidant pathway.

At2g26400 has been characterized as acireductone dioxygenase 3 (*AtARD3*), which is one of the four members in the ARD family in *Arabidopsis* that are required for methionine (Met) salvage. The Met salvage pathway is critical in plants due to high demand for S-adenosylmethionine (AdoMet) in ethylene, polyamine and phytosiderophore synthesis. During synthesis of any of these molecules, methylthioadenosine (MTA) is formed as a by-product that can be recycled through the Met cycle to regenerate AdoMet. In plants, members of the ARD family were first described in rice. These include *OsARD1,* which is regulated by ethylene, and *OsARD2*, which is constitutively expressed (Sauter 2005). In *Arabidopsis*, four ARD genes were identified as members of the methionine cycling pathway. *AtARD1*, *AtARD2* and *AtARD4* are not regulated by ethylene and transcripts of *AtARD3* were unable to be

detected and further studies were not performed. Previous work has also shown that supplementation of low levels of Met to *mtk*, a mutant that disrupts the Met cycle, can restore the growth rate to wt levels (Bürstenbinder 2007). When Col-0 wt and *als7-1* were grown on low levels of Met, there was a dramatic increase in root length of *als7-1* that only occurred in the presence of $AlCl_3$. Based on Northern analysis, *AtARD3* expression requires *ALS7* in the presence of $AlCl_3$, indicating that plants require Met recycling in the presence of $AlCl_3$. It was attempted to supplement a higher amounts of Met to the same levels reported in Bürstenbinder, 2007, but severe toxicity was observed. Quantitative analysis of Met metabolism in *Lemna paucicostata* has shown that up to 80% of this amino acid is used for the synthesis of AdoMet (Giovanelli 1985). Since *Lemna* is not a higher plant and does not produce ethylene, it is difficult to use their data to determine what the contribution of the Met cycle to the Met and AdoMet pools will be in *Arabidopsis*. When Col-0 wt and *als7-1* were grown with AdoMet in the presence of $AlCl_3$, *als7-1* had an increase in root length upon supplementation, suggesting that the AdoMet pool in this mutation is low.

Due to the increase in root length went *als7-1* was grown in the presence of Al, and the requirement for decarboxylated AdoMet for polyamine biosynthesis it was of interest to determine if polyamines were required for Al tolerance. When Col-0 wt and *als7-1* were grown in the presence of the polyamines spermidine and spermine, there was a two-fold increase in root length that was only observed when seedlings were grown in the presence of 25μM Al and reversed the root growth inhibition due to Al see in *als7-1*. What was even more exciting was the 6-fold increase observed when *als7-1* was grown

on 50μM Al in hydroponics, an extremely high level of Al. On the other hand, difluoromethylornithine (DFMO), an inhibitor of ornithine decarboxylase, which is a key enzyme in putrescine biosynthesis and a precursor of the polyamines spermidine and spermine, caused a reduction in root growth only in the presence of Al. High levels of DFMO can cause root growth inhibition in *Arabidopsis* since high enough levels will reduce polyamine levels to the point where the plant cannot survive, but the level in this study has been previously shown to not be inhibitory to *Arabidopsis* roots (Mirza 1991). This indicates that there is a need to maintain a perfect balance of polyamine levels to maintain Al tolerance in plants. To date there has been limited evidence that polyamines can enhance the plant's ability to tolerate Al stress, possibly because most of the research on Al-tolerance has been focused on anions that can chelate Al, and not cations that would compete with Al.

Polyamines are small aliphatic polycationic molecules found in all organisms except for some Archaea. In plants, polyamines have been described to be involved in cell division, embryogenesis, root formation, fruit development, ripening, and abiotic and biotic stress. Polyamines are also involved in many fundamental cellular processes such as RNA modification, transcription, protein synthesis and the modulation of enzyme activities (Takahashi 2010). The simplest polyamine, putrescine has been found to be required for stress tolerance. In plants, putrescine is primarily synthesized by the enzyme arginine decarboxylase (ADC), but can also be synthesized utilizing ornathine decarboxylase (ODC). In the *Arabidopsis* genome there are two copies of ADC. *ADC1* is constitutively expressed, and *ADC2* is expressed in response to abiotic stress, such as

drought. Loss of function mutants for *ADC2* in *Arabidopsis* results in increased salinity sensitivity, but no reduction of spermine or spermidine levels, while loss of function mutants of both *ADC1* and *ADC2* results in lethality due to the lack of ability to produce polyamines (Urano 2004, 2005).

While putrescine might confer greater tolerance on $AlCl_3$, the two polyamines that are of greater interest due to requirement of the aminopropyl group from decarboxylated AdoMet are spermidine and spermine. Decarboxylated AdoMet is produced by *S*-adenosylmethionine decarboxylase (SAMDC) and it is thought to be the major regulatory enzyme for production of spermidine and spermine. In *Arabidopsis*, two genes encode spermidine synthase. While a mutation in either spermidine synthase does not result in a phenotype, a double mutant causes lethality (Takahashi 2010). Attempts were made to produce an *Arabidopsis* line that overexpressed *SPDS2*, one of the two spermidine synthase genes, under the *ACT2* promoter but the transgenic lines that were created displayed limited Al-tolerance. This could be due to the fact that polyamine levels are tightly regulated, so it is possible that the polyamine of greatest interest in this study, spermine, was not being properly synthesized either due to the regulation of spermine synthase (*SPMS*) and *ACAULIS5* (*ACL5*), or due to a limited pool of AdoMet.

Unlike spermidine, it has been shown that spermine is not required for plant growth under normal conditions (Imai 2004). When spermine deficient plants (*spms/acl5*) were challenged with salt and drought stress, they were more sensitive than wild type (Yamaguchi 2007). This phenotype might be related to the fact that intracellular polyamines can block inward potassium currents across the plasma

membrane of guard cells (Liu 2000). The blocking of ion channels by polyamines has also been reported for vacuolar cation cannels in barley and red beet, and for non-selective cation channels in pea mesophyll cells (Dobrovinskaya 1999, Shabala 2007). This is very interesting since one of the proposed mechanisms of Al toxicity is the alteration of ion channels due to Al at the root. Additionally spermine has another, more significant hypothesized role on the cell, protecting DNA from free radical attack and subsequent mutation (Ha 1998). On the other hand, spermine plays a role as a mediator in defence signaling against plant pathogens. This pathway involves accumulation of spermine in the apoplast, which triggers spermine-derived H_2O_2, upregulation of defense-related genes and programmed cell death by the hypersensitive response (Yamakawa 1998, Kusano 2008). This creates a paradoxical role for spermine, where in the nucleus it scavenges for free radicals, but in the apoplast it acts as a source of free radicals. It cannot be ruled out that spermine may interact with other molecules when it is required for cell death.

The phenotypes of these knockout lines are similar to *als7-1*/*swa2* indicating that low polyamine levels are probably due to not only the increased sensitivity of *als7-1* to $AlCl_3$ but also the homozygous lethal nature of *swa2*. Although there has been no published work relating $AlCl_3$ stress to polyamine levels in *Arabidopsis*, similar work has been completed in other plant species. Polyamine accumulation in response to Al stress has been described in suspension culture of *Catharanthus roseus*. Within four hours of exposure, putrescine levels increased 20-25% and twenty-four hours after $AlCl_3$ treatment, spermine levels increased at least 2 fold (Minocha 1992). In saffron, improved

$AlCl_3$ tolerance was observed with the application of 1mM polyamines in hydroponics, with putrescine being most effective (Chen 2008). At physiological pH, polyamines are positively charged and it is possible that polyamines are binding to negatively charged DNA and aiding in protection during $AlCl_3$ challenge. In acidic soils, $AlCl_3$ and polyamines could also be competing for binding sites at the cell well and cellular membrane preventing uptake of $AlCl_3$.

In this study it was found that treatment with spermine reduces Al uptake in Col-0 wt using ICP-OES. In a previous study with saffron, Al uptake was analyzed using a qualitative method by hematoxylin staining. In that study, exogenous polyamines putrescine, spermidine and spermine were all able to reduce the Al content of saffron roots (Chen 2008). This current work in *Arabidopsis* is the first quantitative evidence that polyamines reduce Al uptake and support the work performed in saffron.

Furthermore, it previously has not been shown that an *in vivo* reduction of polyamines results in Al sensitivity. The loss-of-function *als7-1* mutant provides the first genetic evidence that altered polyamine content has a direct relationship to the capability of plants to grow in an Al toxic environment. *als7-1* has a significantly lower level of spermine within its roots. Ideally it would have been interesting to measure the levels of polyamines at the root tip since the site of Al-toxicity is at the root tip. Unfortunately it would be incredibly difficult to isolate enough tissue to complete this analysis or to even isolate the same area of the root for each seedling. It is possible that there are even lower levels of spermine at the root tip of *als7-1*.

Given the evidence that spermine is required for plant Al tolerance, it is possible that application of spermine to agriculturally relevant plant species could be beneficial for agriculture in regions with acidic soils. Although there are no studies with foliar application of polyamines as a method of Al tolerance in plants, there have been similar studies done with heavy metal tolerance. Foliar spraying with 0.25 to 0.50mM spermidine on cattail (*Typha latifolia* L.) that were grown under Cd^{2+} stress was studied. The generation of superoxide anion, H_2O_2 and malondialdehyde (MDA), a product of lipid peroxidation in both leaves and caudices were decreased after treatment with spermidine. It was suggested that exogenous spermidine elevated the tolerance of *Typha latifolia* L. grown in Cd^{2+} by increasing glutathione reductase activity and increasing the glutathione level (Tang 2005). Additionally, sunflower leaf discs that were treated with spermidine or spermine reversed the cadmium and copper-induced thiobarbituric acid reactive substances (TBARS) increase. Also treatment with 1mM spermidine or spermine was able to restore activities of glutathione reductase and superoxide dismutase to levels that were seen before treatment with copper or cadmium (Groppa 2001). This previous work as well as this current study clearly demonstrates that endogenous polyamines play a critical role in mediating Al resistance and it is likely that altering polyamine content in roots is an effective strategy for improving crop productivity in Al toxic environments.

CHAPTER EIGHT

DNA Crosslinks are Detected by ALT2, which Indicates that Al is a Weak DNA Crosslinker

Even though it is important to identify factors that confer plant Al tolerance to further understand the stress response pathway, it is also important to identify factors in plants that can enhance Al tolerance. To date, there is little known about how plants respond to internalized Al, since there are many predicted binding sites for Al within the cell. By using an *als3-1* suppressor screen, mutations can be easily identified that confer enhanced $AlCl_3$ tolerance.

The second mutation that was isolated that suppresses *als3-1* phenotype, *alt2-1,* was characterized in this study. Using map-based cloning, *alt2-1* was identified as a WD40 protein that has not been described fully due to current lines being embryonic lethal or dying shortly after germination. It was previously characterized as *tanmei/emb2757* (*tan*) a mutation that causes defects in both embryo and seedling development. *TAN* functions in both the early and late phases of embryo development and the *tan* mutant embryos share many characteristics with the *leafy cotyledon* (*lec*) class of mutants since they accumulate anthocyanin, are intolerant of desiccation, form trichomes on cotyledons, and have reduced accumulation of storage proteins and lipids. The *tan* mutants die as embryos, but immature mutant seeds can be germinated in culture yet the seedlings are defective in shoot and root development, their hypocotyls fail to elongate in the dark, and they die as seedlings (Yamagishi 2005).

In *Arabidopsis* there are approximated 237 WD40 repeat proteins, representing a class of proteins that are involved in mediating interactions between other proteins (van Nocker 2003). They are a very diverse superfamily of regulatory proteins that play roles in signal transduction, nuclear export, RNA processing, chromatin modification, flowering, apoptosis, and many cellular processes and mechanisms. The average WD40 repeat protein has between four and sixteen WD repeats (WDR), with ALT2 containing seven WDRs. The basic structural unit of a WD40 repeat protein is four antiparallel beta strands, which fold into a higher order structure called a beta propeller (Higa 2007). This structure is conserved among all WD repeat proteins, suggesting that the large surface area created by the beta propeller is useful for organizing, stabilizing and interacting with other proteins.

WD40 proteins have been shown to associate with a variety of protein complexes, including E3 ubiquitin ligases. In eukaryotes, proteins are targeted for degradation via the ubiquitination-proteasome system. This process requires the activities of ubiquitination activating enzyme (E1), ubiquitin conjugating enzyme (E2) and ubiquitin ligase (E3). The specificity of the pathway relies on E3 ligases since they bind to the substrate. In plants, cullins, which are part of a family of scaffolding proteins, form the largest family of E3 ligase complexes. E3 ubiquitin ligases are based on Cullins 1, 2, 3 or 4. The recruiting mechanism in Cullin 4 (CUL4) is not well understood in plants. CUL4 has been shown to associate with adaptor proteins to recruit substrate receptors. One of these adapter proteins is DDB1 (Damaged DNA Binding 1). Recent studies in mammals have shown that WD40 repeat proteins, such as DDB2 (Damaged DNA Binding 2)

associate with CUL4-DDB1 complexes and act as substrate targeting subunits of CUL4-DDB1 complex (Higa 2007). Most of the WD40 proteins that associate with CUL4-DDB1 contain a conserved motif of 16 amino acids called the DWD (DDB1 binding WD40) box. There are four highly conserved residues Asp-7 (or Glu), Trp-13 (or Tyr), Asp-14 (or Glu) and Arg-16 (or Lys) with Arg-16 being required for DDB1 binding (He 2006).

Recently, a genome wide analysis was completed in *Arabidopsis* that identified a group of WD40 proteins that potentially associate with CUL4-DDB1 complexes. A group of 85 putative DWD proteins were found in *Arabidopsis* and were classified into five subgroups based on phylogenetic tree analysis (Lee 2008). ALT2 contains a DWD domain, and is one of 17 that have a similar structure. This research did not specifically target ALT2, but a representative protein from each subgroup was shown to bind to DDB1A *in vitro* using yeast two-hybrid analysis (Lee 2008). Analyses with yeast two-hybrid and *in vitro* pulldowns show that ALT2 does not bind to DDB1A but there are two copies of DDB1 in *Arabidopsis*, DDB1A and DDB1B. Both proteins are highly similar and using *in vitro* pulldowns, it was found that ALT2 binds to very weakly to DDB1B and not DDB1A.

CUL4-DDB1 complexes are not well described in *Arabidopsis*, but there has been recent work that has shown a relationship between the CUL4-DDB1A-DDB2 complex in *Arabidopsis* to DNA repair in response to UV damage. Even though studies have shown that mutations in AtATR cause increased UV sensitivity it was still of interest to understand other CUL4-DDB1 complexes in *Arabidopsis* (Molinier 2008). This also

provides a starting point to find other factors that might be required for detecting DNA damage in response to $AlCl_3$ challenge. Under normal growth conditions, DDB1A resides in the cytoplasm while DDB2 and CUL4 reside in the nucleus. This study found that upon UV exposure, DDB2 recognizes the lesions created due to UV damage, which causes DDB1A to shuttle into the nucleus in an ATR dependent manner. This event then allows for degradation of DDB2 by the 26S proteasome and probably allows for subsequent steps to occur in nucleotide excision repair process (Molinier 2008).

This study gave a link between DWD proteins and AtATR in plants, which suggested that *ALT1* (*AtATR*) and *ALT2* are functioning in the same pathway in detecting DNA damage in response to $AlCl_3$ stress. In support of this, a double mutation of *alt1-1* and *alt2-1* showed no increased $AlCl_3$ tolerance compared to the single mutants, further suggesting that these two factors are both part of the same pathway. There are some differences between *alt1-1* and *alt2-1* such as their tolerance to heavy metals and sensitivity to HU. Previous studies have shown that *alt1-1* is hypersensitive to HU but *alt2-1* is not hypersensitive to short term HU treatment compared to Col-0 wt and is able to induce *CycB1;1* accumulation and stabilization. In addition, *alt1-1* is tolerant to low levels of both $NiCl_2$ and $CdCl_2$ while *alt2-1* is only slightly tolerant. Both of these factors suggest that *ALT1* is a master factor required for the detection of a wide range of DNA damage, while *ALT2* is specifically targeting DNA damage due to $AlCl_3$ challenge.

To confirm that ALT2 functions similarly to other DWD proteins, yeast-two-hybrid analyses and *in vitro* binding assays were performed. Unlike previous studies on DWD proteins, ALT2 displayed no interaction with DDB1A in both the yeast-two-hybrid

and the *in vitro* binding assays. It is possible that the system used for the yeast-two-hybrid did not produce functioning proteins, or the correct vectors were not used. According to Dr. Jae-Hoon Lee of the Deng lab, DDB1A has to be in the bait vector or an interaction will not be observed. Also the empty vector causes some background β-galactosidase activity, but when a negative control is added, the β-galactosidase activity is almost abolished (personal communication and Lee 2008). None of these results were observed in this study, so it is possible that ALT2 could still indeed interact with DDB1. In the *in vitro* binding assays, an extremely weak interaction was observed between ALT2 and DDB1B. It is difficult to tell if this interaction is a positive interaction since it was so weak. Additionally, a stronger interaction was observed between ALT2 and DDB2, but it was still a weak interaction. It is possible that ALT2 is directly interacting with DDB2 since it has previously described that there are multiple factors that have been shown to interact with DDB2 such as XPC, CSN, Ku70, and Ku86 in mammals (Takedachi 2010). In support of these two interactions, T-DNA insertion mutations *ddb1b* and *ddb2* display slight Al tolerance, indicating they are playing a minor role in the plant's response to Al stress.

Since a link was been shown between ALT2 and AtATR, it was important to complete the same experiments that were performed on the *alt1-1* mutation on the *alt2-1* mutation. ATR responds to single-stranded DNA breaks and replication fork poisons, making knockout mutants susceptible to hydroxyurea, aphidicolin, UV-B and γ-radiation (Culligan 2006). Upon sensing the appropriate form of DNA damage, ATR phosphorylates its downstream targets to activate the G2/M cell cycle checkpoint and

DNA damage repair pathway (Lydall 2005). Like the *alt1-1;CycB1;1* plants grown in the presence of Al, the *alt2-1;CycB1;1* plants displayed no altered pattern of GUS staining when compared to untreated plants. This was in contrast to the dramatic upregulation of *CycB1;1* in Col-0 wt when they were grown in the presence of Al. It can been inferred that the *alt2-1* mutation affects the ability to induce *CycB1;1* expression in the presence of Al and is failing to arrest at G2/M DNA damage checkpoint. Although this suggests that the *alt2-1* mutation causes a defect in properly inducing *CycB1;1* in all types of DNA damage, *alt2-1* does have the capacity to induce *CycB1;1* after treatment with HU, indicating that *alt2-1* is specifically required for induction of *CycB1;1* in the presence of Al-mediated DNA damage. *CycB1;1* may play a further role in DNA damage as cyclin B proteins appear to be upregulated in response to genotoxic treatments (Culligan 2006). In Al-exposed roots, the expression of *CycB1;2* remained relatively unaffected whereas *CycB2;1* transcription was downregulated in Col-0 wt. Interestingly, *CycB* expression in Al-treated roots of *alt1-1* displayed elevated expression for both *CycB* genes. This may indicate enhanced cell cycle progression in *alt1-1* (Rounds 2008). If this is also occurring in *alt2-1* plants, the hypothesis that normal or enhanced mitosis could be occurring is supported by the healthy appearance of roots grown in the presence of Al and the maintenance of the quiescent center. This suggests that *alt2-1*, like *alt1-1* fails to properly respond to Al-dependent DNA damage and this failure enables the roots of *alt2-1* to continue growing in the presence of Al.

With the characterization of these two mutants, the biggest concern became identifying the type of DNA damage that occurs as a result of Al accumulation. It seems

counterintuitive to enhance a plant's tolerance to an agent that causes DNA damage by reducing the function of a factor that is necessary for DNA damage detection, so it is easy to assume that Al is not an agent of DNA damage. The data from the Comet assay displays that DNA fragmentation is occurring in response to Al treatment, but both the *alt1-1* and *alt2-1* mutations do not affect the accumulation of DNA fragmentation. Treatment with bleomycin, a mimic of radiation also did not cause an altered growth on *alt2-1* plants compared to wt. These data indicate that Al-mediated damage that is detected by AtATR and ALT2 is not due to DNA fragmentation. In an attempt to further identify the type of Al-mediated DNA damage, other factors have been previously characterized in *Arabidopsis* that have been shown to be required for DNA damage repair, AtUVH1 (AtRAD1) and AtRAD17, were analyzed.

AtUVH1 (AtRAD1) is the *Arabidopsis* homolog of *Saccharomyces cerevisiae* RAD1, *Schizosaccharomyces pombe* RAD16 and human XPF, all of which are enzymes required for DNA repair and recombination processes. *AtRAD1* is an endonuclease in nucleotide excision repair, involved in the excision of UV-induced damage. The *rad1* mutants are more sensitive to UV light and to mitomycin C, suggesting an active role of *AtRAD1* in plant nucleotide excision repair like pathway and recombination (Gallego 2000). When *uvh1-1* plants were grown in the presence of Al, there was slight hypersensitivity at moderate to high levels of Al. This suggests that a minor portion of the repair that is performed by *AtRAD1* is required for Al tolerance, possibly due to DNA crosslinks since *alt2-1* mutants are not sensitive to double and single stranded DNA breaks by bleomycin, which mimics γ-irradiation or UV damage.

AtRAD17, an *Arabidopsis* homolog of yeast RAD17, is involved in DNA checkpoint control in yeast and human cells and is necessary for S phase and G2/M arrest in response to both DNA damage and stalled DNA replication. *AtRAD17* mutants show increased sensitivity to bleomycin and mitomycin C, which suggests that *rad17* plants cause a defect in DNA repair in plant cells. Also the mutant displays a delay in the general repair of double-strand breaks, which is associated with a deficiency in non-homologous double strand break repair (Heitzeberg 2004). Like the AtUVH1 mutant, *rad17-1* mutants displayed hypersensitivity to Al, but to all concentrations of Al and to a greater extent. Since *alt2-1* mutants are not hypersensitive to bleomycin, it further suggests that the damage caused by Al could be similar to MMC.

Using the previously published work completed on AtRAD17 and AtUVH1 and their sensitivity on Al, *alt2-1* was challenged with the crosslinking agents MMC and CDDP. Both chemicals resulted in severe hypersensitivity of *alt2-1* to these agents, while minor sensitivity was observed with Col-0 wt, which was unlike any other chemical treatment tested on *alt2-1*. This was very interesting because *alt2-1* displays extreme tolerance on Al, but extreme sensitivity to interstrand and intrastrand crosslinking agents. This suggests that ALT2 is required for detection of DNA crosslinks and not the actual repair. If ALT2 was required for actual repair, *alt2-1* mutants would be hypersensitive to Al, since detection would occur, cell cycle would be arrested and recruitment of repair machinery would follow. This would cause *CycB1;1* stabilization since the cell cycle needs to be halted in order for repair to occur. When *alt2-1;als3-1* carrying ALT2:GFP were challenged with $AlCl_3$, MMC and CDDP, all three chemicals

were able to cause ALT2:GFP accumulation in the nucleus. Additionally, using a modified protocol of the Comet assay designed to measure DNA interstrand crosslinks, it was determined that Al is a weak DNA crosslinker *in vivo*. MMC, a potent interstrand crosslinker, caused a 93.0±0.04% decrease in the tail moment and 38.8±0.06% decrease in the tail moment of the Al treated nuclei. The decrease in tail moment upon treatment with Al, although significantly lower than the MMC treated cells suggests that Al is a weak DNA interstrand crosslinker.

The culmination of these experiments provides an *in vivo* link between Al and DNA crosslinking. Based on the *CycB1;1* results, growth of *alt2-1* on crosslinking agents and the GFP studies, ALT2 is required for detection of DNA crosslinking events. It is possible that "ignoring" the Al crosslinking event has limited short-term consequence in *Arabidopsis*. When a potent and permanent crosslinking agent is added, if the plants "ignore" those events such as in *alt2-1*, transcription and replication would permanently halted causing hypersensitivity to those agents due to the inability to resolve blocked replication forks.

Proposing that Al acts as a DNA crosslinker is not a new hypothesis, but identifying a genetic link and having *in vivo* evidence is novel. Starting in the 1970s, scientists made a link between Alzheimer's disease and accumulation of aluminum (Crapper 1973). From these studies, it was discovered that 95% of Al accumulation in the grey matter of the mammalian brain is within the nuclear compartment. Also that 14% of the total tissue Al associates with is euchromatin, the portion of transcriptionally active chromatin. This indicates that if Al concentration in this compartment increases

that it can have a powerful impact on gene transcription and DNA repair. Al *in vitro* can also cause linker histones to bind more tightly to DNA causing further silencing of gene expression (Crapper McLachlan 1989). This work then led to the many *in vitro* studies that demonstrated Al acts as an interstrand and intrastrand DNA crosslinker. Al forms at least three different complexes with DNA; Complex I occurs at high pH and displays helix-stabilizing characteristics of a phosphate-binding metal such as Mg^{2+}, Complex II occurs low pH and exhibits properties similar to base-binding metals (destabilization and crosslinking) and Complex III that occurs at range of different pHs and combines features of both complex I and II. Of these three complexes, Complex II is the most interesting because it occurs at pH < 6, contains high aluminum levels of > 0.4 Al(III)/DNA(P) and forms interstrand crosslinks with DNA of all base compositions (Karlik 1980, Karlik 1989). To further demonstrate that Al is causing interstrand DNA crosslinking, electron microscopy was utilized to examine the morphological effects of Al on DNA. Using concentrations of Al that have been reported to be encountered in the brain cells in Alzheimer's disease it was shown that even at room temperature double stranded DNA aggregation is present. Studies were also completed with heated samples in the presence of Al and the DNA-Al complexes displayed compaction and the formation of toroidal (doughnut) structures, and that these structures can be reversed by chelation (Karlik 1989). This indicates that although Al is a potent crosslinker, the effects of Al on the DNA are completely reversible.

Interstrand crosslinks are a particularly deleterious type of DNA lesion since they covalently link both strands of the DNA helix together. This prevents strand separation

and as a result, interstrand crosslinks are extremely cytotoxic, particularly for proliferating cells since this prevents vital cellular processes such as DNA replication and transcription. Unfortunately, crosslink repair is not well understood but there are several DNA repair pathways that have been described in mammalian systems for the repair of DNA damage caused by radiation and reactive chemicals. These pathways include nucleotide excision repair, transcription coupled repair, base excision repair, mismatch repair, nonhomologous end joining, homology directed repair, single strand break repair and translesion synthesis. Although the repair of crosslinks is not well understood, it is known that some or all of these repair pathways are activated once a crosslink is detected (Muniandy 2010).

One of the major issues with understanding how organisms repair crosslinked DNA is due to the severity of the crosslinking event since some interstrand crosslinking agents cause extreme helical distortion and other agents cause less of a distortion. Given that helical distortion is an important determining factor of DNA repair, this structural variability can make it difficult to compare results from experiments with different agents. Additionally, crosslinking agents produce more than just interstrand crosslinks, and in some compounds interstrand crosslinks are also usually a minority product of the agent. This can skew the interpretation of experiments. For example, mitomycin C has six possible DNA adducts, with the interstrand crosslinking event accounting for 90% of the products, 4 being mono adducts and one being an intrastrand crosslink event between adjacent guanines. Cisplatin reacts with a range of cellular targets including RNA, protein, phospholipids, as well as DNA. Additionally, the major DNA adducts include

1,2 intrastrand crosslinks at GpG (65%) and ApG (25%) sites. Interstrand crosslinks occur up to 8% of the time and form at GpC sites linking the N7 of both guanines. The interstrand crosslinks formed by cisplatin are not stable and can spontaneously convert to intrastrand crosslinks. Finally, crosslink repair can occur at any phase of the cell cycle but some repair pathways are only operative during certain phases of the cell cycle (Muiandy 2010).

There are four major methods that have been described to detect and repair interstrand DNA crosslinks, which are summarized in Figure 52. The major event for crosslink repair is unhooking the crosslink so it can be excised and the gap can be filled. In the absence of replication, the crosslink is detected as a lesion that distorts the local structure of the DNA duplex (Figure 53A and B). This causes activation of base excision repair, nucleotide excision repair and mismatch repair damage detection pathways. One of these pathways, NER has been thoroughly described with the CUL4-DDB1^{DDB2} machinery and the detection of UV-lesions. Unfortunately, many DNA crosslinks actually stabilize the DNA duplex and in the previously described nucleotide excision repair pathways, the bases that are part of the lesion are flipped out so excision can occur. It is currently unknown how this occurs in the repair of DNA crosslinks (Muniandy 2010). The detection and repair pathway of crosslinks that has received much more attention is caused by the encounter of a blocked replication fork (Figure 53C). Defects in this pathway cause the human disease Fanconi Anemia (FA) a disorder that causes cancer predisposition, progressive bone marrow failure, congenital developmental defects, chromosomal abnormalities, and hypersensitivity to DNA interstrand

Figure 53. Intrastrand crosslinks can be detected and repaired in four basic methods. (A) In the absence of replication, the distortion of the DNA structure caused by the lesion attracts protein(s) involved in the global damage surveillance of DNA. This process has been shown to involve proteins of the NER pathway, with XPC leading the initial recognition. The first incision step on either side of the lesion on one strand of the duplex by the XPF-ERCC1 endonuclease, and generates a gapped structure, which serves as a substrate for bypass polymerases. The now flipped out monoadduct-like structure can be recognized by DDB2 and possibly by also glycosylases such as MPG or Neil1. The nucleotide excision repair pathway will start a second cycle of repair and remove the remaining adduct on the opposite strand. (B) Stalling of RNA polymerases at the site of lesion during transcription can also serve as a means of interstrand crosslink recognition in non-replicating DNA. (C) and (D), a stalled replication fork, either due to a single or dual fork encounter, causes activation of the Fanconi Anemia (FA) pathway and recruitment of proteins such as Mus81-EME1/2, Snm1B, and MRN. FANCM-FAAP24 complex, which then becomes part of the FA core complex is thought to recognize the blocked replication fork. The FA core complex recruits the FANCD2 and FANCI proteins, which are modified by ubiquitination and phosphorylation. The interstrand crosslink is incised by XPF-ERCC1 and Mus81-EME1 on the leading strand, generating a double strand break at the replication fork. In the case of converging forks (D), the first incision cycle may occur on either strand. The gapped structure will be filled in by lesion bypass polymerases, including polζ, polκ, polι, polN, polη and Rev1. When a single fork is stalled by the interstrand crosslink, polymerase(s) will extend a parental strand to fill the gap. When two forks converge on the ICL a leading daughter strand is extended to bypass the lesion. Upon removal of the remaining single adduct on the opposite strand using the nucleotide excision repair pathway, the broken fork will be reconstructed by recombinational repair.

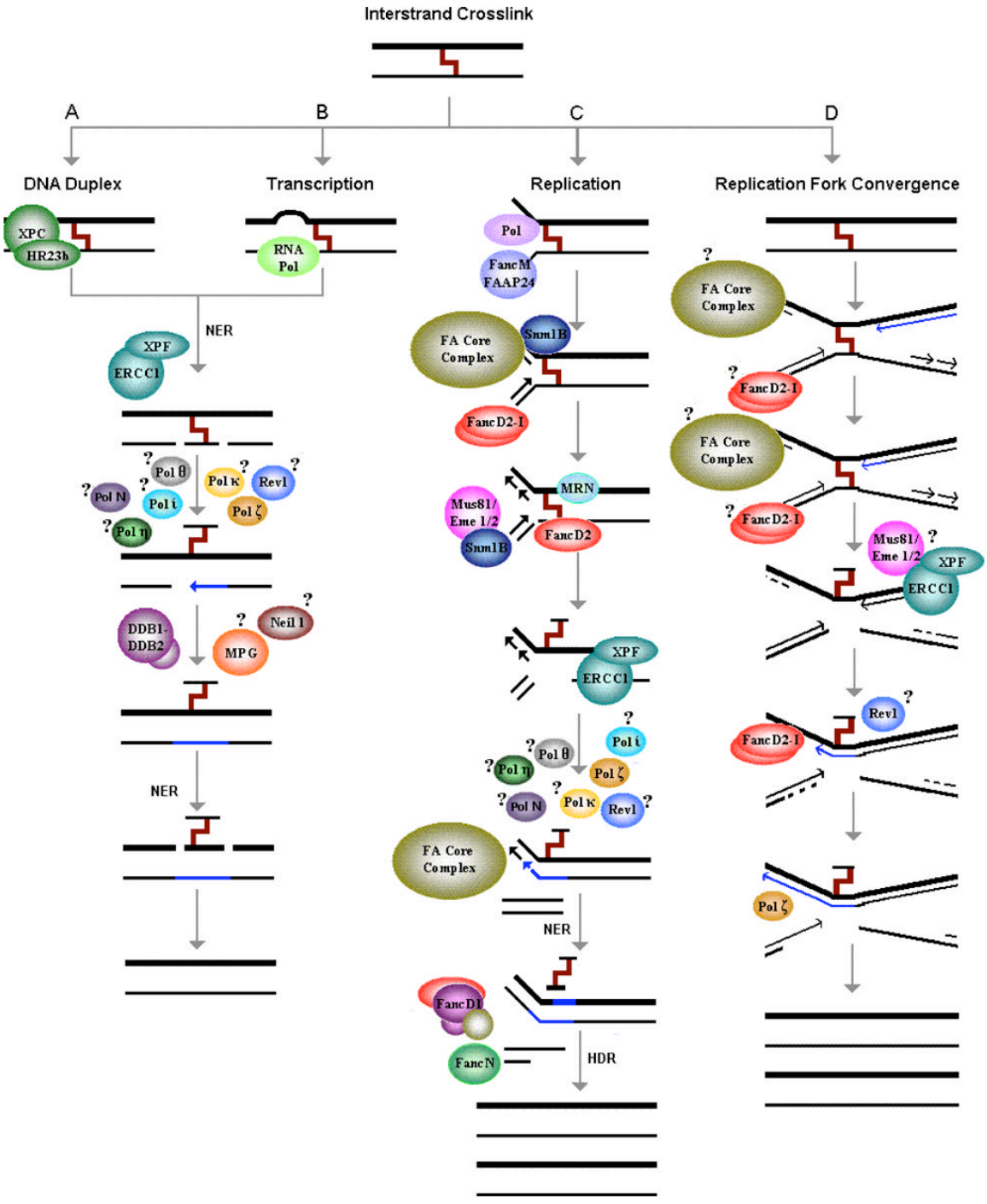
Interstrand Crosslink
A
B
C
D
DNA Duplex
Transcription
Replication
Replication Fork Convergence
XPC
HR23b
RNA Pol
Pol
FancM FAAP24
FA Core Complex
Snm1B
FancD2-I
NER
XPF
ERCC1
Pol θ
Pol κ
Rev1
Pol N
Pol ι
Pol ζ
Pol η
MRN
Mus81/ Eme 1/2
FancD2
DDB1-DDB2
MPG
Neil 1
NER
HDR
FancD1
FancN

crosslinking agents. This pathway contains a family of 15 FANC proteins that are required for the detection and repair of DNA crosslinks. The basic overview of this repair pathway involves activating a FANCM–ATR-dependent S-phase checkpoint, mediating enzymatic replication-fork breakage and crosslink unhooking, filling the resulting gap by translesion synthesis by error-prone polymerase(s), and restoring the resulting one-ended double-strand break by homologous recombination repair (Thompson 2009). Finally another possibility for the detection and repair of DNA crosslinks is the encounter of a crosslink by two converging replication forks (Figure 53D). It appears that nucleotide excision repair pathway is not functioning in the repair of this type of encounter. In this pathway, two converging replication forks stall and translesion bypass synthesis occurs using the nascent leading strand as the primer. To unhook the crosslink a double sided double strand break occurs and repair occurs by nonhomologous end joining (Raschle 2008).

Considering the previous work on Al acting as a DNA crosslinker and the current work on DNA crosslink repair in mammalian systems, a proposed model of Al-mediated crosslinking and detection has been made. Upon Al treatment, the Al enters the cell, and potentially fluxes on and off of the DNA either mimicking crosslinking or acting as a weak crosslinker. ALT2 and/or AtATR detect the crosslinking event by recognition of a stalled or collapsed replication fork. This initiates *CyclinB1;1* stabilization and the DNA repair pathway for crosslinks. It is also possible that ALT2 is required for detecting crosslinking in the presence of replication and during global damage surveillance of DNA. In the case of the global damage surveillance of DNA, ALT could recognize the

distortion, this recruits an endonuclease to excise the crosslink and help recruit DDB2 to the lesion caused by Al binding to the DNA. Repair then occurs using nucleotide excision repair after the recruitment of the CUL-DDB1 complex. In *alt2-1* plants, the Al-mediated DNA crosslinking event is not property detected. Since Al is not a permanent DNA crosslinker or a weak crosslinker, the *alt2-1* plants can ignore this stress with minor immediate consequence. The blocked replication fork could eventually become unblocked or the DNA lesion caused by Al could dissipate once Al fluxes off of the DNA.

Currently little is known on how these detection and repair pathways function in *Arabidopsis*, possibly because many of T-DNA knockout lines are homozygous lethal and the lack of plant homologs for previously characterized mammalian factors. Many of the factors characterized in plants such as RAD5A, MUS81 and RECQ4A are members of the actual repair pathway, and factors required for the detection of crosslinks such as AtATR have only been described to be involved in the detection of DNA damage due to γ-irradiation, UV-B, Al, and telomere maintenance (Mannuss 2010, Furukawa 2010, Sakamoto 2009, Rounds 2008, Vespa 2005). Also, plants differ greatly from animals in terms of cell differentiation so DNA repair strategies might have a different impact on cell fate, even though these repair strategies are conserved among higher eukaryotes. It is likely that the ALT2 mediated detection and repair that is completed by replication is through a pathway similar to what has been characterized in mammalian systems for FA (Figure 54). There have been a few members of the FA pathway that have been characterized that exhibit altered growth patterns in the presence of Al, such as AtATR.

Figure 54. The Fanconi Anemia repair pathway. (1) An interstrand crosslink is formed. (2) The interstrand crosslink physically blocks DNA replication, which causes the activation of ATR. ATR phosphorylates a number of proteins, including FANCD2. Phosphorylated FANCD2 is then monoubiquitinated by the FANCL subunit of the Fanconi Anemia (FA) core complex. This triggers the accumulation of numerous proteins involved in homologous recombination and translesion synthesis creating nuclear foci. (3) The blocked replication fork also causes the creation of a double strand break, which occurs by incision of one of the template strands upstream of the crosslink by an endonuclease (depicted as scissors). (4) To separate the two template strands, a second incision needs to occur, so the crosslinked DNA is unwound by a helicase such as FANCM. (5) The interstrand crosslink is then unhooked by a second incision that occurs on the same strand but on the other side of the crosslink likely by the ERCC1-XPF endonuclease. This is facilitated by RPA, the single stranded binding protein that dictates which strand is cut. (6) The second incision creates a gap and a new 3′ end that can be used to prime DNA synthesis. (7) An error-prone translesion polymerase fills in the gap to restore the damaged template strand. (8) The translesion polymerase frequently inserts incorrect bases, creating a mutation at the site of the damage. (9) The interstrand crosslink is unhooked by hydrolysis or nucleotide excision repair and strand integrity is restored. Double strand break repair can now occur by homologous recombination. This is initiated by the resection of the broken end to yield a 3′ single-strand overhang able to pair with its sister chromatid. (10–11) Repair requires the homologous-recombination machinery, including RAD51, BRCA1, BRCA2, PCNA, and RPA. The FANCJ helicase is also probably involved at this step. (12) The resolution of Holliday junction recombination intermediates permits replication to continue and may or may not result in the formation of a sister-chromatid exchange. Deubiquitination at the end of S phase turns the pathway off. Copy by Laura J. Niedernhofer, Astrid S. Lalai, and Jan H.J. Hoeijmakers, 2005.

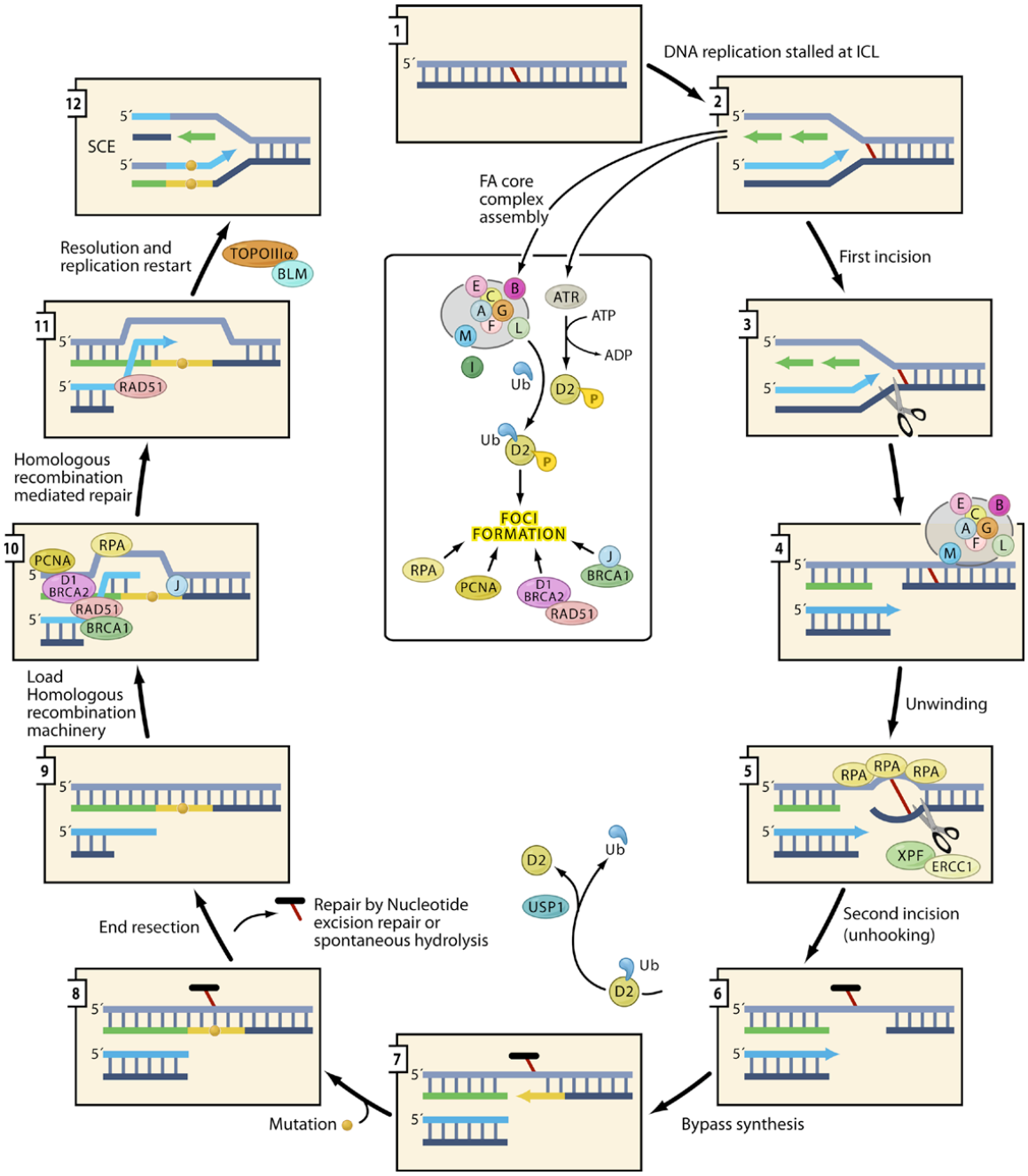
1
5´
DNA replication stalled at ICL
2
5´
5´
FA core complex assembly
First incision
3
5´
5´
E
C
B
A
G
F
M
L
I
ATR
ATP
ADP
Ub
D2
P
FOCI FORMATION
RPA
PCNA
D1 BRCA2
J
BRCA1
RAD51
4
5´
5´
Unwinding
5
5´
5´
RPA
RPA
RPA
XPF
ERCC1
Second incision (unhooking)
6
5´
5´
Bypass synthesis
7
5´
5´
Mutation
8
5´
5´
End resection
Repair by Nucleotide excision repair or spontaneous hydrolysis
9
5´
5´
Load Homologous recombination machinery
10
5´
5´
PCNA
RPA
D1 BRCA2
J
RAD51
BRCA1
Homologous recombination mediated repair
11
5´
5´
RAD51
Resolution and replication restart
TOPOIIIα
BLM
12
SCE
5´
5´
D2
Ub
USP1
Ub
D2

There are five members of the core FA complex that display sequence homology to factors in *Arabidopsis*. These include FANC-M, FANC-L, FANC-D2, FANC-D1 (BRCA2), FANC-J/BRIP1, all of which have not been previously characterized except for BRCA2A and BRCA2B (Knoll 2011, Siaud 2004, Wang 2010). Although there are a few members that do have limited homology to the FA core complex, the vast majority of factors that have been previously characterized in mammalian systems do not have homologs in plants. With this current work it is evident that Al can be used as an effective model to identify and characterize other factors that are required to detect DNA crosslinks in plants and will provide insights about the strategies that plants set in action to cope with this environmental challenge.

Materials and Methods

Growth Media and Conditions

For all soaked gel and hydroponic experiments, seedlings were surface sterilized before planting. Seeds were immersed in 70% ethanol and then washed 4 times with sterile water. Seeds were then soaked in 50% bleach (Clorox) for 5 minutes, after which seeds were washed 4 times with water. Seeds were wrapped in foil and imbibed at 4^{o}C for 3 days before planting.

The Al-screening medium was prepared by pouring a lower gel layer consisting of 80mL of nutrient medium (pH 4.2) plus 0.125% gellan gum (Gel-Gro, ICN Biomedicals) in Nunc Lab-Tek Extra-Depth Polystyrene Dishes 100x25mm (Fisher Scientific, Pittsburg, PA). Nutrient medium consisted of 2mM KNO_3, 0.2mM KH_2PO_4, 2mM $MgSO_4$, 0.25mM $(NH_4)_2SO_4$, 1mM $Ca(NO_3)_2$, 1mM $CaSO_4$, 1μM $MnSO_4$, 5μM H_3BO_3, 0.05μM $CuSO_4$, 0.2μM $ZnSO_4$, 0.1μM $CaCl_2$, 0.02μM Na_2MoO_4, 0.001μM $CoSO_4$, and 1% sucrose. Al was introduced by overlaying the solidified lower layer with 20 mL of "soak solution" consisting of the nutrient solution medium described above but with 0.75mM $AlCl_3$. To adjust the pH of the soak solution, the amount of base (0.1N KOH) to be added was determined empirically by adjusting the pH on an aliquot of the soak solution containing 0.75mM $AlCl_3$. The amount of base determined from the trial pH adjustment was added to the actual soak solution prior to adding $AlCl_3$. This was done to

prevent the formation of the very toxic polymeric Al species $AlO_4Al_{12}(OH)_{24}(H_2O)_{12}^{7+}$ called Al_{13} (Bertsch 1986, Bertsch 1987, Parker 1989) at high pH. The soak solution was allowed to equilibrate with the lower layer for 2 days and was then poured off. This method was used for all concentrations of $AlCl_3$ for plants grown in a gel soaked environment. For media that was supplemented with methionine (Met), 10μM Met was added to both the lower gel layer and soak solution.

In hydroponics experiments, Al-screening media was prepared as above without gellan gum and $AlCl_3$. Seeds were sowed on 250-μm mesh, polypropylene screen (Small Parts, Inc., Miami Lakes, FL). After 6 days of growth, screens were transferred to new Al-screening media supplemented with either 0μM, 25μM $AlCl_3$ or 50μM $AlCl_3$. In polyamine experiments, 0μM, 25μM or 50μM $AlCl_3$ supplemented with either 0μM or 25μM spermine or spermidine was added to the media on the first day of growth. For polyamine inhibition, 1.5mM difluoromethylornithine (DFMO) was added to 0μM or 25μM $AlCl_3$ hydroponics.

For treatment with 15 μg/mL mitomycin C (Fisher Scientific, Pittsburg, PA), 0.1μg/mL bleomycin (EMD Chemicals, Gibbstown, NJ), or 5μM cisplatin (Sigma-Aldrich, St. Louis, MO) were added to plant nutrient media plus sucrose (PNS). Seeds were sowed and allowed to grow for seven days, after which roots were measured.

For other experiments seeds were planted on plant nutrient media plus sucrose (PNS), which consisted of 5mM KNO_3, 2.5mM KH_2PO_4, 2mM $MgSO_4$, 2mM $Ca(NO_3)_2$, 50μM FeEDTA, 1μM $MnSO_4$, 100nM $CaCl_2$, 100nM $CoSO_4$, 5nM H_3BO_3, 50nM $CuSO_4$, 20nM $NaMoO_4$, 0.8M Sucrose, 0.8% agar. Plants were grown in 24-hour light at

20°C in I-36LLVL biological incubator (Percival Scientific, Perry, IA). After one week, plants were repotted in Sunshine Special Blend potting soil with controlled release fertilizer, 15-9-12 + minors (Lehle Seeds, Round Rock, TX). Plants were grown in 24-hour continuous light at 22°C in a plant growth room with Sylvania Gro-Lite fluorescent bulbs until maturity.

Identification of *als7-1* and *alt2-1*

To generate the *als7-1* mutation, Col-0 wt seeds were treated with EMS. M_2 seedlings were screened for mutants with increased sensitivity of Al by using a two-layer gel system. The lower layer consisted of the screening media as previously described soaked with 0.75mM $AlCl_3$ and the upper layer consisted of the screening media without $AlCl_3$. EMS treated seeds were planted around the periphery of the plates and were grown for 6 days at 20°C with a day/night cycle of 16 hrs/8 hrs. After 6 days, seedlings with roots that grew through the upper layer but not the lower layer were marked. The marked seedlings were then allowed to grow for an additional 24 hours. Seedlings that did not grow significantly were rescued on nutrient media. After 2 weeks, putative mutants were transferred to soil and were selfed. M_3 seeds were collected from each mutant and were screened using the same 2-layer gel system. One of the lines that was unable to penetrate through the $AlCl_3$ layer was then further characterized and named *als7-1*.

To generate the *alt2-1* mutation, *als3-1* seeds were treated with EMS. M_2 seedlings were screened for mutants that suppressed the hypersensitivity of *als3-1* to Al

on 0.75mM $AlCl_3$ gel soaked plates. EMS treated seeds were planted around the periphery of the plates and were grown for 7 days at 20°C with a day/night cycle of 16 hrs/8 hrs. After 7 days, seedlings with roots that grew to the bottom of the plate were rescued on nutrient media. After 2 weeks, putative mutants were transferred to soil and were selfed. M_3 seeds were collected from each mutant and were screened using the same system. One of the lines that was able to restore growth on the $AlCl_3$ media was then further characterized and named *alt2-1*.

DNA Extraction

DNA extraction on plants was performed using a modified version of the method described by Fulton, et al (1995). DNA extraction buffer was freshly prepared by using 2.5 parts of Extraction buffer (0.35M sorbitol, 0.1M Tris-base, 5 mM EDTA; pH 7.5) 2.5 parts Nuclei Lysis Buffer (0.2 M Tris, 0.05 M EDTA, 2 M NaCl, 2% CTAB), 1 part 5% Sarkosyl and between 0.3-0.5g sodium bisulfite per 100mL DNA extraction buffer. Heat buffer at 65^{o}C for 5 minutes. A small amount of tissue was collected and ground in 250µl of fresh DNA extraction buffer, after which another 250µl buffer was added. Samples were incubated for 30-60min at 65^{o}C, after which 500µl cholorform/isoamyl alcohol (24:1) was added. Sampled were mixed well and centrifuged at 10,000g for 5 minutes. The aqueous phase was kept and had 1 volume ice-cold isopropanol added. The samples were mixed immediately and centrifuged for 5 minutes. The supernatant was discarded and 400µl of 70% ethanol was added. The samples were centrifuged for 5

minutes and the supernatant was discarded. The pellet was dried in a vacuum desiccator and 50μl of sterile distilled water was added to the dry pellet.

Mapped Based Cloning

Both *als7-1* and *alt2-1*, which are both in the Col-0 wt background, were crossed with Ws-0 wt and *als3-4*, which is in the La-0 wt background, respectively and the F1 generation was allowed to self. The seeds from the F2 generation were screened for either the *als7-1* or *alt2-1* phenotype.

To determine the location of the *als7-1* and *alt2-1* mutations, PCR based markers either CAPS (Cleaved Amplified Polymorphic Sequences) or SSLPs (Single Sequence Length Polymorphisms) were used that represented many different areas of the genome. Most marks displayed a recombination frequency of about 50% indicating no linkage for the appropriate mutation. For the *als7-1* mutation, linkage was localized to chromosome 1. Markers used for this fine scale analysis included *Nga111* and *At1g72480*. A novel CAPS marker, *At1g72480*, was identified. Primers for this marker were

5'- ATGCAGAAGCGAATAGCCTTG

3'- CAAAATCCAGATAAGCACCTC

The PCR product was digested with *AccI* giving two DNA fragments for Col-0 and one for Ws. Candidate genes from this region were amplified by PCR and sequenced by the ICBR (University of Florida, Gainsville). For sequencing the *At1g72440* gene, it

was divided into three, approximately 2 kilobase parts that were cloned into pGEMT-Easy (Promega, Madison, WI) and transformed into *E. coli* strain DH5α.

Part 1: 5'-CACATTCACATCACTAAGTTCAATATTT

3'-CATGAATCATATAAACCATCAACC

Part 2: 5'-GTATAGGATCAATGATGCGAATATTG

3'-GTAACGTGATTCGGATCTTTCCTTC

Part 3: 5'-GGAACAATTAAAGGGATCACAACTGAG

3'-GGAGTGATGGATTTGCGTTGTTAG

For the *alt2-1* mutation, linkage was localized to a narrow region of chromosome 4. Markers used for this fine scale analysis included *Nga1107*, *PRNA*, and *Ag*. Candidate genes from this region were amplified by PCR and sequenced by the ICBR (University of Florida, Gainsville). For sequencing the *At4g29860* gene, it was divided into two approximately two kilobase parts that were cloned into pGEMT-Easy (Promega, Madison, WI) and transformed into *DH5α*.

Part 1: 5'-CAAGTCAATCATTGCTATAGAG

3'-CGAGTCGATGGGAAAATTGCAG

Part 2: 5'-ATCAGTGCATAGCATGAGGATG

3'-GTTGTGTGTTCGCTTGGTTTC

Sequences were compared to the published *Arabidopsis thaliana* genome on TAIR to identify potential mutations. Putative mutations were resequenced for verification.

Identification of *als7-2* and *alt2-2*

The *als7-2* and *alt2-2* mutations were identified by screening EMS treated plants using TILLING (*Arabidopsis* TILLING Project, Henikoff 2004). Allele *als7-2* was identified as CS94028 from the *Arabidopsis* Biological Resource Center (ABRC) (Ohio State University, Columbus, Ohio). The mutation can be followed using PCR primers listed below followed by loss of the *Mbo*II digestion site.

5'-CAGTATACTTAAGCTTTTGAT

3'-CAGATGACGAAGAGGCTTTG

Allele *alt2-2* was identified as CS95089 from ABRC (Ohio State University). The mutation can be followed using PCR primers listed below followed by loss of the *Hinf*I digestion site.

5'-TCTCTGCAAGAAGCTGAAAGTC

3'-TAAGCAAGTTCAAAGGTGAAC

alt2-1 and *alt2-1,alt1-1* lines

To generate *alt2-1* without *als3-1*, *alt2-1*;*als3-1* were crossed with Col-0 wt. F1 lines were allowed to self and F2 lines were screened for wild type ALS3 by PCR. The *als3-1* mutation can be followed by amplification with CAPS markers:

5'-CTCTCTGTTATCGGATTTGTTC

3'-GACAGAGAGATCACTAGTGC

The PCR product is then digested with *ClaI*. The wild typeALS3 contains a *ClaI* site, while *als3-1* mutation causes a loss of a site. Lines that were homozygous for ALS3 were then screened for the *alt2-1* mutation. The *alt2-1* mutation can be followed by the amplification with the following primers:

5'-CGAGTCGATGGGAAAATTGCAG

3'-AGATATCGAGAGATTTATGGGGAGGATATAG

The PCR product then is sequenced using the following primer as a gene specific sequencing primer.

5'-ATCCTCATGCTATGCACTG.

The *alt2-1* mutation has a single base pair change from a G to an A.

To generate the *alt2-1;alt1-1* double mutant, *alt2-1* was crossed with *alt1-1*. F1 lines were allowed to self and F2 lines were screened first for the *alt1-1* mutation. The *alt1-1* mutation can be followed by amplification with CAPS markers:

5'-CCTTCCTTCTCTTTCTCTAAGAAG

3'-TTCTTCGGTTCAGTTGTATCTG

The PCR product is then digested with *BstXI*. The wild type ALT1 product contains a restriction site, while the *alt1-1* mutation loses the *BstXI* site. The *alt2-1* mutation was then identified using PCR followed by sequencing as previously described.

T-DNA insertion lines

The *atr-2* T-DNA insertion line is the homozygous line SALK_032841. Its mutation can be followed by the lack of PCR amplification with the *AtATR* wild type primers.

5'-AGTTTGGATGATCAAGCTGATC

3'-ACTGCATGCCATTTACTCCTAC

The *atr-2* T-DNA mutation is then identified by the PCR amplification with the LBa1 T-DNA primer with the 3' *AtATR* wild type primer.

5'-TGGTTCACGTAGTGGGCCATCG

3'-ACTGCATGCCATTTACTCCTAC

The *ddb1a* T-DNA insertion line is the homozygous line SALK_038757C that was used without further identification.

The *ddb1b* T-DNA insertion line was obtained from INRA Versailles Genetics and Plant Breeding Laboratory *Arabidopsis thaliana* Resource Center as line FLAG_348G01, in the WS background. The *ddb1b* T-DNA mutation can be followed by lack of PCR amplification with the *DDB1B* wild type primers.

5'-ACTCGAACTCAGTGAAGCCTAGTGAGTTC

3'-GTTATGTTCACAAGAACTCACC

The *ddb1b* T-DNA mutation is then identified by the PCR amplification with the LBa1 T-DNA primer with the 3' *DDB1B* wild type primer.

5’-TGGTTCACGTAGTGGGCCATCG

3’-GTTATGTTCACAAGAACTCACC

To confirm that the *ddb1b* T-DNA line was a knockout line, RT-PCR was performed. RNA was extracted from WS wt and *ddb1b* seedlings using TRIzol reagent (Invitrogen, Carlsbad, CA) following the manufacturer’s instructions. From 1μg of RNA, cDNA was synthesized using the SuperScriptIII First-Strand Synthesis System (Invitrogen, Carlsbad, CA), following the manufacturer’s instructions for the oligo(dT) primers. *DDB1B* was then amplified from the cDNA from both WS wt and *ddb1b* using specific primers for the cDNA.

5’-GAAGAGGAGAGCTTGGATTTGC

3’-ATGATGACATCTACCTCGGTAC

The *ddb2* T-DNA insertion line was obtained from Riken as line DDB2 line 53-3351-1, in the Nossen background. The *ddb2* T-DNA mutation can be followed by the lack of PCR amplification with the *DDB2* wild type primers.

5’-CTCAACCATCTCTCTGTATTATC

3’-GAGAGATTGTTCATAGTAATG

The *ddb2* T-DNA mutation is then identified by the PCR amplification with the DS3-2a primer with the 3’ *DDB2* wild type primer.

5’-CCGGATCGTATCGGTTTTCG

3’-GAGAGATTGTTCATAGTAATG.

To confirm that the *ddb2* T-DNA line was a knockout line, RT-PCR was performed. RNA was extracted from Nos-0 wt and *ddb2* seedlings using TRIzol reagent (Invitrogen, Carlsbad, CA) following the manufacturer's instructions. From 1μg of RNA, cDNA was synthesized using the SuperScriptIII First-Strand Synthesis System (Invitrogen, Carlsbad, CA), following the manufacturer's instructions for the oligo(dT) primers. *DDB2* was then amplified from the cDNA from both Nos-0 wt and *ddb2* using specific primers for the cDNA.

5'-CTCAACCATCTCTCTGTATTATC

3'-GAGAGATTGTTCATAGTAATG

Generation of Transgenic Plants

To generate the *ALS7* functional complementation, full-length *At1g72440* including the 5' and 3' UTR was amplified from genomic DNA in two parts using the following primer sets:

Part 1: 5'-AAGGTACCACATAATCGTACAGTTATTCTC

3'-GTCATAAGTCATAACATGAAATCTTTC

Part 2: 5'-ACTAGTGAAAGATTTCATGTTATGAC

3'-AACTGCAGAAAACTTCAATATCTACTTTGTC

PCR was performed using a high fidelity Taq polymerase, Phusion (NEB, Ipswich, MA) following the manufacturer's instructions. The full-length wild type *At1g72440* that was amplified above was introduced into pBI101. The construct was

electroporated into *Agrobacterium tumefaciens* strain Aglo, which was then used to transform Col-0 wt. F_0 lines were screened for kanamycin resistance. Kanamycin resistant lines were allowed to self and F_1 lines were then screened again on 0.75mM $AlCl_3$ to identify homozygous lines that complement the *als7-1* phenotype.

To generate the *ALS7:*GFP line, the full length of *At1g72440* including the promoter was amplified from genomic DNA in two parts using the follower primer sets:

Part 1: 5'-AAGTCGACAAAACTTCAATATCTACTTT

3'-GTCATAAGTCATAACATGAAATCTTTC

Part 2: 5'-GATGATGTTGATGATAATGCTGTG

3'-AACCCGGGCTCTGATGCTTTAGACTTCTTC

PCR was performed using a high fidelity Taq polymerase, Phusion (NEB, Ipswich, MA) following the manufacturer's instructions. The two parts were assembled in the pGEM-T EASY vector and then cloned into PBI101 containing GFP to create the ALS7:GFP fusion. The construct was electroporated into *Agrobacterium tumefaciens* strain Aglo, which was then used to transform Col-0 wt. F_0 lines were screened for kanamycin resistance. Kanamycin resistant lines were allowed to self and F_1 lines were then screened again on kanamycin to identify homozygous lines. Images were taken with a Lecia SP2 confocal microscope and nuclei were counterstained with Hoescht 33342 or DAPI.

To generate the *ALT2* functional complementation, full length *At4g29860* including the 5' and 3' UTR was amplified from genomic DNA in two parts using the

following primer sets:

Part 1: 5’-AGATATCCATTTCTGTGTTGGAACTTCTTTG

3’-CACATTCCTGCAGATGACCATA

Part 2: 5’-TATGGTCATCTGCAGGAATGTG

3’-AGCGGCCGCGATATCTATTTATAGATATGTAAGTATAAATG

The two parts were assembled in the pGEM-T EASY vector and then transferred into PBI101 that contained GFP. The construct was electroporated into *Agrobacterium tumefaciens* strain Aglo, which was then used to transform *alt2-1;als3-1*. T_0 seeds were initially screened for kanamycin resistance. Kanamycin resistant plants were allowed to self, and T_1 plants were screened on 0.75mM $AlCl_3$ to identify lines that complement *alt2* phenotype.

To create the *ALT2* GUS lines, *At4g29860* promoter was amplified using the following primers and then cloned into pBI101.

5’-AGATATCTCCTCTGATTCAACTACTACAC

3’-ATCTAGATATGTAAATACACAGCATTCAG

The construct was electroporated into *Agrobacterium tumefaciens* strain Aglo, which was then used to transform Col-0 wt. F_0 lines were screened for kanamycin resistance. Kanamycin resistant lines were allowed to self and F_1 lines were then screened again on kanamycin to identify homozygous lines. Kanamycin resistant homozygous lines were then GUS stained.

To generate the *ALT2* GFP lines, full length *At4g29860* including the promoter was amplified in two parts.

Part 1: 5'-AGATATCCATTTCTGTGTTGGAACTTCTTTG

3'-CACATTCCTGCAGATGACCATA

Part 2: 5'-TATGGTCATCTGCAGGAATGTG

3'-AGATATCGAGAGATTTATGGGGAGGATATAG

The two parts were assembled in pGEM-T EASY and was then cloned into pBI101 with GFP. The construct was electroporated into *Agrobacterium tumefaciens* strain Aglo, which was then used to transform flowering *alt2-1;als3-1* plants. T_0 seeds were initially screened for kanamycin resistance. Kanamycin resistant plants were allowed to self, and T_1 plants were screened on 0.75mM $AlCl_3$ to identify lines that complement *alt2* phenotype. Images were taken with a Lecia SP2 confocal microscope and nuclei were counterstained with Hoescht 33342 or DAPI.

To create the over-expression *AtARD3* lines, full length *AtARD3* not including the promoter was amplified from Col-0 wt cDNA with the following primers:

5'-GCCATGGGTGAAGCCGCTAAGGATC

3'-CGAGCTCTTACGCTGAAGCGTCTATGTTAC

The PCR product was cloned into pGEMT EASY, and then cloned into pBS with ACTII promoter. The full length *AtARD3* with over-expression promoter was then cloned into pBI101. The construct was electroporated into *Agrobacterium tumefaciens*

strain Aglo, which was then used to transform Col-0 wt. F_0 lines were screened for kanamycin resistance. Kanamycin resistant lines were allowed to self and F_1 lines were then screened again on kanamycin to identify homozygous lines.

To create the over-expression *SPDS2* lines, full length *SPDS2* (*At1g70310*), excluding the promoter reason was amplified from Col-0 wt cDNA using the following primers.

5'-AAGATCTCTAGTTGGCTTTCGAATCAATC

3'-AAGATCTATGTCTTCAACACAAGAAGCGTC

The PCR product was cloned into pGEMT EASY, and then cloned into pBS with ACTII promoter. The full length *SPDS2* with over-expression promoter was then cloned into pCGN18. The construct was electroporated into *Agrobacterium tumefaciens* strain Aglo, which was then used to transform Col-0 wt. F_0 lines were screened for kanamycin resistance. Kanamycin resistant lines were allowed to self and F_1 lines were then screened again on kanamycin to identify homozygous lines.

Agrobacterium-mediated transformation

All pBI101 and pCGN18 constructs were electroporated into *Agrobacterium tumefaciens* strain Aglo using a Bio-Rad MicroPulser (Bio-Rad, Hercules, CA) following the manufacturer's instructions. Colonies that appeared to contain the plasmid were grown and tested via PCR for the insert. Genomic DNA from the *Agrobacterium* line was grown overnight in 1mL YEP medium at 28^{o}C. Cells were pelleted and resuspened

in 0.1mL of ice-cold Solution I (4mg/mL lysozyme, 50mM glucose, 10mM EDTA, 25mM Tris-HCl, pH 8.0). Cells were incubated for 5 minutes at room temperature. To the cell suspension, 30μL of phenol equilibrated with two volumes of solution II (1%SDS, 0.2N NaOH) was added and vortexed gently for a few seconds. To this mixture, 150μL of 3M sodium acetate, pH 4.8 was added and the tube was shaken briefly. The tube was incubated at -20^{o}C for 15 minutes, centrifuged for 3 minutes and then supernatant was poured into a new 1.5mL tube. The tube was filled with ice-cold 95% ethanol, mixed by inversion and stored at -80^{o}C for 15 minutes. The tube was centrifuged for 3 minutes and the supernatant was discarded. To the pellet, 0.5mL of 0.3M sodium acetate, pH 7.0 was added and the pellet was resuspended. The tube was filled with ice-cold 95% ethanol and mixed well by inversion. The tube was then stored at -80^{o}C for 15 min. The tube was centrifuged for 3 minutes, the supernatant was decanted and the tube was inverted on a paper towel to drain remaining supernatant. To the tube, 1mL of ice-cold 70% ethanol was added, the tube was vortexed briefly and centrifuged for 1 minute. All the supernatant was discarded and the pellet was dried briefly in a vacuum desiccator. The pellet was resuspended in 50μL of TE (1mM EDTA, 10mM Tris-HCl, pH 8.0).

Flowering Col-0 wild type *Arabidopsis thaliana* was transformed with *Agrobacterium* lines that were confirmed to contain the appropriate plasmid. *Agrobacterium* lines carrying the appropriate plasmid were grown over night at 30^{o}C in 500mL of LB with appropriate antibiotics from a 5mL starter culture. The overnight culture was pelleted at 5,000 rpm in a GSA rotor for 10 minutes. The supernatant was

decanted and the cells were resuspended in 500mL of infiltration medium (0.5x MS salts, 1x B5 vitamins, 5% (w/v) sucrose, 44nM benzylaminopurine, 0.02% (v/v) Silwet L-77). Invert flowering plants into *Agrobacterium* solution and swirl for 1 minute making sure that the leaves and flowers were fully submerged. The top of the pots were wrapped with saran wrap and covered for 3 days, after which plants were hand-watered until seeds were fully set.

Callose staining

Col-0 wt, *alt2-1;als3-1*, *als3-1* and *als7-1* were grown in a gel soaked environment with 0mM or 0.75mM $AlCl_3$ for 7 days. Seedlings were fixed in 5mL of FAA (50% ethanol, 5% formaldehyde, 10% acetic acid) for one hour under a vacuum. The fixed seedlings were washed twice with 0.1M K_2HPO_4, pH 9.0 and stained with 0.1% aniline blue (Sigma-Aldrich, St. Louis, MO), 0.1M K_2HPO_4, pH 9.0 overnight. Images were taken with a Lecia fluroscope.

ICP-OES analysis

Roots of ten-day-old Col-0 wt and *als7-1* seedlings were grown hydroponically and were treated with 0μM or 25μM $AlCl_3$, pH 4.2 for 48 hours. For Al analysis with treatment with spermine, Col-0 wt plants were grown for six days with 25μM spermine and then treated with 0μM or 25μM $AlCl_3$, pH 4.2 for 48 hours with 25μM spermine. Roots of six day old Col-0 wt, *alt2-1;als3-1* and *als3-1* were treated with 0μM or 25μM $AlCl_3$, pH 4.2 for 48 hours. After treatment, roots were washed with nutrient medium

briefly. Roots were harvested, dried at 65°C for two days, weighed and ashed in 50µl 90% nitric acid. Samples were resuspended in 5mL of 1% nitric acid and analyzed using a Perkin-Elmer Optima 7300 DV ICP-OES (Perkin-Elmer, Norwalk, CT).

RNA extraction and Northern Analysis

Seedlings were grown in hydroponics, which consists of the Al media without GelGro in the absence of $AlCl_3$. After ten days of growth for *als7-1* experiments or six days for *alt2-1* experiments, seedlings were transferred to hydroponic media supplemented with either zero or 25µM $AlCl_3$ for 24 hours. Roots were collected and frozen in liquid nitrogen. Total RNA was extracted using TRIzol reagent (Invitrogen, Carlsbad, CA) following the manufacturer's instructions. RNA yield was measured on Beckman DU730 spectrophotometer (Beckman Coulter, Brea CA). Loading buffer (1xMOPS, 18% formaldehyde, 50% formamide, 10% glycerol, 2µL/mL ethidium bromide) was added to 10µg of total RNA. Total RNA was run on a 1% agarose gel containing 1xMOPS and 18% formaldehyde (Sambrook 1989). Even loading was verified by the relative amount of RNA in each lane by ethidium bromide staining. RNA was transferred to a Zeta Probe GT nitrocellulose membrane (BioRad, Hercules, CA) through RNA Capillary Transfer as per manufacturer's instructions. RNA was crosslinked using optimal crosslink setting on a SpectroLinker XL-1000 UV Crosslinker (Spectronics Corporation, Westbury, NY). The blot was pre-hybridized by incubating at 65°C in prehybridization solution (6x SSC, 2x Denhardt's solution, 50% formamide, 100ug/mL Herring sperm DNA, 0.1% SDS) for at least one hour before adding the probe.

The probe was made using [^{32}P]-labeled dCTP (PerkinElmer, Waltham, MA) with the RadPrime kit (Invitrogen, Carlsbad, CA) following manufacturer's instructions. The probes were cleaned up using an illustra MicroSpin G-50 column (GE Heathcare, Buckinghamshire, UK) following the manufacturer's instructions. The probes were boiled, quick chilled then injected into the prehybridization solution and allowed to hybridize overnight at 65^{o}C. The blots were then washed in progressively more stringent washes in the following order 2x SSC, 0.1% SDS; 0.5xSSC, 0.1% SDS; 0.1% SSC, 0.1% SDS, for 30 minutes each. The blots were exposed to BioMax Light film (Kodak, Rochester, NY) and developed using a MiniMedical Automatic Film Processor (AFP ImageWorks, Elmsford, NY).

To create the probes, the following genes were amplified from Col-0 wt cDNA and cloned into pGEM-T Easy (Promega, Madison, WI) using the following primers.

AtALMT1 (*At1g08430*)

5'-ATGGAGAAAGTGAGAGAGATAGTG

3'-TTACTGAAGATGCCCATTACTTAATG

ALS7 (*At1g72440*)

Part 1: 5'-ATGTCAAAGATAAAGCCTTTGAG

3'-CATCTTCCATAGAGGTGGCCTTG

Part 2: 5'-CAAGGCCACCTCTATGGAAGATG

3'-ACATAATCGTACAGTTATTCTC

AtARD3 (*At2g26400*)

5’-ATGGGTGAAGCCGCTAAGGATG

3’-TGTTTAGCTTATAGAAATCTGATC

Oxidoreductase (*At4g10500*)

5’-ATGGCAACTTCTGCAATATCTAAG

3’-ATAGCTAAAGAGCCAATTCAAG

ALT2 (*At4g29860*)

5’-ATGAGTAAGAGACCTCCGCCTG

3’-TCAGAGAGATTTATGGGGAG

GeneChip Analysis

Total RNA was isolated from the roots of Col-0 wt and *als7-1* that were grown in the presence of 0μM or 25μM $AlCl_3$ in hydroponics using TRIzol reagent (Invitrogen, Carlsbad, CA), following the manufacturer’s instructions. cDNA was synthesized using 1μg of total RNA that was reverse transcribed with the SuperScriptIII First-Strand Synthesis System (Invitrogen, Carlsbad, CA). Samples were then processed using an Affymatrix *Arabidopsis* ATH1 Genome Array by the Nottingham *Arabidopsis* Stock Centre (University of Nottingham, UK).

Quantitative RT-PCR

Col-0 wt and *als7-1* seedlings were grown for 7 days on PNS medium after which seedlings were harvested and RNA isolated with TRIzol reagent (Invitrogen, Carlsbad,

CA). One μg of total RNA from each sample was reverse transcribed into cDNA with the SuperScriptIII First-Strand Synthesis System (Invitrogen, Carlsbad, CA) following the manufacturer's instructions. Two μL of 1:5 diluted cDNA was used for each reaction with the iQ SuperMix with SYBR Green (Bio-Rad, Hercules, CA), along with primers specific to AtARD3 (*At2g26400*), oxidoreductase (*At4g10500*) and Actin2, listed below. Reactions were performed on a Bio-Rad iQ5 Real-Time PCR Detection System and analyzed using the manufacturer's iQ5 software. Three replicates were performed per sample per gene from two separate biological samples. Expression ratios were determined with the Pfaffl equation, using primer efficiencies calculated by standard dilution curves.

AtARD3 (*At2g26400*)

5'-AAGATACAAATTCCTTAGGATCC

3'-ACACAAAAGAAGAATAACCATGG

Oxidoreductase (*At4g10500*)

5'-TTCCGACTTTCTATTTCCCTTC

3'-ATAGCTTAAAGAGCCAATTCAAG

ACT2 (*At3g18780*)

5'-ATGTTTCTAAGCTCTCAAGATC

3'-GTCACACACAAGTGCATCATAG

Polyamine analysis

Col-0 wt and *als7-1* were grown hydroponically in the presence of 0μM or 25μM $AlCl_3$. Root tissue was harvested and ground in 10mM Tris-HCl, pH 7.5. Samples centrifuged for 5 minutes at 4°C and the supernatants were kept. The supernatants were digested with ice-cold 0.2N perchloric acid (PCA) at a concentration of 100mg of tissue per 1mL PCA for 15 minutes on ice. Samples were centrifuged for 10 minutes at 4°C. Dr. Leo Hawel analyzed the supernatants for polyamines using an Agilent 1100 HPLC with an autosampler, a Hitachi F1000 fluorscence detector. Agilent's ChemStation software was used to run the HPLC.

Briefly, the PCA precipitates all macromolecules and leaves the polyamines and amino acids and other small ions in solution. The supernatant is then made basic by addition of Na carbonate (to pH about 10.5) and reacted with DANSYL-Cl (a fluorescent adduct that reacts with amino groups). The carbonate was precipitated after the reaction by addition of MeOH. Samples were then injected onto the HPLC to quantitate the DANSYL-polyamines (Gilbert 1991).

The pellets from the PCA reaction were neutralized by the addition of 500μL 0.1N NaOH and were left overnight to dissolve. Protein concentrations were quantified by using the microassay procedure of the Bio-Rad Protein Assay (Bio-Rad, Hercules, CA), following the manufactures instructions. Concentration of polyamines within the plant tissue was depicted as picograms of polyamines per milligrams of total protein.

Yeast Two Hybrid

ALT2, *ALS7*, *DDB1A*, *DDB1B*, *DDB2*, and *CUL4* full-length coding sequences were amplified by PCR using cDNA synthesized from Col-0 wt root tissue as a template, expect for *ALT2*, which was also amplified using *alt2-1* cDNA. A truncated version of *AtATR* was amplified that included a predicted binding domain. All of the genes were cloned first into pGEM-T EASY vector system, then cloned into both the pACTII and pLexA vectors (Clontech Laboratories, Palo Alto, CA). pACTII vector contains the Gal4 activation domain II and encodes for the LEU2 gene for selection. The Gal4 activation domain was fused in frame to the N-terminal end of all proteins listed. pLexA vector contains the bacterial repressor LEXA DNA-binding domain and the *TRP1* gene for selection. Primers that were used are as follows.

ALT2 (*At4g29860*)

5’-ACCCGGGGATGAGTAAGAGACCTCGCCTGA

3’-ACTCGAGTCAGAGAGATTTATGGGGAGG

ALS7 (*At1g72440)*

5’-ACCCCGGGGAACATCATTCCGGAAAATAAG

3’-ACTCGAGTTACTCTGATGCTTTAGACTTC

AtATR (*At5g40820*)

5’-ACCCGGGGATGGCGAAGGACGACAATAATC

3’-ACTCGAGTTACTCATCTTTCTTTAAATCTTC

CUL4 (*At5g46210*)

5’-CGAATTCGAATGTCTCTTCCTACCAAACGCTC

3’-AGTCGACCTAAGCAAGATAATTGTATATC

DDB1A (*At4g05420*)

5’-ACCCCGGGGATGAGCTCATGGAACTACGTTG

3’-AGAATTCTCAGTGTTGCCTAGTGAGTTC

DDB1B (*At4g21100*)

5’-CGAATTCGAATGACGGTATGGAACTACGC

3’-ACTCGAGTCAGTGAAGCCTAGTGAGTTC

DDB2 (*At5g58760*)

5’-ACCATGGAGATGAGTTCAACGAGGAGCAGAAG

3’-ACTCGAGTTAAGTTTTTGTCTTCTTGGTG

Both pACTII and pLEX fusion constructs were simultaneously transformed into *Saccharomyces cerevisiae* strain L-40 using the lithium acetate method (Rose 1990). Yeast were grown overnight at 30^{o}C in YPAD media. Yeast were pelleted and resuspended in yeast transformation buffer (0.4M lithium acetate, 0.1M DTT, 35% PEG-3350, 0.5 mg/ml denatured herring sperm DNA), vortexed and incubated at 42^{o}C for 45 minutes. Cells were grown on SD media (1.2g/L yeast nitrogen based w/o amino acids and ammonium sulfate, 2.5 g/L ammonium sulfate, 5g/L succinic acid, 3g/L NaOH, 10g/L sucrose, 0.05g/L of amino acids adenine, arginine, cysteine, leucine, lysine, threonine, tryptophan and uracil, 0.025g/L amino acids asparagine, histidine, isoleucine,

methionine, phenylalanine, proline, serine, tyrosine, and valine) lacking leucine and tryptophan and to select for yeast that contain both pACTII and pLEX constructs at 30^{o}C overnight.

Yeast transformants were tested for the ability to drive the HIS3 reporter gene onto SD media lacking histidine, leucine and tryptophan, with a positive interaction indicated by growth on the dropout media. Transformants were also tested for the ability to drive the LacZ reporter gene (regulated by the LexA operator in strain L-40) by utilizing X-gal filter assay. Transformants were grown as patches on SD media lacking leucine and tryptophan for 24 hours at 30^{o}C. Filter paper was placed on top of the yeast plated and pressed down gently. The lifted yeast was frozen on the filter paper (Fisher Scientific, Pittsburg, PA) in liquid nitrogen and allowed to thaw, twice, to break open the cells. The thawed filters were then placed on Whatman grade 3MM paper (Bio-Rad, Hercules, CA) soaked in Z buffer (60 mM Na_2HPO_4, 40 mM NaH_2PO_4, 10 mM KCl, 1 mM $MgSO_4$, pH 7.0) plus 0.1% Triton X-100 and 1.5 mg/ml X-Gal. The filters were incubated at 37^{o}C until blue color develops.

In-vitro binding assay

A maltose binding protein (MBP) was fused to the ALT2 protein by using pMAL-c2E vector (New England Biolabs, Beverly, MD). The entire coding sequence of *ALT2* was fused to the C-terminal end of MBP.

ALT2 (*At4g29860*)

5’-AGGATCCATGAGTAAGAGACCTCCGCCTG

3’-ACTCGAGTCAGAGAGATTTATGGGGAGG

To create ALT2^{G340R} in pMAL-c2E, mutagenesis was performed using pMAL-c2E with ALT2 and the QuikChange II XL Site-Directed Mutagenesis Kit (Agilent Technologies, Santa Clara, CA), following the manufacturer’s instructions. The site-directed mutagenesis kit utilizes high fidelity PCR to create point mutations in large plasmids.

ALT2^{G340R}

5’-CGAGTCTATAATTAGCGCAAAGGAAATGCTCTAGCAATACTAAAG

3’-CTTTAGTATTGCTAGAGCATTTCCTTTGCGGTAATTATAGACTCG

Both of these constructs were introduced into *E. coli* strain BL21-DE3 (Promega, Madison, WI). Transformants were grown overnight at 30^{o}C in Rich Media (10g/L tryptone, 5g/L yeast extract, 5g/L NaCl, 2g/L dextrose) supplemented with 100μg/mL carbenicillin and 34μg/mL chloramphenicol. The starter culture was used to inoculate 50mL Rich Media with carbenicillin and chloramphenicol and grown for six hours at 30^{o}C. Cultures were then induced to produce the protein fusion with 0.3mM IPTG for three hours. The cultures were then pelleted and then frozen at -80^{o}C and freeze/thawed twice. After the second thaw cycle, 5U of RQ1 DNase (Promega, Madison, WI) was added and allowed to incubate for 20 minutes at room temperature. After the incubation

period, 5mL of column buffer (20mM Tris-HCl, pH 7.5, 5mM EDTA, 20mM NaCl) with the addition of 0.07% β-mercaptoethanol was added, the cellular debris was spun down and the supernatant was taken.

The fusion proteins were purified on 300µL of amylose resin (New England Biolabs, Beverly, MD) that had been washed 3 times in column buffer. The fusion protein and resin were incubated for 1 hour at 4^{o}C on a clip bar of a Labquake tube rotator (Fisher Scientific, Pittsburg, PA). Beads were spun down and washed twice with 4mL column buffer. Remaining 1mL of washed beads were transferred to a microcentrifuge tube, were spun down and washed 1 more time with 1mL of column buffer. The beads were resuspended in 100µL of column buffer.

Samples were run on a SDS-PAGE gel stained with Coomassie blue to visualize the amount and size of the fusion protein. The gel was prepared as a 10% resolving gel (10% bisacrylamide, 0.25M Tris-HCl, pH 8.0, 0.1% SDS, 6.6µL/mL 10% ammonium persulfate, and 13.3µL/L TEMED) and overlayed with a 4.5% stacking gel (4.5% bisacrylamide, 0.125M Tris-HCl, pH 6.8, 0.1% SDS, 6.6µL/mL 10% ammonium persulfate, and 13.3µL/L TEMED. The gel was run at 150 volts until the sample ran to the resolving gel and then was turned up to 200 volts until the dye front ran off the end of the gel. The gel was stained in Coomassie brilliant blue (2.5g/L Coomassie brilliant blue, 45.5% ethanol, 9% glacial acetic acid) for one hour and then detained (45.5% ethanol, 9% glacial acetic acid) overnight. The protein size and quantity was based on estimation using the Kaleidoscope Prestained Standards protein ladder (Bio-Rad, Herculus, CA) and BSA protein standards of 1.0µg, 5.0µg and 10.0µg.

For *in-vitro* translation, AtATR, DDB1a, DDB1b, DDB2 and CUL4 were amplified from cDNA using PCR with the addition of Kozak sequences added before the start codon and were subcloned into pGEM-T EASY.

AtATR (*At5g40820*)

5’-AAGCCATGGCGAAGGACGACAATAATC

3’-ACTCGAGTTACTCATCTTTCTTTAAATCTTC

DDB1A (*At4g05420*)

5’-ACCATGAGCTCATGGAACTACGTTG

3’-AGAATTCTCAGTGTTGCCTAGTGAGTTC

DDB1B (*At4g21100*)

5’-ACCATGAGCGTATGGAACTACGCC

3’-ACTCGAGTCAGTGAAGCCTAGTGAGTTC

DDB2 (*At5g58760*)

5’-ACCATGAGTTCAACGAGGAGCAGAAG

3’-ACTCGAGTTAAGTTTTTGTCTTCTTGGTG

CUL4 (*At5g58760*)

5’-ACCATGTCTCTTCCTACCAAACGC

3’-AGTCGACCTAAGCAAGATAATTGTATATC

The protein from each of these constructs was produced as radiolabeled [^{35}S] methionine using the TnT Quick Coupled Transcription/Translation System (Promega, Madison, WI), following the manufacturer’s instructions. *AtATR*, *DDB1A*, *DDB2* and

CUL4 all utilized the T7 promoter, while *DDB1B* utilized the Sp6 promoter.

The *in-vitro* binding assay was performed using 10µL of the purified fusion protein with the amylose beads, mixed with either 5µL or 25µL of the ^{35}S labeled *in-vitro* translated protein in 400µL of bead binding buffer with BSA (50mM KH_2PO_4, 150mM KCl, 1mM $MgCl_2$, 10% glycerol, 10mg/mL BSA, 0.5% Triton X-100). The samples were rocked overnight at 4^oC. Protein samples were then gently washed 3 times with bead binding buffer without BSA. At the last wash, all remaining buffer was removed with a skinny pipette tip, and samples were resuspended in SDS protein sample buffer and separated on a 10% SDS-PAGE gel. The gel was fixed (25% isopropanol, 10% acetic acid) for 20 minutes and then soaked in Amplify solution (Amersham, Piscataway, NJ) for 20 minutes. The gel was dried in a gel dryer vacuum system (Fisher Scientific, Pittsburg, PA) and then exposed to BioMax Light film (Kodak, Rochester, NY) and developed using a MiniMedical Automatic Film Processor (AFP ImageWorks, Elmsford, NY).

Comet Assay

Col-0 wt and alt2-1 seedlings were grown for 7 days on a gel soaked environment with 0 or 1.50 mM $AlCl_3$. Roots of ~100 seedlings were harvested and chopped finely with pre-chilled razor blades on ice with ice-cold 1xPBS (Ca^{2+}-and Mg^{2+}-free, 20 mM EDTA, pH 7.4) in the dark. Cell lysate was transferred and filtered through 40 µm nylon cell strainers (BD Falcon, Franklin Lakes, NJ) to isolate nuclei in a total volume of 50µL. The nuclei were then used to perform a comet assay using the CometAssay kit (Trevigen,

Gaithersburg, MD), following the manufacturer's instructions. Briefly, 50µL of the nuclei were added to 500µL warm LMAgarose and 75µL was plated on the CometSlide. Slides were incubated at 4^{o}C for 20 minutes. Slides were then incubated in pre-chilled Lysis Solution at 4^{o}C for 45 minutes. After incubation, excess buffer was tapped off and slides were immersed in Alkaline Solution for 40 minutes at room temperature. Excess buffer was tapped off and the slides were washed in 1xTBE buffer (89 mM Tris base, 89 mM boric acid, 2.5 mM EDTA disodium salt) twice for 5 minutes each. Slides were transferred to a 15 cm length electrophoresis box and were run for 10 minutes at 15 volts in 1xTBE. Excess TBE was tapped off and slides were immersed in 70% ethanol for 5 minutes. Following the assay, air-dried slides were stained with 1X SYBR Green and visualized with a Leica MZFLIII fluorescence stereomicroscope and a Spot Diagnostics Pursuit 4Meg Slider digital camera. Comet tails were analyzed with CometScore software (TriTek Corp, Sumerduck, VA).

Measurement of DNA Interstrand Crosslinking Using the Comet Assay

A modified protocol based on Spanswick, et al was utilized to measure interstrand crosslinking in *Arabidopsis*. Col-0 wt was grown in hydroponics media, pH 5.5 on pegs. After five days of growth, three pegs were transferred to hydroponics media with no chemicals, pH 5.5; 0.1µg/mL bleomycin, pH 5.5; 20µg/mL MMC with 0.1µg/mL bleomycin, pH 5.5 or 100µg/mL $AlCl_3$ with 0.1µg/mL bleomycin, pH 4.2. Root tips (~0.5cm portion of the root) were harvested and chopped finely with pre-chilled razor blades on ice with ice-cold 1xPBS (Ca^{2+}-and Mg^{2+}-free, 20 mM EDTA, pH 7.4) in the

dark. The cell lysate was transferred and filtered through 40 μm nylon cell strainers (BD Falcon, Franklin Lakes, NJ) to isolate nuclei in a total volume of 50μL. The nuclei were then used to perform the modified comet assay using the CometAssay kit (Trevigen, Gaithersburg, MD). Briefly, 20μL of the nuclei were added to 200μL warm LMAgarose and 75μL was plated on the CometSlide. Slides were incubated at 4°C for 10 minutes. Slides were then incubated in pre-chilled Lysis Solution at 4°C for 60 minutes. After incubation, excess buffer was tapped off and slides were immersed in ice-cold alkali buffer (50mM NaOH, 1mM disodium EDTA, pH 12.5) for 45 minutes in a large electrophoresis tank, in the dark at 4°C. The slides were electrophoresed in the same tank, using the same buffer for 25 minutes at 16V (0.6V/cm) in the dark at 4°C. Excess alkali buffer was tapped off and slides were immersed twice in dH_20 for 5 minutes each, then 70% ethanol for 5 minutes and dried for 15 minutes at 45°C. Following the assay, air-dried slides were stained with 1X SYBR Green and visualized with a Leica MZFLIII fluorescence stereomicroscope and a Spot Diagnostics Pursuit 4Meg Slider digital camera. Comets of 200 nuclei were analyzed with the Comet Assay IV software (Perspective Instruments, Suffolk, UK). To calculate the percent decrease in tail moment, the following formula was used:

$$\% \text{ decrease in tail moment} = \left[1 - \left(\frac{(TMdi - TMcu)}{(TMci - TMcu)}\right)\right] \times 100$$

TMdi=tail moment of the treated bleomycin sample

TMcu=tail moment of untreated control

TMci=tail moment of untreated bleomycin control

Treatment with Hydroxyurea

Col-0 wt and *alt2-1* were grown in hydroponics media, pH 5.5. After four days of growth, half of the seedlings were measured. The remaining seedlings were transferred to new medium with or without 1mM hydroxyurea (Sigma-Aldrich, St. Louis, MO). After three additional days, root lengths were measured.

Cell Cycle and Quiescent Center Reporter Lines

To generate the *alt2-1* lines carrying either the *CycB1;1::GUS* or *QC46* reporters, parent lines of *alt2-1;als3-1* were crossed and F_1 seeds allowed to self-pollinate. Genomic DNA was extracted from F_2 plants for genotyping. Plants homozygous for the *als3*-1 mutation were identified by amplification of the gene via PCR using the following primers.

als3-1 PCR primer

5'-CTCTCTGTTATCGGATTTGTTC

3'-GACAGAGAGATCACTAGTGC

The PCR product was subsequently digested with *ClaI*, the *als3-1* mutation results in a loss of a *ClaI* site.

Plants that were identified as wild type *ALS3* were GUS stained to identify lines that were homozygous for the reporter line, either *CycB1;1* or *QC46*. Homozygous lines for the reporter genes were then screened to identify the *alt2-1* mutation. The *alt2-1* mutation was identified by PCR amplification, followed by sequencing the PCR product

and identifying a G to an A basepair change.

alt2-1 PCR primer

5’- AGATATCGAGAGATTTATGGGGAGGATATAG

3’-CGAGTCGATGGGAAAATTGCAG

alt2-1 sequencing primer

5’-ATCCTCATGCTATGCACTG

Gus staining

CycB1;1 and *QC46* lines were grown with the appropriate chemical treatment conditions as previously mentioned. An adapted protocol on GUS staining from Jefferson, et al (1987) and Rodrigues-Pousada et al (1993) was performed. Briefly, tissue was fixed in 90% ice-cold acetone and incubated on ice for 15 to 20 minutes. The acetone was removed and replaced with rinse solution (50mM $NaPO_4$, pH 7.2 (68.4 parts Na_2HPO_4, 31.6 parts NaH_2PO_4), 0.5mM $K_3Fe(CN)_6$, 0.5mM $K_4Fe(CN)_6$) to rinse the tissue. The rinse solution was then replaced with X-gluc staining solution (50mM $NaPO_4$, pH 7.2, 0.5mM $K_3Fe(CN)_6$, 0.5mM $K_4Fe(CN)_6$, 2mM X-Gluc (Gold Biotechnology, St. Louis, MO), 1 drop of Triton X-100) and was vacuum infiltrated for 30 minutes. The tissue was then transferred to 37^{o}C incubator until a blue color developed, about 2 hours. Staining was stopped by replacement of the X-gluc staining solution with 70% ethanol.

Propidium iodide and Evan's Blue staining

Col-0 wt and *alt2-1* seeds were sterilized and planted on 0mM, 0.75mM and 1.5mM $AlCl_3$ soak plates as previously described. Seedlings were grown for 7 days. A drop of propidium iodide (PI) solution (5μg/mL in water) was placed on each 3-6 root tips. Seedlings were immediately transferred to microscope slides already wetted with PI. Images were taken using a Leica MZFLIII fluorescence stereomicroscope with a DsRED filter and a Spot Diagnostics Pursuit 4Meg Slider digital camera.

CycB1;1 reporter lines were grown in the presence of crosslinking agents. Seedlings were harvested and stained with 0.1% (w/v) Evan's Blue (Sigma-Aldrich, St. Louis, MO) for 2 minutes. Seedlings were then washed with dH_20. DIC images were immediately taken with a Leica DMR microscope fitted with a Spot Diagnostics RT Color-2000 digital camera.

TRF Analysis

Col-0 wt, *alt2-1*, and *alt1-1* were grown for 7 days on a gel soaked environment with 0, 1.0mM, or 1.5mM $AlCl_3$. Seedlings were harvest and genomic DNA was extracted using ArchivePure DNA Plant Kit (5 Prime, Gaithersburg, MD) following the manufacturers instructions. 5μg of DNA from each sample was digested overnight with *Tru*1I (Fermentas, Glen Burne, MD) and run out on a 0.8% agarose gel at 80 volts. To prepare the gel for transfer it was soaked in depurination solution (0.125M HCl) for 10 minutes, immediately transferred to denaturation solution (1.5M NaCl, 0.5M NaOH) for 30 minutes and finally transferred to neutralization solution (1.5M NaCl, 0.5M Tris-HCl,

pH 7.5) for 30 minutes. The gel was transferred overnight to an Amersham Hybond-N+ positively charged membrane (GE Healthcare, Buckinghamshire, UK), following the manufacturer's instructions for capillary transfer. The DNA was crosslinked to the membrane using optimal crosslink setting on a SpectroLinker XL-1000 UV Crosslinker (Spectronics Corporation, Westbury, NY) and rinsed in 5xSSC. The membrane was then incubated at 55^{o}C in prehybridization buffer (6xSSC, 0.05xBLOTTO (1xBLOTTO is 5% (w/v) non-fat dry milk)) for at least one hour. The ssDNA oligo probe (5'-TTTAGGG$_{14}$) was labeled with [γ^{32}P]ATP with the DNA 5'-End Labeling System (Promega, Madison, WI) according to the manufacturer's directions. The end-labeling reaction was cleaned up with an illustra MicroSpin G-50 column (GE Heathcare, Buckinghamshire, UK) following the manufacturer's instructions. The probe was injected into the prehybridization solution and allowed to hybridize with the membrane overnight. The membrane was then washed with increasingly stringent conditions. The membrane was washed twice with 2xSSC, 0.1% SDS at 37^{o}C for 10 minutes each, then one time with 0.2xSSC, 0.01% SDS at 55^{o}C for 15 minutes. The membrane was exposed to BioMax Light film (Kodak, Rochester, NY) and developed using a MiniMedical Automatic Film Processor (AFP ImageWorks, Elmsford, NY).

Literature Cited

Ahn SJ, Sivaguru M, Osawa H, Chung GC, Matsumoto H (2001) Aluminum inhibits the H^+-ATPase activity by permanently altering the plasma membrane surface potentials in squash roots. Plant Physiol 126:1381–1390.

Alcázar R, Garcia-Martinez JL, Cuevas JC, Tiburcio AF, Altabella T (2005) Overexpression of *ADC2* in *Arabidopsis* induces dwarfism and late-flowering through GA deficiency. Plant J 43:425-436.

Andersson M (1988) Toxicity and tolerance of aluminum in vascular plants: a literature review. Water, Air, Soil Pollut 39:439-462.

Babourina O, Rengel Z (2009) Uptake of aluminum into *Arabidopsis* root cells measured by fluorescent lifetime imaging. Ann Bot 104:189-195.

Barceló J, Poschenrieder C (2002) Fast root growth responses ,root exudates and internal detoxification as clues to the mechanisms of aluminum toxicity and resistance: a review. Environ Exper Bot 48:75-92.

Bertch PM, Thomas GW, Barnhisel RI (1986) Characterization of hydroxy-aluminum solutions by aluminum-27 nuclear magnetic resonance spectroscopy. Soil Sci Soc Am J 50:825-830.

Bertsch PM, Thomas GW, Barnhisel RI (1986) Characterization of hydroxy-aluminum solutions by aluminum-27 nuclear magnetic resonance spectroscopy. Soil Sci Sco Am J 50:825-830.

Bertsch PM (1987) Conditions of AL13 polymer formation in partially neutralized alumium solutions. Soil Sci Soc Am J 51:825-828.

Blancaflor EB, Jones DL, Gilroy S (1998) Alterations in the cytoskeleton accompany aluminum-induced growth inhibition and morphological changes in primary roots of maize. Plant Physiol 118:159–172.

Boscolo PRS, Menossi M, Jorge RA (2003) Aluminum-induced oxidative stress in maize. Phytochemistry 62:181–189.

Bürstenbinder K, Rzewuski G, Wirtz M, Hell R, Sauter M (2007) The role of methionine recycling for ethylene synthesis in *Arabidopsis*. Plant J 49:238-249.

Carver BF, Ownby, JD (1995) Acid Soil Tolerance in Wheat. Adv Agron 54:117-173.

Chen W, Xu C, Zhao B, Wang X, Wang Y (2008) Improved Al tolerance of saffron (*Crocus sativus* L.) by exogenous polyamines. Acta Physiol Plant 30:121-127.

Colbert T, Till BJ, Tompa R, Reynolds S, Steine MN, Yeung AT, McCallum CM, Comai L, Henikoff S (2001) High-throughput screening for induced point mutations. Plant Physiol 126:480-484.

Culligan KM, Robertson CD, Foreman J, Doerner P, Britt AB (2006) ATR and ATM plat both distinct and additive roles in response to ionizing radiation. Plant J 48:947-961.

Crapper DR, Krishnan SS, Dalton AJ (1973) Brain aluminum distribution in Alzheimer's disease and experimental neurofibrillary degeneration. Science 180:511-513.

Crapper McLachlan DR, Lukiw WJ, Kruck TPA (1989) New evidence for an active role of aluminum in Alzheimer's disease. Can J Neurol Sci 16:490-497.

Delhaize E, Ryan PR, Randall PJ (1993) Aluminum tolerance in wheat (*Triticum aestivum* L.) II. Aluminum-stimulated excretion of malic acid from root apices. Plant Physiol 103:695–702.

Delhaize E, Ryan PR, Hebb DM, Yamamoto Y, Sasaki T, Matsumoto H (2004) Engineering high-level aluminum tolerance in barley with the ALMT1 gene. Proc Natl Acad Sci USA 101:15249–15254.

Dobrovinskaya OR, Muñiz J, Pottosin H (1999) Inhibition of vacuolar ion channels by polyamines. J Membrane Biol 167:127-140.

Dorr RT (1992) Bleomycin pharmacology: mechanism of action and resistance, and clinical pharmacokinetics. Semin Oncol 19:3-8.

Edskes HK, Ohtake Y, Wickner RB (1998) Mak21p of *Saccharomyces cerevisiae*, a homolog of human CAATT-binding protein, is essential for 60 S ribosomal subunit biogenesis. J Biol Chem 273: 28912–28920.

Edwards D, Murray JAH, Smith AG (1998) Multiple genes encoding the conserved CCAAT-box transcription factor complex are expressed in *Arabidopsis*. Plant Physiol 117:1015-1022.

Ezaki B, Katsuhara M, Kawamura M, Matsumoto H (2001) Different mechanisms of four aluminum (Al)-resistant transgenes for Al toxicity in *Arabidopsis*. Plant Physiol 127:918–927.

Fidantsef AL, Mitchell DL, Britt, AB (2000) The *Arabidopsis* UVH1 Gene Is a Homolog of the Yeast Repair Endonuclease RAD1. Plant Physiol 124:579-586.

Furukawa J, Yamaji N, Wang H, Mitani N, Murata Y, Sato K, Katsuhara M, Takeda K, Ma JF (2007). An aluminum-activated citrate transporter in barley. Plant Cell Physiol 48:1081-1091.

Furukawa T, Curtis MJ, Tominey CM, Duong YH, Wilcox BW, Aggoune D, Hays JB, Britt AB (2010) A shared DNA-damage-response pathway for induction of stem-cell death by UVB and by gamma irradiation. DNA Repair (Amst) 9:940-948.

Fulton TM, Chunwongse J, Tanksley SD (1995) Microprep Protocol for Extraction of DNA from Tomato and other Herbaceous Plants. Plant Mol Biol Rep 13(3):207-209.

Gabrielson KM, Cancel JD, Morua LF, Larsen PB (2006) Identifcation of dominant mutations that confer increased aluminium tolerance through mutagenesis of the Al-sensitive *Arabidopsis* mutant, als3–1. J Exp Bot 57:943–951.

Gallego F, Fleck O, Li A, Wyrzykowska J, Tinland B (2000) AtRAD1, a plant homologue of human and yeast nucleotide excision repair endonucleases, is involved in dark repair of UV damages and recombination. Plant J 21:507-518.

Gilbert RS, Gonzalez GG, Hawel L 3rd, Byus CV (1991) An ion-exchange chromatography procedure for the isolation and concentration of basic amino acids and polyamines from complex biological samples prior to high-performance liquid chromatography. Anal Biochem 199(1):86-92.

Giovanelli J, Mudd SH, Datko AH (1985) Quantitative analysis of pathways of methionine metabolism and their regulation in *Lemna*. Plant Physiol 78: 553–560.

Groppa MD, Tomaro ML, Menavides MP (2001) Polyamines as protectors against cadmium or copper-induced oxidative damage in sunflower leaf discs. Plant Sci 161:481-488.

Groppa MD, Benavides MP (2008) Polyamines and abiotic stress: recent advances. Amino Acids 34: 35-45.

Ha HC, Sirisoma NS, Kuppusamy P, Zweier JL, Woster MP, Casero RA Jr. (1998) The natural polyamine spermine functions directly as a free radical scavenger. Proc Natl Acad Sci USA 95:11140-11145.

He YJ, McCall CM, Hu J, Zeng Y, Xiong Y (2006) DDB1 functions as a linker to recruit receptor WD40 proteins to CUL4–ROC1 ubiquitin ligases. Genes Dev 20:2949–2954.

Hede AR, Skovmand B, López-Cesati J (2001) Acid soils and aluminum toxicity. In: *Application of physiology in wheat breeding* (Reynolds MP, Ortiz-Monasterio JI, NcNab A, eds). CIMMYT, Mexico D. F. Pp. 172-173.

Heitzeberg F, Chen IP, Hartung F, Orel N, Angelis KJ, Puchta H (2004) The Rad17 homologue of *Arabidopsis* is involved in the regulation of DNA damage repair and homologous recombination. Plant J 38:954-968.

Henikoff S, Till BJ, Comai L (2004) TILLING. Traditional mutagenesis meets functional genomics. Plant Physiol 135: 630–636.

Hoekenga OA, Maron LG, Piñeros MA, Cançado GM, Shaff J, Kobayashi Y, Ryan PR, Dong B, Delhaize E, Sasaki T, Matsumoto H, Yamamoto Y, Koyama H, Kochian LV (2006). *AtALMT1*, which encodes a malate transporter, is identified as one of several genes critical for aluminum tolerance in *Arabidopsis*. Proc Natl Acad Sci USA 103:9738-9743.

Horst WJ, Asher CJ, Cakmak I, Szulkiewicz P, Wissemeier AH (1992) Short-term responses of soybean roots to aluminium. J Plant Physiol. 140:174–178.

Horst WJ, Wang Y, Eticha D (2010) The role of the root apoplast in aluminum-induced inhibition of root elongation and in aluminum resistance of plants: a review. Ann Bot 106:185-197.

Huang CF, Yamaji N, Mitani N, Yano M, Nagamura Y, Ma JF (2009) A bacterial type ABC transporter is involved in aluminum tolerance in rice. Plant Cell 21:655-667.

Illéš P, Schlicht M, Pavlovkin J, Lichtscheidl I, Baluška F, Ovečka M (2006) Aluminium toxicity in plants: internalization of aluminium into cells of the transition zone in *Arabidopsis* root apices related to changes in plasma membrane potential, endosomal behaviour, and nitric oxide production. J Exp Bot 57: 4201-4213.

Imai A, Akiyama T, Kato T, Sato S, Tabata S, Yamamoto KT, Takahashi T (2004) Spermine is not essential for survival of *Arabidopsis*. FEBS Lett 556:148-152.

Javed MI, Bagni N (1991) Effects of exogenous polyamines and difluoromethylornithine on seed germination and root growth of *Arabidopsis thaliana*. Plant Growth Regul 10:163-168.

Jefferson RA, Kavanagh TA, Devan MW (1987) GUS fusions: beta-glucuronidase as a sensitive and versatile gene fusion marker in higher plants. EMBO 6:3901-3907.

Jones DL, Gilroy S, Larsen PB, Howell SH, Kochian LV (1998) Effect of aluminum on cytoplasmic Ca^{2+} homeostasis in root hairs of *Arabidopsis thaliana* (L.). Planta 206:378–387.

Karlik SJ, Eichhorn GL, Lewis PN, Crapper DR (1980) Interaction of aluminum species with deoxyribonucleic acid. Biochemistry 19:5991-5998.

Karlik SJ, Eichhorn GL (1989a) Polynucleotide cross-linking by aluminum. J Inorg Biochem 37:259-269.

Karlik SJ, Chong AA, Eichhorn, DeBoni U (1989b) Reversible toroidal compaction of DNA by aluminum. Neurotoxicology 10:167-176.

Kasprzak KS, Sunderman FW Jr, Salnikow K (2003) Nickel carcinogenesis. Mutat Res 533:67-97.

Kauss H, Waldmann T, Jeblick W, Euler G, Ranjeva R, Domard A (1989) Ca^{2+} is an important but not the only signal in callose synthesis induced by chitosan, saponins and polyene antibiotics. (Lugtenberg BJJ, ed) Signal molecules in plant and plant–microbe interactions. Berlin: Springer-Verlag Pp. 107–116.

Khan MSH, Tawaraya K, Sekimoto H (2009) Relative abundance of delta5-sterols in plasma membrane lipids of root-tip cells correlates with aluminum tolerance of rice. Physiol Plantarum 135: 73–83.

Kidd PS, Llugany M, Poschenrieder C, Gunse B, Barcelo J (2001) The role of root exudates in aluminium resistance and silicon-induced amelioration of aluminium toxicity in three varieties of maize (*Zea mays* L.). J Exp Bot 52:1339–1352.

Knoll A and Puchta H (2011) The role of DNA helicases and their interaction partners in genome stability and meiotic recombination in plants. J Exp Bot 62:1565-1579.

Kochian LV (1995) Cellular mechanisms of aluminum toxicity and resistance in plants. Annu Rev Plant Physiol Plant Mol Biol 46:237–260.

Kochian LV, Hoekenga OA, Piñeros MA (2004) How do crop plants tolerate acid soils? Mechanisms of aluminum tolerance and phosphorous efficiency. Annu Rev Plant Biol 55:459-493.

Kochian LV, Piñeros MA, Hoekenga OA (2005) The physiology, genetics and molecular biology of plant aluminum resistance and toxicity. Plant Soil 274:175-195.

Kollmeier M, Felle HH, Horst WJ (2000) Genotypical differences in aluminum resistance of maize are expressed in the distal part of the transition zone. Is reduced basipetal auxin flow involved in inhibition of root elongation by aluminum? Plant Physiol 122:945-956.

Kumar A, Altabella T, Taylor M, Tiburcio AF (1997) Recent advances in polyamine research. Trends Plant Sci 2:124–130.

Kusano T, Berberich T, Tateda C, Takahashi T (2008) Polyamines: essential factors for growth and survival. Planta 228:367-381.

Larsen PB, Tai CY, Kochian LV, Howell SH (1996) *Arabidopsis* mutants with increased sensitivity to aluminum. Plant Physiol 110:743–751.

Larsen PB, Kochian LV, Howell SH (1997) Al inhibits both shoot development and root growth in als3, an Al sensitive *Arabidopsis* mutant. Plant Physiol 114:1207–1214.

Larsen PB, Degenhardt J, Tai C-Y, Stenzler LM, Howell SH, Kochian LV (1998) *Arabidopsis* mutants with increased aluminum resistance exhibit altered patterns of aluminum accumulation and organic acid release from roots. Plant Physiol 117:9-17.

Larsen PB, Geisler M.J, Jones CA, Williams KM, Cancel JD (2005) ALS3 encodes a phloem-localized ABC transporter-like protein that is required for aluminum tolerance in *Arabidopsis*. Plant J 41:353–363.

Larsen PB, Cancel JD, Rounds MA, Ochoa V (2007) *Arabidopsis ALS1* encodes a root tip and stele localized half type ABC transporter required for root growth in an aluminum toxic environment. Planta 225:1447-1458.

Lee JH, Terzaghi W, Gusmaroli G, Charron JBF, Yoon HJ, Chen H, He YJ, Xion Y, Deng XW (2008) Characterization of *Arabidopsis* and rice DWD proteins and their roles as substrate receptors for CUL4-RING E3 ubiquitin ligases. Plant J 20:152-167.

Li N, Yuan L, Liu N, Shi D, Li X, Tang Z, Liu J, Sundaresan V, Yang WC (2009) *SLOW WALKER2*, a NOC1/MAK21 homologue, is essential for coordinated cell cycle progression during female gametophyte development in *Arabidopsis*. Plant Physiol 151:1486-1497.

Liu K, Fu H, Bei Q, Luan S (2000) Inward potassium channel in guard cells as a target for polyamine regulation of stomatal movements. Plant Physiol 124:1315-1326.

Liu Q, Yang JL, He LS, Li YY, Zheng SJ (2008) Effect of aluminum on cell wall, plasma membrane, antioxidants and root elongation in triticale. Biol Plantarum 52:87–92.

Liu Z, Hossain GS, Islas-Osuna MA, Mitchell DL, Mount DW (2000) Repair of UV damage in plants by nucleotide excision repair: *Arabidopsis* UVH1 DNA repair gene is a homolog of *Saccharomyces cerevisiae* Rad1. Plant J 21:519-528.

Lukiw WJ (2010) Evidence supporting a biological role for aluminum in brain chromatin compaction and epigenetics. J Inorg Biochem 104:1010-1012.

Lum LSY, Sultzman LA, Kaufman RJ, Linzer DIH, Wu BJ (1990) A cloned human CCAAT-box-binding factor stimulates transcription from the human hsp70 promoter. Mol Cell Biol 10:6709-6717.

Lydall D, Whitehall S (2005) Chromatin and the DNA damage response. DNA Repair (Amst) 4:1195-1207.

Ma JF, Hiradate S, Nomoto K, Iwashita T, Matsumoto H (1997) Internal detoxification mechanism of Al in hydrangea (identification of Al form in the leaves). Plant Physiol 113:1033–1039.

Ma JF, Hiradate S, Matsumoto H (1998) High aluminum resistance in buckwheat. II. Oxalic acid detoxifies aluminum internally. Plant Physiol 117:753-759

Ma JF (2000a) Role of organic acids in detoxification of aluminum in higher plants. Plant Cell Physiol 41:383-390.

Ma JF, Hiradate S (2000b) Form of aluminum for uptake and translocation in buckwheat (*Fagopyrum esculentum* Moench). Planta 211:355–360.

Ma JF, Furukawa J (2003) Recent progress in research of external Al detoxification in higher plants: a minireview. J Inorg Biochem 97:46-51.

Ma JF (2008) Syndrome of aluminum toxicity and diversity of aluminum resistance in higher plants. Int Rev Cytol 264: 225–253.

Magalhaes JV, Liu J, Guimarães CT, Lana UG, Alves VM, Wang YH, Schaffert RE, Hoekenga OA, Piñeros MA, Shaff JE, Klein PE, Carneiro NP, Coelho CM, Trick HN, Kochian LV (2007). A gene in the multidrug and toxic compound extrusion (MATE) family confers aluminum tolerance in sorghum. Nat Genet 39:1156-1161.

Mannuss A, Dukowic-Schulze D, Suer S, Hartung F, Pacher M, Puchta H (2010) RAD5A, RECQ4A, and MUS81 have specific functions in homologous recombination and define different pathways of DNA repair in *Arabidopsis thaliana*. Plant Cell 22:3318-3330.

Martin RB (1988) Metal Ions in Biological Systems: Aluminum and its Role in Biology, Vol 24. (Sigel H, Sigel A, eds) Marcel Dekker, NY Pp 1-57.

Matsumoto H, Hirasawa E, Morimura S, Takahashi E (1976) Localization of aluminium in tea leaves. Plant Cell Physiol 17:627–631.

McBride MB (1994) Environmental chemistry of soils. Oxford University Press, NY. Pp 48, 173-175, 180.

Minocha R, Minocha SC, Long SL, Shortle WC (1992) Effects of aluminum on DNA synthesis, cellular polyamines, polyamine biosynthetic enzymes and inorganic ions in cell suspension cultures of a woody plant *Catharanthus roseus*. Physiol Plant 85:417-424.

Mirza JI, Bagni N (1991) Effects of exogenous polyamines and difluoromethylornithine on seed germination and root growth of *Arabidopsis thaliana*. Plant Growth Regul 10:163-168.

Molinier J, Lechner E, Dumbliauskas E, Genschik P (2008) Regulation and role of *Arabidopsis* CUL4-DDB1A-DDB2 in maintaining genome integrity upon UV stress. PLoS Genet 4: e1000093.

Morita A, Horie H, Fujii Y, Takatsu S, Watanabe N, Yagi A, Yokota H (2004) Chemical forms of aluminium in xylem sap in tea plants. Phytochemistry 65:2775–2780.

Muniandy P, Liu J, Majumdar A, Liu S, Seidman MM (2010) DNA interstrand crosslink repair in mammalian cells: step by step. Crit Rev Biochem Mol Biol 45:23-49.

Niedernhofer LJ, Lalai AS, Hoeijmakers JHJ (2005) Fanconi anemia (cross)linked to DNA repair. Cell 123:1191-1198.

Parker DR, Kinraide TB, Zelazny LW (1989) On the phytotoxicity of polynuclear hydroxy-aluminum complexes. Soil Sci Soc Am J 53:789-796.

Pellet DM, Grunes DL, Kochian LV (1995) Organic acid exudation as an aluminum tolerance mechanism in maize (*Zea mays* L.) Planta 196:788-795.

Pfaffl MW, Horgan GW, Dempfle L (2002) Relative expression software tool (REST) for group-wise comparison and statistical analysis of relative expression results in real-time PCR. Nucleic Acids Res 30:e36.

Raschle M, Knipsheer P, Enoiu M, Angelov T, Sun J, Griffith JD, Ellenberger TE, Scharer OD, Walter JC (2008) Mechanism of replication-coupled DNA interstrand crosslink repair. Cell 134:969–980.

Rengel Z, Zhang WH (2003) Role of dynamics of intracellular calcium in aluminium-toxicity syndrome. New Phytol 159:295–314.

Rodrigues-Pousada RA, De Ryche R, Dedonder A, Van Caeneghem W, Engler G, Van Montagu M, Van Der Straeten D (1993) The *Arabidopsis* 1-Aminocyclopropane-1-Carboxylate Synthase Gene 1 is expressed during early development. Plant Cell 5:897-911.

Rose MD, Winston FM, Hieter P (1990) Methods in yeast genetics: a laboratory course manual. (Cold Spring Harbor, NY: Cold Spring Harbor Laboratory).

Rounds MA, Larsen PB (2008) Aluminum-dependent root-growth inhibition in *Arabidopsis* results from AtATR-regulated cell-cycle arrest. Curr Biol 18:1-6.

Ryan PR, Shaff JE, Kochian LV (1992) Aluminum toxicity in roots: Corelation among ionic currents, ion fluxes, and root elongation in aluminum-sensitive and aluminum-tolerant wheat cultivars. Plant Physiol 99:1193-1200.

Sabatini S, Heidstra R, Wildwater M, Scheres B (2003) *SCARECROW* is involved in positioning the stem cell niche in the *Arabidopsis* root meristem. Genes Dev 17: 354–358.

Sakamoto AN, Lan VT, Puripunyavanich V, Hase Y, Yokota Y, Shikazono N, Nakagawa M, Narumi I, Tanaka A (2009) A UVB-hypersensitive mutant in *Arabidopsis* thaliana is defective in the DNA damage response. Plant J 60:509-17.

Sambrook J, Fritsch EF, Maniatis T (1989) Molecular cloning: a laboratory manual. (Cold Spring Harbor, NY: Cold Spring Harbor Laboratory).

Sasaki T, Yamamoto Y, Ezaki B, Katsuhara M, Ahn SJ, Ryan PR, Delhaize E, Matsumoto H (2004) A wheat gene encoding an aluminum-activated malate transporter. Plant J 37:645–653.

Sauter M, Lorbiecke R, Ouyang B, Pochapsky TC, Rzewuski G (2005) The immediate-early ethylene response gene *OsARD1* encodes an acireductone dioxygenase involved in recycling of the ethylene precursor S-adenosylmethionine. Plant J 44:718-729.

Shabala S, Cuin TA, Pottosin H (2007) Polyamines prevent NaCl-induced K+ efflux from pea mesophyll by blocking non-selective cation channels. FEBS Lett 581:1993-1999.

Shen R, Ma JF, Kyo M, Iwashita T (2002) Compartmentation of aluminum in leaves of an Al-accumulator, *Fagopyrum esculentum* Monench. Planta 215:394-398.

Siaud N, Dray E, Gy I, Gérard E, Takvorian N, Doutriaux MP (2004) Brca2 is involved in meiosis in *Arabidopsis thaliana* as suggested by its interaction with Dmc1. EMBO J 23:1392-1401.

Siddik Z (2003) Cisplatin: mode of cytotoxic action and molecular basis of resistance. Oncogene 22:7265–7279.

Silva IR, Smyth TJ, Moxley DF, Carter TE, Allen NS, Rufty TW (2000) Aluminum accumulation at nuclei of cells in the root tip. Fluorescence dection using lumogallion and confocal laser scanning microscopy. Plant Physiol 123:543-552.

Spanswick VJ, Hartley JM, Hartley JA (2010) Measurement of DNA interstrand crosslinking in individual cells using the single cell gel electrophoresis (Comet) assay. Methods Mol Biol 613:267-282.

Sun P, Tian Q, Chen J, Zhang W (2010) Aluminum-induced inhibition of root elongation in *Arabidopsis* is mediated by ethylene and auxin. J Exp Bot 61:347-356.

Takahashi T, Kakehi J (2010) Polyamines: ubiquitous polycations with unique roles in growth and stress responses. Ann Bot 105:1-6.

Takedachi A, Saijo M, Tanaka K (2010) DDB2 Complex-mediated ubiquitylation around DNA damage is oppositely regulated by XPC and Ku and contributes to the recruitment of XPA. Mol Cell Biol 30:2708-2723.

Tang CF, Lui YG, Zeng GM, Li X, Xu WH, Li CF (2005) Effects of exogenous spermidine on antioxidant system responses of *Typha latifolia* L. under Cd^{2+} stress. J Integ Plant Biol 47:428-434.

Taylor GJ, McDonald-Stephens JL, Hunter DB, Bertsch DB, Elmore D, Rengel Z, Reid RJ (2000) Direct measurement of aluminum uptake and distribution in single cells of *Chara corallina*. Plant Physiol 123:987-996.

Thompson LH and Hinz JM (2009) Cellular and molecular consequences of defective Fanconi anemia proteins in replication-coupled DNA repair: Mechanistic insights. Mutat Res 668:54-72.

Tolrà R, Vogel-Mikuš K, Hajiboland R, Kump P, Pongrac P, Kaulich B, Gianoncelli A, Babin V, Barceló J, Regvar M, Poschenrieder C (2011) Localization of aluminum in tea (*Cammellia sinensis*) leaves using low energy X-ray fluorescence spectro-microscopy. J Plant Res 124:165-172.

Tomasz M (1995) Mitomycin C: small, fast and deadly (but very selective). Chem Biol 2:575-579.

Tyler G, Berggren D, Bergkvist B, Falkengren-Grerup U, Folkeson L, Rühling Å (1987) NATO ASI Series G16, effects of atmospheric pollutants on forests, wetlands and agricultural ecosystems (Hutchinson TC and Meema KM, eds) Springer-Verlag, Berlin, p 347.

Ulrich B (1983) Pollution Stresses on Forest Ecosystems (Cammerer A, ed.), Environment Canada.

Urano K, Yoshiba Y, Nanjo T, Ito T, Yamaguchi-Shinozaki K, Shinozaki K (2004) *Arabidopsis* stress-inducible gene for arginine decarboxylase *AtADC2* is required for accumulation of putrescine in salt tolerance. Biochem Biophys Res Comm 313:369-375.

Urano K, Hobo T, Shinozaki K (2005) *Arabidopsis ADC* genes involved in polyamine biosynthesis are essential for seed development. FEBS Lett 579:1557-1564.

van Nocker S, Ludwig P (2003) The WD-repeat protein superfamily in I: conservation and divergence in structure and function. BMC Genomics 4:50.

Vázquez MD, Poschenrieder C, Corrales I, Barceló J (1999) Change in apoplastic aluminum during the initial growth response to aluminum by roots of tolerant maize variety. Plant Physiol 119:435-444.

Vespa L, Couvillion M, Spangler E, Shippen DE (2005) ATM and ATR make distinct contributions to chromosome end protection and the maintenance of telomeric DNA in *Arabidopsis*. Genes Dev 19:2111-2115.

von Uexkull HR, Mutert E (1995) Global extent, development and economic impact of acid soils. Plant Soil 171:1–15.

Waisberg M, Joseph P, Hale B, Beyersmann D (2003) Molecular and cellular mechanisms of cadmium carcinogenesis. Toxicology 192:95-117.

Wang C and Liu Z (2006) *Arabidopsis* ribonucleotide reductases are critical for cell cycle progression, DNA damage repair and plant development. Plant Cell 18:350-365.

Wang S, Durrant WE, Song J, Spivey NW, Dong X (2010) *Arabidopsis* BRCA2 and RAD51 proteins are specifically involved in defense gene transcription during plant immune responses. Proc Natl Acad Sci USA 107:22716-22721.

Wang Y, Stass A, Horst WJ (2004) Apoplastic binding of aluminum is involved in silicon-induced amelioration of aluminum toxicity in maize. Plant Physiol 136:3762-3772.

Wehr JB, Menzies NW, Blamey FPC (2004) Inhibition of cell-wall autolysis and pectin degradation by cations. Plant Physiol Bioch 42:485–492.

Westerman RL (1987) Soil reaction: Acidity, alkalinity, and salinity. In "Wheat and Wheat Improvement" (E. G. Heyne, ed.), 2nd Ed., pp. 340-344. Agron. Monogr. 13, ASA, CSSA, SSSA, Madison.

Xia J, Tamaji N, Kasai T, Ma JF (2010) Plasma membrane-localized transporter for aluminum in rice. Proc Natl Acad Sci USA 107:18381-18385.

Wong MTF, Swift RS (2003) Role of organic matter in alleviating soil acidity. In: Handbook of soil acidity (Rengel Z, ed). Marcel Dekker, NY Pp. 349-351.

Xue YJ, Tao L, Yang ZM (2008) Aluminum-induced call wall peroxidase activity and lignin synthesis are differentially regulated by jasmonate and nitric oxide. J Agric Food Chem 56:9676-9684.

Yamagishi K, Nagata N, Yee KM, Braybrook SA, Pelletier J, Fujioka S, Yoshida S, Fischer RL, Goldberg RB, Harada JJ (2005) TANMEI/EMB2757 Encodes a WD Repeat Protein Required for Embryo Development in *Arabidopsis*. Plant Physiol 139:163-173.

Yamaguchi K, Takahashi Y, Berberich T, Imai A, Takahashi T, Michael AJ, Kusano T (2007) A protective role for the polyamine spermine against drought stress in *Arabidopsis*. Biochem Biophys Res Commun 352:486-490.

Yamakawa H, Kamada H, Satoh M, Ohashi Y (1998) Spermine is a saliclate-independent endogenous inducer for both tobacco acidic pathogenesis-related proteins and resistance against tobacco mosaic virus infections. Plant Physiol 118:1213-1222.

Yamamoto Y, Kobayashi Y, Matsumoto H (2001) Lipid peroxidation is an early symptom triggered by aluminum, but not the primary cause of elongation inhibition in pea roots. Plant Physiol 125:199–208.

Zdobnov EM, Apweiler R (2001) InterProScan - an integration platform for the signature-recognition methods in InterPro. Bioinformatics 17:847-848.

Zhang J, He Z, Tian H, Zhu G, Peng X (2007) Identification of aluminium responsive genes in rice cultivars with different aluminium sensitivities. J Exp Bot 58:2269–2278.